REGULATION OF SODIUM TRANSPORT ACROSS EPITHELIA DERIVED FROM HUMAN MAMMARY GLAND

by

QIAN WANG

B.S., Capital Normal University, 2008

AN ABSTRACT OF A DISSERTATION

submitted in partial fulfillment of the requirements for the degree

DOCTOR OF PHILOSOPY

Department of Anatomy and Physiology
College of Veterinary Medicine

KANSAS STATE UNIVERSITY
Manhattan, Kansas

2014

Abstract

The first aim of this project is to define the cellular mechanisms that account for the low Na^+ concentration in human milk. MCF10A cells, which were derived from human mammary epithelium and grown on permeable supports, exhibit amiloride- and benzamil-sensitive short circuit current (I_{sc}), suggesting activity of the epithelial Na^+ channel, ENaC. When cultured in the presence of cholera toxin (Ctx), MCF10A cells exhibit greater amiloride sensitive I_{sc} at all time points tested, an effect that is not reduced with Ctx washout for 12 hours or by cytosolic pathways inhibitors. Ctx increases the abundance of both β and γ-ENaC in the apical membrane and increases its monoubiquitination but without changing total protein and mRNA levels. Additionally, Ctx increases the levels of both the phosphorylated and the nonphosphorylated forms of Nedd4-2, a ubiquitin-protein ligase that regulates ENaC degradation. The results reveal a novel mechanism in human mammary gland epithelia by which Ctx regulates ENaC-mediated Na^+ transport.

The second project aim is to develop a protocol to isolate mammary gland epithelia for subsequent *in vitro* culture. Caprine (1°CME) and bovine mammary epithelia (1°BME) were isolated and cultured on permeable supports to study hormone- and neurotransmitter-sensitive ion transport. Both 1°CME and 1°BME cells were passed for multiple subcultures and all passages formed electrically tight barriers. 1° CME were cultured in the presence of hydrocortisone and exhibited high electrical resistance and amiloride-sensitive I_{sc}, suggesting the presence of ENaC-mediated Na^+ transport. 1° BME were grown in a complex media in the presence or absence of dexamethasone. In contrast to 1°CME, 1°BME exhibited no detectable amiloride-sensitive I_{sc} in either culture condition. However, 1°BME monolayers responded to an adrenergic agonist, norepinephrine, and a cholinergic agonist, carbamylcholine, with rapid increases in I_{sc}. Thus, this protocol for isolation and primary cell culture can be used for future studies that focus on mammary epithelial cell regulation and functions.

In conclusion, the results from these projects demonstrate that mammary epithelial cells form electrically tight monolayers and can exhibit neurotransmitter- and/or hormone-induced net ion transport. The mechanisms that regulate Na^+ transport across mammary gland may provide clues to prevent or treat mastitis.

REGULATION OF SODIUM TRANSPORT ACROSS EPITHELIA DERIVED FROM HUMAN MAMMARY GLAND

by

QIAN WANG

B.S., Capital Normal University, 2008

A DISSERTATION

submitted in partial fulfillment of the requirements for the degree

DOCTOR OF PHILOSOPY

Department of Anatomy and Physiology
College of Veterinary Medicine

KANSAS STATE UNIVERSITY
Manhattan, Kansas

2014

Approved by:

Major Professor
Dr. Bruce D. Schultz

Copyright

Abstract

The first aim of this project is to define the cellular mechanisms that account for the low Na^+ concentration in human milk. MCF10A cells, which were derived from human mammary epithelium and grown on permeable supports, exhibit amiloride- and benzamil-sensitive short circuit current (I_{sc}), suggesting activity of the epithelial Na^+ channel, ENaC. When cultured in the presence of cholera toxin (Ctx), MCF10A cells exhibit greater amiloride sensitive I_{sc} at all time points tested, an effect that is not reduced with Ctx washout for 12 hours or by cytosolic pathways inhibitors. Ctx increases the abundance of both β and γ-ENaC in the apical membrane and increases its monoubiquitination but without changing total protein and mRNA levels. Additionally, Ctx increases the levels of both the phosphorylated and the nonphosphorylated forms of Nedd4-2, a ubiquitin-protein ligase that regulates ENaC degradation. The results reveal a novel mechanism in human mammary gland epithelia by which Ctx regulates ENaC-mediated Na^+ transport.

The second project aim is to develop a protocol to isolate mammary gland epithelia for subsequent *in vitro* culture. Caprine (1°CME) and bovine mammary epithelia (1°BME) were isolated and cultured on permeable supports to study hormone- and neurotransmitter-sensitive ion transport. Both 1°CME and 1°BME cells were passed for multiple subcultures and all passages formed electrically tight barriers. 1° CME were cultured in the presence of hydrocortisone and exhibited high electrical resistance and amiloride-sensitive I_{sc}, suggesting the presence of ENaC-mediated Na^+ transport. 1° BME were grown in a complex media in the presence or absence of dexamethasone. In contrast to 1°CME, 1°BME exhibited no detectable amiloride-sensitive I_{sc} in either culture condition. However, 1°BME monolayers responded to an adrenergic agonist, norepinephrine, and a cholinergic agonist, carbamylcholine, with rapid increases in I_{sc}. Thus, this protocol for isolation and primary cell culture can be used for future studies that focus on mammary epithelial cell regulation and functions.

In conclusion, the results from these projects demonstrate that mammary epithelial cells form electrically tight monolayers and can exhibit neurotransmitter- and/or hormone-induced net ion transport. The mechanisms that regulate Na^+ transport across mammary gland may provide clues to prevent or treat mastitis.

Table of Contents

List of Figures

List of Tables

Acknowledgements

Thanks to my mentor, Dr. Bruce Schultz, for support, guidance and encouragement throughout the years. Without him, I would not have had opportunities to study what I truly love and to chase my dream. Thanks, Dr. Schultz, you are patient and always encourage me to work hard and to never give up. Your wisdom, hard work and enthusiasm for scientific research set a golden example for me in my future career. I cannot describe how much I appreciate that you are my mentor.

Also, I want to thank to my committee professors, Dr. Peying Fong, Dr. Daniel Marcus, and Dr. David Grieger for their expert advice and guidance throughout my studies. Thank you to my wonderful current and previous lab mates, Florence Wang, who gives me lots of help whenever I need assistant with cell culture, Dr. Fernando Pierucci-Alves, Dr. Vladimir Akoyev, Pradeep Reddy Malreddy, Sheng Yi and Jacob Hull.

I also want to extend my deep appreciation to my beloved husband, Feng Zhang and my little angel, Caroline. Without you as a family and without your support, I would never have been able to chase my dreams and to experience success. Thank you to my Mom, Liya Zhang and my Dad, Yi Wang. Thank you so much for your accompany and support in all these wonderful adventures.

Dedication

To my beloved husband, to my wonderful little angel, to my parents, to my great mentor, and to my friends… without your support, I would not be able to achieve my dream. Thank you very much!

Chapter 1 - Overview of Mammary Gland Epithelial Function and Regulation of Epithelial Na^+ Transport

The mammary gland is a defining characteristic of all mammals. Lactation is critical for neonate survival and thus is required for reproductive success and species propagation. However, mechanisms that contribute to and regulate ion transport across mammary epithelium, which contribute to milk composition and volume, are poorly understood. This dissertation focuses on regulation of ion transport, particularly Na^+ transport through the epithelial sodium channel (ENaC) in two experimental systems, a human mammary epithelial cell line and primary cultures of cells isolated from caprine and bovine mammary gland. The goal of research reported in chapter 2 is to describe underlying mechanisms that link cholera toxin (Ctx), a toxin secreted by *Vibrio cholera,* to the regulation of Na^+ absorption *via* ENaC in a human mammary epithelial cell line, MCF10A. Chapter 3 focuses on defining and optimizing a protocol to isolate and grow bovine and caprine mammary epithelia in culture. This introduction provides a brief review of the literature describing mammary gland development, mechanisms of milk secretion, and regulation of ion transport with particular focus on ENaC-mediated Na^+ transport across mammary epithelia as a general background for the materials covered in subsequent chapters.

Mammary gland development

Mammary glands are unique in that their development, which includes embryonic, pubertal and gestational, mostly occurs after birth. Many changes that allow for milk formation and secretion occur in the epithelium during gestation and early in the post-partum period. Although mammary glands achieve their full function only after pregnancy, the formation of these glands is initiated during embryogenesis (70). The initial formation of mammary glands in humans is reported as early as the sixth week of gestation and includes the formation of a milk line on the anterior surface of the embryo (84). Figure 1.1 shows a schematic review of three stages of murine mammary gland development: embryonic, pubertal and gestational (70). At murine embryonic day (E) 11.5, five pairs of placodes are formed, which are epithelial structures that will develop into discrete organs. Between E10 and E20, mammary epithelial buds and initial fat pads are formed. The epithelial buds further elongate to invade the fat pad and branch to form ductal structures. Rudimentary ducts are present at birth and will remain at this developmental

stage until puberty. Mammary glands undergo rapid development at puberty with exposure to elevated levels of ovarian hormones such as estrogen. The blind end of prepubertal rudimentary ducts includes a multilayer structure that is called the terminal end bud. In mature mammary ducts and acini, epithelial cells form the inner layer and are surround by myoepithelial cells. These structures are surrounded by a basement membrane and embedded within the mammary fat pad. During pregnancy, lactogenic hormones such as estrogen, progesterone, and prolactin regulate further development culminating in a fully mature functional mammary gland at parturition (84). Ducts extend and branch during gestation and luminal epithelial cells proliferate and differentiate to the extent that milk secretion can occur in alveoli. During lactation, decreased progesterone and increased prolactin stimulate milk synthesis (84). The hormonal regulation of milk section will be reviewed later in this chapter. In humans, about 10-15 ducts are open at each nipple to secrete milk (160). The volume secreted is determined by the number of mammary epithelial cells (238). After milk is made, it is stored in alveoli and ducts (132). Milk removal ('ejection') is initiated by the contraction of myoepithelial cells in response to oxytocin, which is released from the anterior pituitary (84).

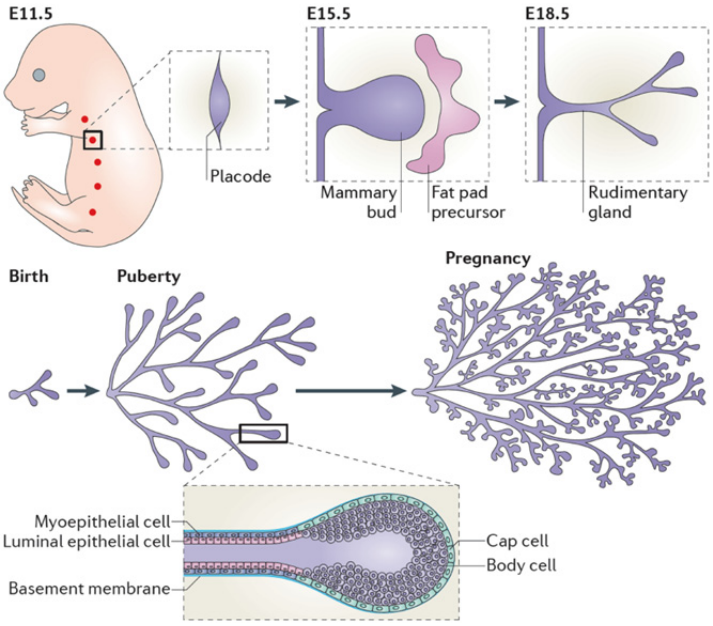

Figure 1.1 Mammary gland development from embryonic stages to birth, through puberty and pregnancy.

Mouse embryos develop five pairs of placodes at E11.5, each of which develops to form a mammary bud. At E18.5, the rudimentary gland is formed. During puberty, hormones lead to the formation of terminal end buds. During pregnancy, mammary glands expand further and elongate. Figure modified from Gjorevsk, *et. all* Ref. [70].

Hormonal regulation of mammary gland and milk secretion will be further introduced in detail here. Many reviews have summarized endocrine regulation of mammary function (41, 118, 161, 238). During development, estrogens and progesterone are essential hormones that regulate ductal growth and alveolar expansion (87). A complex signaling network between mammary

epithelial and stromal cells is influenced by these steroid hormones and other factors (70). Estrogens are suggested to regulate mammary gland ductal elongation and branching, which are influenced also by growth hormone and/or insulin-like growth factor 1 (70, 87). By contrast, progesterone contributes to alveolar expansion (87). Only progesterone receptor-positive cells can develop and be incorporated in functional alveoli (22). Two isoforms of progesterone, A and B, reportedly play different roles in the regulation of alveolar development (87). Progesterone B is essential for regulation of alveolar development and proliferation, whereas deletion of progesterone A does not alter mammary gland development (155). During pregnancy, high levels of progesterone and prolactin trigger further expansion of mammary epithelia (161). In addition, estrogens are required to maintain progesterone receptor expression and production of prolactin (143, 161). Low estrogen levels during pregnancy reportedly are associated with low post-partum prolactin levels and the inability to lactate (143). Other agents such as transforming grow factor α, and epidermal growth factor (EGF) that activate the receptor tyrosine kinases ERBB1 (EGF receptor 1) and ERBB4 (EGF receptor 4), also are required for mammary gland epithelial proliferation and differentiation (87). Mice harboring mutant forms of ERBB1 show impaired alveolar development (61). Similarly, mice with mammary gland-targeted deletion of ERBB4 fail to develop functional alveoli (136). The initiation of lactation is triggered by a precipitous withdraw in circulating progesterone, which in humans is produced by the placenta during late gestation (122, 161).

During lactation, milk synthesis by epithelia is regulated by prolactin, growth hormone and other hormones. Prolactin is named for its function to promote lactation. That prolactin is essential to maintain lactation is demonstrated by the complete loss of lactation that accompanies exposure to dopamine receptor antagonists such as ergot alkaloids, which inhibit prolactin release from the pituitary (87). Prolactin binds to the prolactin receptor, which is a class I cytokine receptor family member. The receptor undergoes dimerization, binds to Janus kinase-2 (JAK2) and phosphorylates specific tyrosine residues to activate STAT5 (signal transducer and activator of transcription 5) (87). STAT5 serves as a downstream signaling component of the pathways activated by either the prolactin receptor or ERBB4. STAT5 also activates the transcription of genes that encode for milk proteins (87). Growth hormone increases milk yield and the commercialized form is called “bovine somatotropin,” which is used in the dairy industry to increase milk yield (161). Inhibition of growth hormone secretion during lactation decreases

milk yield in rats (161). However, the mechanism by which growth hormone affects lactation is not fully defined and remains the subject of ongoing studies.

Other hormones play substantial roles in stimulating milk secretion and ejection. Oxytocin promotes milk ejection and enhances milk production (8). Hormones that regulate body metabolism, such as thyroid hormone, insulin, and leptin, can impact milk secretion (28, 83, 267). Moreover, feedback inhibitor of lactation (FIL), β-casein 1 to 28 (βCN1-28) and serotonin (5-HT) can reduce milk secretion (41). FIL is proposed to be a glycoprotein that can inhibit milk secretion. However the peptide sequence has not yet been published and the mechanism of action remains to be determined (41, 255). Similarly, βCN1-28, is proposed to reduce milk secretion in response to heat stress, perhaps by inhibiting apical K^+ channels (41, 211, 212). 5-HT also plays a role in reducing milk secretion. 5-HT receptors and components of the 5-HT metabolic pathway are reportedly present in bovine mammary gland and 5-HT can be detected in milk (41). It has been suggested that 5-HT can act through multiple pathways to regulate milk synthesis. *In vitro*, 5-HT reduced tight junction formation of MCF10A cells, a human mammary epithelia cell line (41, 142, 237). Block of the 5-HT reuptake transporter, SERT protein, delayed of milk secretion (41, 141, 242). Clearly, the effects of hormones and growth factors on milk production are many and varied with much more work being required to describe these effects fully.

Mechanisms of milk secretion

Although milk composition varies widely across species (reviewed later in this chapter), the mechanisms of milk secretion appear to be similar (132). Five pathways have been used to describe cellular mechanisms that account for the transport, synthesis and secretion of milk constituents by alveolar epithelial cells (152). As depicted in Figure 1.2, pathway I shows exocytotic apical release of lactose, oligosaccharides, phosphate, calcium, citrate and proteins that are synthesized by epithelia and are present in the aqueous phase of milk (152). Similar pathways are present in other cell types in which Golgi vesicles carry substances for secretion at the apical membrane. Concentrations of osmolytes especially lactose are high in Golgi vesicles, which drives water flux into the vesicles and ultimately into secreted milk. Therefore, milk fluid volume is proportional to total lactose secretion (153). Pathway II represents lipid secretion with formation of cytoplasmic lipid droplets that enter milk *via* a pinocytotic process to form a milk fat globule (MFG) that is fully enclosed in membrane derived from the apical aspect of the

epithelial cell (152). Lipids are synthesized in the smooth endoplasmic reticulum and formed into lipid bodies for transport toward the apical membrane where they separate from the cells as MFGs (152). MFGs are the main energy source for breast-fed neonates (152). Pathway III depicts vesicular transcytosis of extra-cellular solutes such as immunoglobulins, albumin and hormones from the interstitial space to the milk (152). Immunoglobulin A has been shown to be transported into milk *via* the transcytotic pathway in rabbit mammary gland (152). Some hormones such as prolactin, insulin and EGF are likely transported into milk via transcytosis, although the underlying mechanisms remain to be defined (160). Pathway IV, which is a focal point of this thesis, depicts processes that facilitate the movement of ions, water, glucose and other small solutes across the apical and/or basolateral membranes (152). The predominant pathway for water movement is not known, but is likely a combination of paracellular and transcellular flux. Aquaporins that facilitate transcellular movement are present in mammary epithelia (153). Pathway V illustrates an avenue for paracellular movement of plasma components and leukocytes (152). Typically, one would expect this pathway to allow little flux during lactation (*i.e.*, that there is tight barrier that separates milk from the interstitial space). However, the pathway may become highly permeant in pathological situations such as mastitis. Further, it is thought that the paracellular pathway is relatively permeant in the non-lactating state.

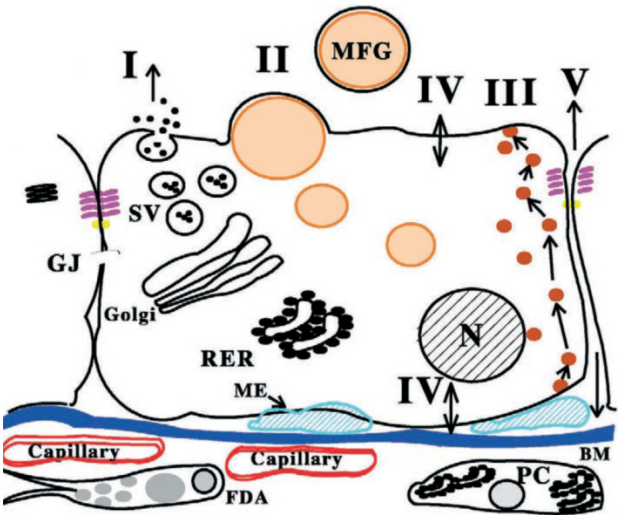

Figure 1.2 Five pathways for milk constituent secretion across mammary alveolar epithelial cells.

Detailed descriptions for each pathway are reported in the text. SV, secretory vesicle; RER, rough endoplasmic reticulum; BM, basement membrane; N, nucleus; PC, plasma cells; FDA, fat depleted adipocyte; GJ, gap junctions; ME, myoepithelial cells. Figure adapted from McManaman and Neville. Ref [151].

Mechanisms of ion transport depicted in Pathway IV are poorly defined. A system to account for ion gradients across the mammary epithelium was first proposed in 1971 based upon observations on cultured guinea pig mammary tissue (Figure 1.3) (132, 204). This model

suggests that the apical membrane is freely permeable to Na^+, K^+, and Cl^-, and that Na^+/K^+ ATPase in the basolateral membrane sets the concentration of Na^+ and K^+ in milk (132, 202). Moreover, the model predicts that a basolateral pump would bring Cl^- into the cells (132, 202). The model, however, fails to account for the distribution of Cl^- across the apical membrane. Further, becuase there is substantial difference in ash (*i.e.*, mineral) content of milk across species, it is unlikely that this initial model is widely applicable.

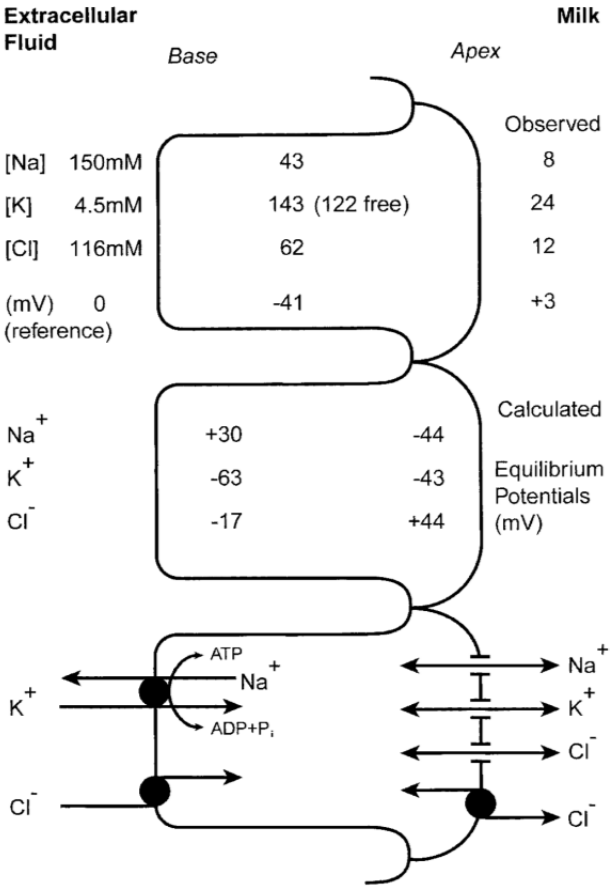

Figure 1.3 An epithelial model illustrates ions distribution and membrane potentials derived for guinea pig mammary tissue.

Image adapted from Shennan and Peaker. Ref [200]

A number of studies have addressed mechanisms of ion transport across mammary epithelia. It has been shown that Ca^{2+}-activated K^+ channels, which are inhibited by Ba^{2+}, are present in mouse mammary epithelial cells (64). Moreover, volume-activated K^+ channels, which can be blocked by quinine, were detected in rat mammary tissue (203), and Ba^{2+}-sensitive K^+ channels were detected in apical membranes stripped from goat MFGs (215). Amiloride-sensitive Na^+ transport, suggesting ENaC activity, was reported to be present in mammary epithelia derived from a number of species (14, 15, 20, 123, 182, 197). Moreover, work from this laboratory that showed steroid hormone regulation in a cell line derived from bovine mammary tissue (182, 197). Regulation of Na^+ transport across mammary epithelia is considered in further detail in this chapter. The cystic fibrosis transmembrane conductance regulator (CFTR) reportedly is present in the apical membrane of mammary epithelia (15, 57, 197), although milk from cystic fibrosis (CF) patients reportedly has normal electrolyte composition (207, 254). Although several ion channels have been identified in mammary epithelial cells, there are ongoing discussions regarding potentially different functions of epithelial cells lining the duct when compared to those lining the alveoli (90, 132, 133, 138,

153, 208). The ductile cells reportedly can absorb Na^+, Cl^- and water selectively, but leave the K^+ in lumen (138). Clearly, additional studies are required to identify ion transport mechanisms in mammary epithelium. It is also needed to determine the distribution of these transport mechanisms within the gland and across species and how the mechanisms are regulated at each location.

Species difference in milk composition

The relative proportions of fats, proteins, carbohydrates and minerals vary widely across mammalian species (132). Table 1.1 shows milk composition at mid-lactation for humans and several other species (167). The osmolality is similar among all species and is isotonic with plasma (132, 167). Human milk contains a higher concentration of sugar than bovine milk (167). Protein, fat and mineral content vary widely among the listed species. Human milk is the lowest in protein. Rabbit milk has the highest proportion of protein and salt (ash). Fat content varies widely with black rhinoceros milk being the lowest (0.2%) and fur seal milk being the highest (nearly 50%). It has been proposed that fat contents may correlate with sucking intervals (167). Species that have long inter-suckling intervals, such as fur seals, secrete milk containing high energy density, including a high fat content. In contrast, species that feed their young more

Table 1.1 Major components in milk derived from various species*

Species	Dry matter (%)	Fat (%)	Protein (%)	Sugar (%)	Ash (%)
Human	12.4	4.1	0.8	6.8	0.2
Pig	20.1	8.3	5.6	5.0	0.9
Cow	12.4	3.7	3.2	4.6	0.7
Rabbit	35.2	14.4	15.8	2.7	2.1
Mouse	29.3	13.1	9.0	3.0	1.5
Guinea-pig	17.5	5.7	6.3	4.8	0.8
Northern fur seal	61.0	49.4	10.2	0.1	0.5
Black rhinoceros	8.8	0.2	1.4	6.6	0.3
Goat	12.0	3.8	2.9	4.7	0.8
Horse	10.5	1.3	1.9	6.9	0.4

* Modified from Oftedal. Ref [164]

frequently (e.g., horse, >1 h^{-1}; rhinoceros, ~1 h^{-1}; human, ~0.5 h^{-1}) produce milk with lower fat content (167). Like other constituents, the concentration of Na^+ varies widely across species, but is lower than plasma in all cases (202). Table 1.2 shows a detailed comparison of major milk constituents (especially mineral concentrations) between human and cow in terms of grams per 100 ml of milk (167). The lowest milk Na^+ concentration among all species is reported for humans, only 5-10 mEq/l (159, 160, 177, 202), compared with 136-145 mEq/l in plasma (202). Rabbit milk contains 60-80 mEq/l Na^+ (175) whereas milk from dairy cows typically contains 20-25 mEq/l (168, 177). Chloride, phosphate and glucose concentrations in milk correlate positively with Na+ concentration, whereas lactose and Ca2+ concentrations correlate negatively (160). However, the mechanisms that control ion transport across mammary epithelium and contribute to the generally low Na^+ concentration in milk, as well as the very low Na^+ concentration specifically in human milk, are not fully understood. This Study seeks to reveal underlying mechanisms that contribute to the Na^+ concentration in milk and to provide a better understanding of Na^+ transport across human mammary gland epithelia.

Table 1.2 Major constituents of bovine milk and human milk*

Components	Bovine Milk (g/100 ml)	Human Milk (g/100 ml)
Water (100-dry matter)	87.3	87.2
Lipids	3.7	4.2
Protein, casein	2.6	0.2
Proteins, whey	0.6	0.7
Carbohydrates	4.8	7
Minerals (Ash)	0.8	0.2
Calcium	0.125	0.033
Phosphorus	0.096	0.015
Sodium	0.058	0.015
Potassium	0.138	0.055
Magnesium	0.012	0.004
Chloride	0.103	0.043

* Modified from Oftedal. Ref [164]

Primary mammary epithelia cell culture and cell lines

Numerous cell lines have been developed from human, cow and mouse mammary epithelia and used successfully as models to study mammary function. Human mammary epithelial cell lines have been derived from two sources, carcinomas and normal or healthy epithelial cells. The

MCF10A cell line arose from a spontaneous immortalization of cells that were isolated from normal mammary epithelia (225). MCF10A cells grown on permeable supports can be used as the *in vitro* model to study tight junction formation and architecture (237). Another human cell line, human mammary epithelial cells (T-HME or HME), arose from normal epithelial cells that were transformed by transfection with human telomerase (hTERT) (107, 123). HME cells also form electrically tight monolayers on permeable supports and the cell have been used to study ion transport associated with P2Y receptors (123, 170). Similarly, HMT-3522 and HBL-100 are cell lines derived from normal human breast epithelia (21, 65). However, epithelial barrier and ion transport characteristics have not been reported. Some commonly used mammary cell lines derived from breast carcinomas are MCF-7 (226), Hs578T (80), T-47D (106), and MDA-MB-231 (30). Similarly, rat and mouse mammary epithelial cell lines have been developed both from normal mammary epithelia and from carcinomas (5, 73). The 31EG4 cell line, which is an untransformed nontumorigenic mouse mammary cell line, is used extensively. These cells can be grown as tight monolayers that respond to lactogenic hormones (186, 236, 263). Immortalized bovine mammary epithelial cell lines such as BME-UV (262), HH2A(93), MAC-T (94) and L-1(68) also are used commonly as model systems to study mammary function. An advantage of these cell lines is that there is homogeneity within the cell population and the potential for consistency over time and between laboratories. Cell lines, with their almost infinite potential for expansion, provide the opportunity to conduct multiple tightly paired experiments with a variety of conditions or treatments. However, the limitations of cell lines, such as the general applicability of the inferences that are drawn, cannot be eliminated. The effect of hormones or drugs on cell lines may not be indicative of physiological function *in vivo*.

In vivo studies of mammary function have been carried out predominantly using rodents. They are small, easy to handle and they progress rapidly through developmental stages. Moreover, transgenic mice can be used to gain important knowledge regarding specific contributions to mammary gland development and the mechanisms of making milk. However, rodents cannot represent all mammals as lactation mechanisms are characterized because there is such wide variation on milk composition among all species. Farm animals, predominantly cows, also are used as models to study mammary function and milk yield (7, 72). Other mammals such as tammar wallaby (164) and grey seals (79) have been used as unique models to study milk components synthesis and secretion. Therefore, animal models are useful to study mammary

development but substantial variation among species and complex mammary structure may limit how broadly the conclusions might be applied.

Primary cultures may provide responses that more closely reflect *in vivo* situations when compared to immortalized or transformed cell lines. Primary culture of mammary gland cells can be traced back to as early as 1961, when the model was used to study glycogen synthesis (52, 53). An obstacle associated with primary culture is the difficulty in isolating and/or maintaining an homogeneous epithelial cell population that is free of fibroblasts. Cholera toxin was used as a component in mammary epithelial cell culture media to eliminate fibroblast proliferation (257). It has been reported that bovine (60), caprine (265) and human (75) mammary epithelial cells were cultured successfully as monolayer or 3D structures, but those reports did not assess or define ion transport. This dissertation focuses on Na^+ transport across normal mammary gland epithelia. The literature reveals that few mammary cell lines have been used as *in vitro* models to study ion transport.

Sodium transport across mammary epithelia

ENaC is present in epithelial cells derived from murine (14, 15, 20), bovine (181, 182, 197), and human (15, 20) mammary gland. In most cases, ENaC is composed by three subunits, α, β and γ, with a stoichiometry of 1:1:1 (34, 120). A fourth subunit, the δ subunit, which replaces the α subunit in the heterotrimer (247), is expressed in a variety of epithelial and non-epithelial tissues (98). Amiloride block is used widely as a first indicator that ENaC contributes to the functionality of a tissue (9, 116). Corticosteroid hormones can enhance ENaC expression in human, mouse and bovine mammary epithelia, which could account for Na^+ movement during lactation and oncogenesis (15, 20, 123, 182, 197). This laboratory reported the presence of amiloride-sensitive ion transport in a bovine mammary epithelial cell line, BME-UV, when cultured in the presence of natural and synthetic corticosteroids (182, 197). The mechanisms underlying corticosteroid-induced amiloride-sensitive current include an increase in mRNA abundance for both β- and γ-ENAC, with a lesser effect on α-ENaC mRNA (182). Mifepristone, an inhibitor of the glucocorticoid receptor, can block the effect of corticosteroids on amiloride-sensitive short circuit current (I_{sc}; a sensitive indicator of net ion transport) and on the elevation of ENaC mRNA abundance (182). Moreover, results from The BME-UV model suggest that luminal Na^+ concentration is an important regulator of tight junction integrity (181). Reduction

in apical Na^+ concentration from plasma-like levels to milk-like levels increased the transepithelial electrical resistance (R_{te}) of BME-UV monolayers (181). These observations demonstrate that ENaC-mediated Na^+ transport is present in bovine mammary glands and that Na^+ transport is regulated by steroid hormones. Corticosteroids are used routinely in the culture of mammary epithelia because of the effects on epithelial integrity (*i.e.*, barrier function) that have been reported (15, 111, 152, 213, 235). Similar observations were reported in both mouse cell lines (31EG4 and HC11) and human cell lines (MCF10A, T-47D and MCF-7) (15, 20). Moreover, β- and γ-ENaC mRNAs were elevated in lactating mouse mammary tissue when compared with non-lactating mammary tissue (20). The authors detected mRNA for α-, β-, and γ-ENaC subunits in both cancerous and noncancerous cell lines that were derived from humans and mice (20). Steroid hormones elevated the expression of mRNA coding for all ENaC subunits in MCF10A cells (20). Dexamethasone increased α- and γ-ENaC mRNA in HC11 cells, which were derived from lactating mouse mammary gland, although mRNA coding for β-ENaC was not detected in the present or absent with dexamethasone (5, 20). In contrast, cells derived from human mammary duct carcinoma (T-47D) (106), dexamethasone increased β- and γ-ENaC mRNA expression but had no effect on α-ENaC mRNA expression (20). Similar to T-47D cells results were found in MCF-7 cells, a cell line derived from a human adenocarcinoma (20, 226). When compared to noncancerous cells, cancerous cells express less α-ENaC mRNA under basal conditions and produce no response to steroid hormone treatment on α-ENaC mRNA expression. These studies demonstrated; 1) the presence of mRNA coding for α-, β-, and γ-ENaC, 2) the presence of ENaC protein subunits, and 3) the regulation of ENaC expression by corticosteroids in human and mouse mammary epithelia. However, no functional data to show ENaC-mediated Na^+ transport were reported in the aforementioned mRNA expression studies.

More recently, others have shown that immortalized HME cells express ENaC and that amiloride-sensitive I_{sc} can be stimulated by purinergic agonists (123). For both primary and immortalized HME cells, it was suggested that basolateral P2Y receptor activation enhances ENaC-mediated Na^+ absorption by increasing the activity of $K_{Ca}3.1$, which hyperpolarizes the cell membrane to increase the electrochemical driving force for Na^+ absorption (123, 170). Taken together, these reports provide a mechanism to whereby K^+ channels activation is coupled with Na^+ absorption, thus modifying milk volume and composition.

Mechanisms of ENaC regulation and its function throughout the body

As early as 1951, Hans Ussing and his colleagues demonstrated the presence of net Na^+ transport in isolated frog skin (243). Following this discovery, Ussing hypothesized that Na^+ is actively pumped out of cells to maintain a low intracellular Na^+ concentration (119). Strong evidence for an apical Na^+ channel was demonstrated first in 1977 by using fluctuation analysis of currents across frog skin in the absence and presence of amiloride (129). Subsequent to these pioneering studies in frog skin, epithelial Na^+ transport was identified on the apical surface of epithelia lining a variety of tissues, including mammary gland, kidney, lung, urinary bladder, colon, salivary glands, inner ear, vas deferens and sweat glands (35, 104, 195).

ENaC was first cloned from a rat distal colon cDNA library (33, 34). Initially, only α-ENaC was identified. Expression of α-ENaC in *Xenopus* oocytes resulted in small current than expected based on endogenous channel activity (33). The identity of additional subunits was determined later (34). Ultimately, β- and γ-ENaC were cloned and expressed in *Xenopus* oocytes with α-ENaC and the resulting current was much larger (34). No channel activity was detected when β- and/or γ-ENaC were expressed in the absence of α-ENaC. Since then, mRNAs encoding for α, β, and γ ENaC subunits have been detected in frog renal epithelial cell line (A6 cells) (180), human kidney, lung, liver, and pancreas (148, 149), mouse kidney (2), toad urinary bladder (117) and cow kidney (63). The sequences of ENaC subunits share homology with *C. elegans* genes mec-4 and deg-1, which when mutated are associated with neuronal degeneration (33, 50). Therefore, the family of cation channels was named the "DEG (degenerin)/ENaC" family of ion channels. Although the heteromeric channel structure was widely accepted, 2α:1β:1γ and 3α:3β:3γ channels structures were also proposed (231). Additionally, δ- (98) and ε-ENaC (4, 247) were identified, either of which can replace α-ENaC to form functional channels, although the physiological functions of these two subunits remain to be determined.

A typical ENaC channel is composed of three subunits, each of which has two hydrophobic domains that pass through the cell membrane resulting in an extracellular loop and short cytoplasmic N- and C- termini (Figure 1.4) (13, 32, 220). The extracellular domains of α- and γ-ENaC can be cleaved by proteolytic enzymes, resulting in increased channel open probability (13, 31). In addition, two N-glycosylation sites (34, 220) and two cysteine-rich domains (54), which are present in the extracellular loops of all three subunits play important roles in channel folding, trafficking and gating. The N-terminus of α-ENaC was suggested to regulate channel

gating because mutations in this region associate with a decrease in channel open times and also cause type I pseudohypoaldosteronism (PHA-1) (38, 78). The C-terminus of all three ENaC subunits can be modified by kinases to increase ENaC gating (205, 246, 258). The presence of a proline-rich 'PY' motif (PPPXYXXL, P, Pro; Y, Tyr; L, Leu; X, any amino acid) in the C-terminus of β and γ subunits plays a critical role in channel degradation. A mutation of this region causes Liddle's Syndrome, which will be reviewed in detail later (55, 103, 196, 210, 223).

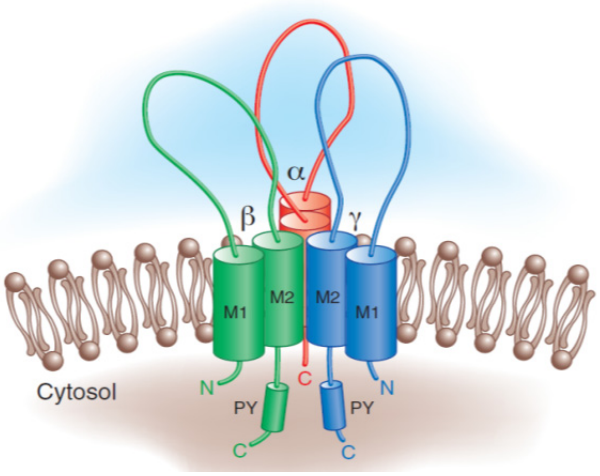

Figure 1.4 Simple representation of ENaC Structure.

A typical ENaC channel is a heterotrimer including an α, β and γ subunit. Each subunit has two hydrophobic domains (M1 and M2) that pass through the cell membrane resulting a large extracellular loop and short cytoplasmic N- and C-termini. Proline-rich 'PY' motifs are present in the C-terminus of β and γ subunits. Adapted from Bhalla and Hallows. Ref [13]

In general, Na^+ absorption through ENaC is tightly regulated by hormones such as aldosterone, hydrocortisone/cortisol, and vasopressin. Dysregulation of ENaC is associated with or contributes to a number of pathological conditions. Two well-characterized diseases associate with mutations in one or more ENaC subunits. PHA-1 results from loss-of-function mutations that lead to renal salt wasting and hyperkalemia (38, 78, 82). PHA-1 is characterized by severe dehydration and hypernatremia in the first week after birth, which is caused by insufficient renal Na^+ reabsorption and a lack of responsiveness to aldosterone. The underlying genetic mutation typically is a premature stop codon leading to a nonfunctional channel (78). In contrast, Liddle's syndrome results from gain-of-function mutations and is characterized by low renin, low aldosterone, and hypertension (210). The syndrome was first documented by Grant Liddle who identified a family in 1963 that suffered severe early onset hypertension (125). Such patients have abnormally low circulating levels of renin and aldosterone, hypertension and high Na^+ retention (210, 218). Therefore, this disease also known as pseudoaldosteronism. Overall gain of ENaC function results from broth point mutations and premature stop codon mutations in the cytoplasmic

carboxyl terminus in β- and/or γ-ENaC (81, 210). These mutations disrupt the 'PY' motif, which is essential for regulation of membrane surface expression (55, 196, 223). Subsequent research identified the PY motif as an important site for interaction with regulatory proteins in the cell. One important example of such an interactor is Nedd4 (Neural precursor cells Expressed Developmentally Downregulated), an E3 ubiquitin-ligase (233). Nedd4-2, a Nedd4 isoform, was reported to interact with ENaC directly *in vitro* (101). Nedd4-2 contains multiple WW domains, conserved tryptophan pairs that can bind directly to the ENaC PY motif (218). After binding, Nedd4-2 catalyzes ubiquitination on lysines residues within the amino terminus of any ENaC subunit (234, 266). ENaC can be regulated by monoubiquitination and polyubiquitination. Monoubiquitination of β-ENaC was associated with elevated surface expression in HEK 293T cells that were transfected with Nedd4-2 with or without mutated lysine residue to prevent formation of polyubiquitin chains (266). Polyubiquitination of ENaC signals their transfer to lysosomes for degradation (266). Therefore, Nedd4-2 decreases ENaC expression at the cell surface.

The cellular mechanisms that contribute to the regulation of ENaC activity is complex. Many cellular signaling pathways are integrated to regulate ENaC expression, trafficking, degradation, retrieval, and open probability. Because Nedd4-2 has a critical role in tagging ENaC for retrieval and degradation, Nedd4-2 regulation is a potential target to manage overall plasma membrane ENaC expression. Nedd4-2 knock out that disrupt its interaction with ENaC lead to salt-sensitive hypertension in mice (206). From *in vitro* studies, it has been reported that phosphorylation of Nedd4-2 will prevent it from binding to ENaC that is resident in the cell membrane. Two pathways increase Nedd4-2 phosphorylation and thereby increase ENaC activities. The renin-angiotensin-aldosterone pathway (*reviewed in the following section*) induces the expression of serum and glucocorticoid-induced kinase (SGK) (39, 157), which can bind to and phosphorylate Nedd4-2 (46, 222). The second pathway is initiated by vasopressin, which increases cAMP and hence, activates protein kinase A (PKA). PKA phosphorylates Nedd4-2 and thus prevents its interaction with ENaC (221). Other signaling pathways also contribute to the regulation of ENaC function. The phosphatidylinositol 3'-kinase (PI3K) pathway stimulates ENaC activity both directly and indirectly. Phosphoinositide products directly bind and simulate ENaC, whereas the PI3K pathway indirectly stimulates ENaC by increasing SGK function (227, 232, 248). The mammalian target of rapamycin complex-2 (mTORC-2) reportedly stimulates ENaC function by

directly binding and activates SGK (218). In contrast, the ERK-MAPK pathway reduces ENaC activity *via* direct phosphorylation, which leads to an increase in ENaC interaction with Nedd4-2 (218). Together, these complex regulatory mechanisms affect ENaC localization to regulate electrolyte homeostasis.

Regulation of ENaC in the kidney

The kidney is a complex organ that reabsorbs Na^+ and is regulated by several hormones (195). In the nephron, four segments reabsorb Na^+, including the proximal convoluted tubule, the thick ascending limb of Henle, the distal convoluted tubule and the collecting duct. ENaC is detected only in the distal convoluted tubule and collecting duct (195). Those segments are called the aldosterone-sensitive distal nephron (ASDN). Although ASDN contributes less than 10% to total Na^+ reabsorption in a nephron, the contribution is important to organismal Na^+ homeostasis (135, 195). Aldosterone, angiotensin and vasopressin play major roles in the regulation of renal ENaC expression and activity. In the distal nephron, aldosterone acts *via* mineralocorticoid receptors to enhance ENaC activity and expression both acutely (1-3 hours) and chronically (over 6-24 hours) (66, 195). During the acute phase, aldosterone increases open probability of membrane-resident ENaC channels (105, 114). In the chronic phase, ENaC channels are synthesized *de novo* and inserted into the epithelial cell apical membranes (218). Moreover, aldosterone also increases SGK expression (39, 157). Coexpression of SGK with ENaC in *Xenopus* oocytes increases amiloride-sensitive Na^+ current over 7-fold when compared to ENaC expression alone (3, 39). SGK increases ENaC membrane availability by increasing membrane trafficking and decreasing protein degradation (195). Angiotensin II (AngII) stimulates aldosterone synthesis and also directly affects ENaC activity independently of aldosterone. However, aldosterone independent mechanisms that link AngII to changes in Na^+ absorption are still under debate (23, 135). At least a portion of angiotensin-induced changes requires the presence of a cognate receptor, AT1, in distal nephron. Targeted AT1 knockout in the distal nephron of mice decreases in α-ENaC expression (23). Additional evidence comes from *in vitro* studies that use AngII acutely to increase ENaC open probability in distal nephron cells or isolated ducts (188, 261). Vasopressin also contributes to the regulation of ENaC. Vasopressin, which binds to its receptor, increases cAMP levels in collecting ducts principal cells (135, 144), which increases ENaC density at the apical membrane (29, 115). Vasopressin

also induces expression of an ubiquitin-specific protease, Usp10, which ultimately increases apical ENaC expression (19). Vasopressin also acts through the cAMP/PKA pathway to phosphorylate Nedd4-2, which ultimately increases ENaC abundance in the apical membrane (221). Additionally, vasopressin increases β- and γ-ENaC mRNA expression in rat kidney (163). Regulations of ENaC activity and expression are complex, which are essential to maintain salt and fluid homeostasis in kidney.

Regulation of ENaC in the lung

ENaC is expressed in airway epithelia where it plays an important role at parturition, transforming the lung from the fetal liquid-filled environment to the neonatal air-filled space. The critical role of ENaC function in the lung was demonstrated using knock-out mouse models. Alpha-ENaC knock-out mice die soon after birth due to the inability to transition from a liquid-filled to an air-filled lung (92). Beta- and γ-ENaC knock-out mice exhibit substantially reduced airway fluid clearance, but typically succumb to electrolyte imbalances and kidney failure shortly after birth rather than pulmonary complications (6, 150, 195). Glucocorticoids act at their cognate receptors in the airway to increase ENaC expression (37). Whether glucocorticoids regulate the expression of one or more specific ENaC subunit in the airway remains the topic of debate. *In vivo* experiments suggest that glucocorticoids enhance on expression of α-ENaC (146, 241), whereas in primary cultures of lung epithelia the expression of all ENaC subunits can be induced (245). Lung epithelia also express mineralocorticoid receptors. However, aldosterone-stimulated ENaC activity is regulated *via* glucocorticoid, rather than mineralocorticoid, receptors (37). AngII reportedly increases both α-ENaC mRNA and protein expression, while there was no detectible change on β- and γ-ENaC mRNA expression and furthermore a decrease in β- and γ-ENaC protein expression (47). AT1 antagonists abolish AngII-induced changes in ENaC expression, suggesting that exogenous AngII altered ENaC expression *via* AT1-dependent mechanism (47).

Regulation of ENaC in the lung also plays an important role in ion transport disorders such as CF, a disease caused by a mutation in CFTR (40). CF patients often have dehydrated mucus and recurrent pulmonary infections throughout their lives (40). The relationship between CFTR and ENaC is still under debate (40). The observation that CF airway cells exhibit increased amiloride-sensitive I_{sc} provided initial evidence for a functional and perhaps physical interaction

between CFTR and ENaC (18). When expressed in *Xenopus* oocytes, the open probability of ENaC is less when CFTR is co-expressed (96). Furthermore, β-ENaC-overexpressing mice show a 'CF-like' phenotype (140). However, CFTR overexpression does not rescue the CF lung phenotype in this mouse model (77, 140). In a porcine CFTR knock-out model, loss of CFTR-mediated anion secretion did not cause Na^+ hyperabsorption (171). In summary, the regulation of ENaC in CF disease is still unclear and requires more studies.

Regulation of ENaC in the vas deferens

Epithelia lining the vas deferens secrete and absorb electrolytes and fluids to modulate the luminal environment, which is critical for sperm function. Amiloride-sensitive Na^+ transport has been identified in vas deferens epithelia derived from humans (35), sheep (12) and pigs (176). Corticosteroid treatment increases amiloride-sensitive I_{sc} in human and pig vas deferens epithelia, which indicates that the steroid hormone induces the expression or activity of ENaC (35, 176). In a recent report from this laboratory, dexamethasone increased amiloride-sensitive I_{sc} in vas deferens epithelia that were derived from newborn pigs that lacked functional CFTR ($CFTR^{-/-}$ and $CFTR^{\Delta F508/\Delta F508}$)(178). These studies provide evidence that ENaC is present in vas deferens and likely plays a role in reproductive success.

Regulation of ENaC in other organs

In colon, ENaC is expressed abundantly and responds to both aldosterone and glucocorticoid stimulation (195). Corticosterone, which is the main glucocorticoid in rats and mice, reportedly regulate Na^+ transport in isolated rat distal colon (76). High concentrations of the mineralocorticoid receptor antagonist, mespirenone, blocked the effect of both aldosterone and glucocorticoids on amiloride-sensitive I_{sc} (76). Another mineralocorticoid receptor antagonist, spironolactone, when combined with a glucocorticoid receptor agonist, RU-28362, increased amiloride-sensitive I_{sc}, but alone has no effect. Thus, both mineralocorticoid and glucocorticoid receptors can be activated to induce electrogenic Na^+ absorption in rat distal colon (76). Colonic ENaC-mediated Na^+ transport is enhanced in a Liddle's syndrome mouse model and also is more sensitive to aldosterone stimulation (11). Aldosterone increases only β- and γ-ENaC mRNA expression in colon but not α-ENaC, suggesting the action of aldosterone on ENaC subunit expression is tissue-specific (11).

In salivary glands, mRNAs and proteins of all three ENaC subunits were detected in mucous tubule and striated ducts in rat (51). *In vitro* studies with an immortalized rat salivary epithelial cell line shows that both glucocorticoids and mineralocorticoids increase amiloride-sensitive I_{sc} and both increase only α-ENaC expression. The presence of a glucocorticoid receptor antagonist blocks both glucocorticoid- and mineralocorticoid-induced effects on ENaC activity. Spironolactone was without effect, suggesting that the effect was mediated exclusively by glucocorticoid receptors (244). Similarly, amiloride-sensitive I_{sc} was detected in mouse mandibular salivary duct cells although experiments to determine regulatory pathways were not conducted (48).

Na^+ transport was first detected in amphibian skin (119). After it was reported that aldosterone stimulated Na^+ transport across toad urinary bladder (201), a similar stimulatory effect on amphibian skin was reported (243). ENaC also has been detected in rat and human skin (191, 256). In keratinocytes, ENaC may play a role in wound healing (256). Several reports indicate upregulation of α- and β-ENaC in human keratinocytes during differentiation, suggesting that ENaC may play a role in epidermal development (24, 166).

ENaC likely plays a significant role in the sensation of taste, hearing, sight, and balance. Three ENaC subunits have been detected in taste cells of the tongue (104, 127, 128), Reissner's membrane of cochlea (43, 110), semicircular canal duct (179), non-sensory cells of the extramacular epithelium of the saccule (109) and retinal photoreceptors (71). ENaC was suggested to have roles in sensing both 'salty' and 'sour' tastes (126-128). Alpha- β- and γ-ENaC mRNA and can be protein have been detected in rat tongue taste cells of the fungiform papillae, where they are regulated by aldosterone (121, 126). However, the function and regulation of ENaC in human taste cells remain unclear (127).

The luminal fluid, endolymph, of inner ear is a K^+-rich fluid that has very low Na^+ concentration (110). Therefore, ENaC channels were suggested to maintain the low Na^+ concentration in endolymph. Indeed, both mRNA and protein for three ENaC subunits were detected in multiple epithelia within the rat cochlea (43). Glucocorticoids increase amiloride-sensitive I_{sc} across structures of the ear including saccule extramacular epithelia (109), semicircular canal duct epithelia (179), and Reissner's membrane, an effect that can be blocked by mifepristone (108). However, the role of ENaC-mediated Na^+ transport during development of inner ear remains unclear (110).

This dissertation focuses on the mechanisms of Na^+ transport across epithelial cells derived from human, bovine and caprine mammary gland. Chapter 2 reports the novel observation that Ctx, a toxin secreted by *Vibrio cholera,* elevates Na^+ absorption across MCF10A human mammary epithelial cells, by increasing the abundance of ENaC in the apical membrane. The underlying mechanism is independent of cAMP/PKA pathway, but includes an increase in the phosphorylation of Nedd4-2. Ctx increases monoubiquitination of ENaC, which likely results in an increase in apical membrane expression. Chapter 3 reports on the outcome of initial studies in which mammary epithelial cells were isolated from bovine and caprine mammary gland and grown on permeable supports in order to establish a protocol for primary isolation, propagation and expansion of mammary epithelia. Electrically tight monolayers were formed by these cultures and electrophysiological studies were conducted with a modified Ussing-style flux chamber. Na^+ transport in response to corticosteroid is examined. Results presented in both Chapter 2 and Chapter 3 demonstrate that glucocorticoids induce or enhance the expression of amiloride-sensitive Na^+ transport across mammary epithelium.

Chapter 2 - Cholera Toxin Enhances Na^+ Absorption across MCF10A Human Mammary Epithelia

Information in this chapter was published by the American Physiology Society

Wang Q and Schultz BD.

Cholera Toxin Enhances Na^+ Absorption across MCF10A Human Mammary Epithelia (250) .

Am J Physiol Cell Physiol.

Published, 1 March 2014.

ePub ahead of print:

http://ajpcell.physiology.org/content/306/5/C471

Abstract

Cellular mechanisms to account for the low Na^+ concentration in human milk are poorly defined. MCF10A cells, which were derived from human mammary epithelium and grown on permeable supports, exhibit amiloride- and benzamil-sensitive short circuit current (I_{sc}; a sensitive indicator of net ion transport), suggesting activity of the epithelial Na^+ channel, ENaC. When cultured in the presence of cholera toxin (Ctx), MCF10A cells exhibit greater amiloride sensitive I_{sc} at all time points tested (2 h to 7 days), an effect that is not reduced with Ctx washout for 12 h. Amiloride sensitive I_{sc} remains elevated by Ctx in the presence of inhibitors for PKA (H-89, Rp-cAMP), PI3K (LY294002) and protein trafficking (brefeldin A). Additionally, the Ctx B subunit, alone, does not replicate these effects. RT-PCR and Western blot analyses indicate no significant increase in either the mRNA or protein expression for α, β, or, γ-ENaC subunits. Ctx increases the abundance of both β- and γ-ENaC in the apical membrane. Additionally, Ctx increases both phosphorylated and nonphosphorylated Nedd4-2 expression. These results demonstrate that human mammary epithelia express ENaC, which can account for the low Na^+ concentration in milk. Importantly, the results suggest that Ctx increases the expression, but reduces the activity of the E3 ubiquitin ligase, Nedd4-2, which would tend to reduce the ENaC retrieval and increase steady-state membrane residency. The results reveal a novel mechanism in human mammary gland epithelia by which Ctx regulates ENaC-mediated Na^+ transport, which may have inferences for epithelial ion transport regulation in other tissues throughout the body.

Keywords: short circuit current I_{sc}; cholera toxin; amiloride; epithelial Na^+ channel; ENaC; mammary gland

Introduction

Milk is secreted by the mammary epithelia of all mammals, but the relative proportions of fats, proteins, carbohydrates and minerals varies widely across species (132). Like other constituents, the concentration of Na^+ varies widely across species, but is lower than plasma in all cases (202). The lowest milk Na^+ concentration is reported for humans, only 5-10 milliequivalents per liter (mEq/l) (159, 160, 202), compared with 136-145 mEq/l in plasma (202). Cl^-, PO_4^{3-} and glucose concentrations in milk are reported to have a positive correlation with Na^+ concentration, whereas, lactose and Ca^{2+} concentrations have negative correlations

(160). However, the mechanisms that control ion transport across mammary epithelium and contribute the low Na^+ concentration in milk across all species and explicitly the very low Na^+ concentration in human milk are not fully understood. Recent reports describe murine (15, 20, 42) and bovine (181, 182, 197) mammary epithelial models to study active ion transport, especially Na^+ transport via the epithelial Na^+ channel (ENaC) in the apical membrane. It has been reported that three ENaC subunits, α, β, and γ, are present in human and mouse mammary gland epithelium (20). Steroid hormones were reported to enhance ENaC expression in human, mouse and bovine mammary epithelia, which could account for Na^+ movement during lactation and oncogenesis (20, 182). Previous reports from this laboratory detail results from a bovine mammary cell line, BME-UV cells, that developed an electrically tight monolayer when cultured on permeable supports. Amiloride sensitive I_{sc} was induced by natural and synthetic corticosteroids (181, 182, 197). Moreover, results from this bovine mammary epithelial model suggest that luminal Na^+ concentration is an important regulator for tight junction integrity (181). Typically, a leaky epithelial barrier is observed *in vivo* before parturition (162). At the onset of lactation, however, the epithelial layer lining the mammary gland becomes relatively impermeable to small solutes such as monovalent ions, sugars and small carbohydrates and substantial concentration gradients for these solutes are generated (162). If the mammary gland develops mastitis, however, the mammary epithelial barrier becomes leaky. Increased Na^+ and Cl^- concentrations are reported in mastitic milk and increased milk electrical conductivity, indicating elevated electrolyte levels, has been used as a preclinical sign of mastitis (67, 130). There is an ongoing question, however, whether mastitis compromises the epithelial barrier to induce an increase in milk electrolytes via mixing with interstitial fluids or whether mastitis induces a decrease in Na^+ absorption and a resultant increase in milk electrolyte concentration, which then causes the epithelia barrier to break down (112, 181, 197).

MCF10A cells, which were derived from non-neoplastic human mammary tissue (225), have been used to study mammary function and regulation (20). In one case, it was reported that MCF10A cells failed to form tight junctions (59). In contrast, another study showed that MCF10A cells not only formed tight junctions, but that an electrically tight monolayer developed that could be used to assess ion transport and responses to agonists (237). In examining these reports further, it was determined that one distinct difference in the culturing systems was the presence or absence of cholera toxin (Ctx) in the growth medium. The use of Ctx in mammary

cell culture can be traced back to 1979 (240). Ctx is widely known to interact with intestinal epithelial cells to increase cytosolic cAMP and ultimately to increase anion secretion (199, 200). Evidence suggests that Ctx also increases cAMP generation in mammary epithelia (172). However, there is no extant report indicating that Ctx has direct effects on ion transport across mammary epithelium and only occasionally has it been suggested that Ctx might have direct effects on epithelial barrier integrity or on cation transport (158, 172, 225). One study reported that Ctx increased cAMP in MCF10A cells, which affected acini lumen formation in a three dimensional culture system (158). This result suggests an increase in anion secretion. Whether there was a Ctx-induced change in either barrier integrity, anion or cation transport, however, was not determined.

In the present study, MCF10A cells were cultured in the presence or absence of Ctx, initially, to determine its effect on barrier formation. Regardless of whether Ctx was present, electrically tight epithelial monolayers were observed and acute changes in net ion transport could be induced. Surprisingly, results from initial experiments suggested that Ctx might promote enhanced levels of Na^+ absorption. Thus, the primary goals for this study were to describe the effects of Ctx on Na^+ absorption across cultured mammary epithelial cells. The outcomes suggest that Ctx builds on corticosteroid-induced ENaC expression to enhance the rate of Na^+ absorption by increasing the amount of ENaC that is resident in the apical membrane.

Methods

Cell culture

The MCF10A cell line, which was derived from non-neoplastic human mammary tissue, was obtained from Dr. Nelson Horseman (University of Cincinnati, Cincinnati, OH) and used throughout this study. Unless indicated otherwise, chemicals were obtained from Sigma-Aldrich (St. Louis, MO). Two media were used for cell culture. Typical medium contained DMEM/F-12 (Cellgro, Herndon, VA), horse serum (5%; Gibco, Grand Island, NY), insulin-transferrin-Na^+ selenite (10 μg/ml), penicillin and streptomycin (1%; Gibco), L-Glutamine (2 mM), hydrocortisone (cortisol, 0.5 μg/ml), and epidermal growth factor (20 ng/ml; RD Systems, Minneapolis, MN). Ctx medium contained typical medium with 100 ng/ml Ctx. Continuous cultures of MCF10A cells were maintained on solid supports (25cm^2 plastic culture flasks; Corning, Lowell, MA) using typical medium. After reaching 80-90% confluence, cells were

detached using trypsin in phosphate buffered saline (PBS) with disodium EDTA (2.4 mM; Gibco) for 7-10 min, suspended in culture medium, and seeded on permeable supports (Snapwell or Transwell; 1.13 cm^2 or 4.67 cm^2, respectively; Corning). Cells were maintained at 37°C in a humidified atmosphere containing 5% CO_2. Media were refreshed every day until experimentation, which typically was 14 days post seeding. In some experiments, MCF10A cells were also cultured in treatment media, such as LY294002 (50 μM), H-89 (10 μM), brefeldin A (10 μg/ml), isoproterenol (100 nM), or R_p-cAMP (100 μM) in typical or Ctx medium, or Ctx B subunit (67 ng/ml) in typical medium. The duration of treatment exposure indicates the last hours or days prior to the experiment during which treatment exposure occurred. For example, when cells were exposed in Ctx for 4 days or 7 days, cells were cultured in medium containing Ctx on days 11-14 or 8-14, respectively. All cell culture-based treatments were administered symmetrically in the mucosal and serosal chambers.

Electrical measurements

A modified Ussing-style system was used to measure active net transepithelial ion transport and electrical resistance as described in detail previously (181, 182, 197). Briefly, the cultured monolayer on its permeable support was inserted to separate the two halves of an acrylic chamber (DCV9; Navicyte, San Diego, CA). The mucosal and serosal hemichambers were filled with equal volumes of Ringer solution (composition in mM; 120 NaCl, 25 $NaHCO_3$, 3.33 KH_2PO_4, 0.83 K_2HPO_4, 1.2 $CaCl_2$, 1.2 $MgCl_2$). Each hemichamber was mixed continually by an airlift system (5% CO_2 with 95% O_2) that also maintained a stable pH (7.4). The system was maintained at 37°C. Custom-made voltage sensing and current injecting electrodes were placed in each chamber and connected to a voltage clamp (model 558C; University of Iowa, Department of Bioengineering, Iowa City, IA) to determine open circuit voltage, to clamp the voltage and to measure short circuit current (I_{sc}). Monolayers were clamped to zero mV with the exception of an intermittent 1 mV bipolar pulse to allow for the determination of transepithelial electrical resistance (R_{te}). Voltage and current measurements were acquired digitally at 1 Hz (MP100A-CE interface and Aqknowledge software, ver. 3.2.6; BIOPAC Systems, Santa Barbara, CA) throughout all experiments. Ion transport modulators were added as 1000x stock solutions to achieve the reported working concentrations either to the mucosal hemichamber (amiloride), to

the serosal hemichamber (bumetanide), or symmetrically (forskolin, Calbiochem, Gibbstown, NJ; glibenclamide).

Semi-Quantitative RT-PCR

To determine the relative copy numbers of mRNA coding for α, β, and γ-ENaC, RNA was isolated from MCF10A monolayers after Ussing chamber experiments were completed by using Micro RNeasy RNA isolation kits (Qiagen Germantown, MD). RNA quality was verified by microfluidics (Nano Labchip, Agilent Technologies, Palo Alto, CA) and concentration was determined spectrophotometrically (Nanodrop Technologies, Wilmington, DE). The sequences of primers to detect mRNA coding for α, β, and γ ENaC were as reported previously (20) with expected products of 159, 84, and 174 bases, respectively. Primers to detect 18s rRNA, which was used as an internal standard, also were as reported previously (253). RT and PCR protocols were performed using One-step RT-PCR kits (Qiagen) and an automated thermocycler (Smart Cycler, Cepeid, Sunnyvale, CA). The PCR products were resolved by electrophoresis on a 1.5% agarose gel to verify a single band of expected mobility.

Western blot analysis

Cell lysates were made from MCF10A monolayers grown on permeable supports in the absence or presence of Ctx by using RIPA lysis buffer (1% Surfact-Amps NP-40, Pierce, Rockford, IL; 0.01% SDS in PBS) including protease inhibitors (cOmplete, Mini; Protease Inhibitor Cocktail, Roche Diagnostics, Indianapolis, Indiana). Monolayers were dislodged by scraping and cells were broken apart by repeated aspiration through a 20-gauge needle. Suspensions were placed on ice for 15 minutes followed by centrifugation at 14,000 rpm for 15 min at 4°C. Supernatants were transferred to fresh tubes and protein concentrations were determined (Micro BCA protein assay kit, Pierce). Proteins (20 μg) were loaded in each well of a polyacrylamide 4%–20% gradient precast gel (Thermo Scientific, Waltham, MA) for electrophoresis in a Tris-HEPES-SDS running buffer (12.1 g/l Tris-base, 23.8 g/l HEPES, 1 g/l SDS). Proteins were resolved at 150 V for one hour or when clearly resolved protein standards (Bio-Rad Laboratories, Hercules, CA) could be observed. Proteins were transferred to a polyvinylidene fluoride microporous membrane (Millipore, Billerica, MA) in buffer (10% methanol, 25 mM Tris base and 192 mM glycine) at 4°C using 55 V for 4 hours. Membranes were blocked with 5% blotting grade milk (Blotto nonfat dry milk, Santa Cruz Biotechnology,

Santa Cruz, CA) in PBS that included 0.1% Tween 20 at room temperature for 4 hours or at 4°C overnight. Membranes were probed with anti-α-ENaC (4 μg/ml, Thermo Scientific cat #PA1-920A, a rabbit polyclonal antibody raised against amino acids 20-42 of rat α-ENaC), anti-β-ENaC (6 μg/ml, Santa Cruz #SC-25354, a mouse monoclonal antibody raised against amino acids 271-460 of human β-ENaC), or anti-γ-ENaC (1 μg/ml, Thermo Scientific #PA1-922, a rabbit polyclonal antibody raised against amino acids 630-649 of rat γ-ENaC) antibodies. Secondary antibodies were goat-anti-rabbit (Thermo Scientific #31460) and goat-anti-mouse (both used at 40 ng/ml; Thermo Scientific #31430). PBS with Tween 20 was used as the washing buffer. Immunized membranes were visualized after being enhanced by chemiluminescence with West Femto Maximum Sensitivity substrate (Thermo Scientific). Nedd4-2 was detected (1:500 dilution, Cell Signaling #4013, a rabbit polyclonal antibody raised against residues surrounding Glu 271 of human Nedd4-2; secondary goat-anti-rabbit at 40 ng/ml, Thermo Scientific #31460) using similar protocols. Occludin (0.5 μg/ml, Invitrogen, Camarillo, CA, #71-1500, a rabbit polyclonal antibody), β-actin (1:1000 dilution, Sigma #A2066, rabbit polyclonal antibody) and Na/K-ATPase α1 subunit (2 μg/ml, Novus Biologicals, Littleton, CO, #NB300-146, a mouse monoclonal antibody) were used in various experiments, as indicated, as internal standards for sample loading.

Cell surface biotinylation

Surface expression on MCF10A cells was assessed using biotinylation followed by Western blotting. MCF10A cells were cultured on permeable supports and exposed to vehicle, Ctx (100 ng/ml) for 24 hours, or Ctx for 2 hours before conducting the biotinylation assay (EZ-link Sulfo-NHS-LC-Biotin and NeutrAvidin Agarose resin, Thermo Scientific) (74). The Ringer solution was adjusted to 300 mosmol/kgH_2O with D-mannitol and was used to wash cells and to dissolve biotin. MCF10A cells were incubated with either mucosal or serosal biotin (500 μg/ml) in Ringer solution at 4°C for 30 minutes. After biotin incubation, cells was washed 5x with glycine (50 mM) in Ringer solution. Cells were lysed in RIPA buffer with protease inhibitors (cOmplete Mini, Roche Diagnostics). Cell lysates were placed on ice for 15 minutes, disrupted by aspiration through a 20-gauge needle and centrifuged at 14,000 rpm for 15 minutes at 4°C. Supernatant was collected and diluted with lysis buffer to achieve equal protein concentrations in all samples. Biotin-labeled proteins were separated using agarose resin with spin columns (Thermo

Scientific) and suspended in Laemmli sample buffer containing DTT (50 mM) prior to electrophoretic resolution as described above.

Immunoprecipitation of ubiquitin

Whole cell lysates (WCL) were derived from MCF10A monolayers as described above. WCL were incubated with protein A/G PLUS-Agarose immunoprecipitation reagent (sc-2003, Santa Cruz) for 1 hour at 4°C to remove proteins that bind to agarose nonspecifically. These samples were centrifuged at 2,500 rpm for 5 min at 4°C and the supernatant was collected. Supernatant protein concentration was determined by the BCA protein assay kit and all samples were adjusted with RIPA buffer to achieve equal concentrations. Equal volumes of protein samples were incubated with anti-ubiquitin antibody (concentration ratio: antibody:protein = 1:1000; Goat polyclonal ubiquitin antibody (N-19), SC-6085, lot # C2312, Santa Cruz) overnight at 4°C. Portions of the WCL are as indicated in the respective figures. The following day, protein A/G PLUS-Agarose was added to each protein-antibody mix and allowed to incubate for 2 hours at 4°C. Ubiquitinated proteins were separated using spin columns with paper filters (Thermo Scientific) and suspended in Laemmli sample buffer containing DTT (50 mM) prior to electrophoretic resolution as described above.

Data Analysis

Statistical analysis was conducted using SigmaPlot (ver. 10.0, Systat Software, Inc. Chicago, IL) and Excel (ver. 14.0.6129.5000, Microsoft, Redmond, WA). Students t-test for unpaired or paired data and ANOVA were used, as appropriate. Dunnett's test was used for post-hoc analysis, when required. Summarized data are presented as mean ± standard error of the mean. Treatment effects were considered significant when the probability of a type I error was ≤0.05.

Results

Ctx elevates amiloride- and benzamil-sensitive I_{sc} across MCF10A cells

MCF10A cells were cultured on permeable supports in the absence or presence of Ctx and mounted in modified Ussing-style flux chambers to test for electrogenic ion transport. Results presented in Figure 2.1A show that these cells formed an electrically tight epithelial barrier that exhibited a positive I_{sc} (4.89 or 11.54 μA cm^{-2}, cultured for the final 24 h in the absence or

presence of Ctx, respectively) indicative of net cation absorption or anion secretion. Using Ohms law, R_{te} across each monolayer was calculated based on the current associated with a periodic 1 mV bipolar pulse. MCF10A cells cultured in typical medium exhibited greater R_{te} (2808 ± 212 Ω•cm^2) when compared to cells exposed to Ctx for 1 day (731 ± 77 Ω•cm^2, n = 4, paired). These data demonstrate that MCF10A cells generate a tight epithelial barrier in both culture conditions, though Ctx is associated with a greater conductivity. Additionally, cells cultured in the presence of Ctx exhibited greater basal I_{sc} (12.04 ± 0.38 μA•cm^{-2}) when compared to their untreated counterparts (4.74 ± 0.21 μA•cm^{-2}, n = 4, paired). Amiloride (10 μM), which blocks ENaC, was added to the apical medium during the recording. Outcomes presented in Figure 2.1A suggest that monolayers exposed to Ctx have greater amiloride-sensitive I_{sc}, indicating enhanced Na^+ absorption. Forskolin and bumetanide cause only modest changes in I_{sc}. There was no detectable effect of Ctx on the response to either forskolin or bumetanide.

Experiments were conducted to determine the time course over which the effects of Ctx occur. MCF10A cells were exposed to Ctx for periods ranging from 2 hours to 7 days. The magnitude of amiloride sensitive current for cells cultured in typical medium was 1.53 ± 0.11 μA•cm^{-2}, which was less than that observed for any duration of Ctx exposure (Figure 2.1B). Amiloride-sensitive I_{sc} was elevated significantly at the earliest time point tested (2 h). The Ctx-induced increment appeared to plateau at 4 hours and remained at or above this level for at least 2 days of exposure, after which the amiloride-sensitive component declined.

Both basal and Ctx-associated I_{sc} were reduced, concentration-dependently, by amiloride and benzamil. Figure 2.2A includes typical tracings in which MCF10A monolayers were cultured with or without Ctx for 1 day, mounted in Ussing chambers and exposed to escalating concentrations of amiloride or benzamil. The magnitude of amiloride and benzamil sensitive current change for each concentration was expressed in proportion to the maximal inhibition and a Michaelis-Menten function was fitted to each data set (Figure 2.2B). The apparent K_ds (K_{app}) for amiloride were 0.41 ± 0.05 μM and 0.36 ± 0.11 μM in the presence and absence of Ctx, respectively. Similarly, the K_{app}s for benzamil were 0.03 ± 0.01 μM and 0.01 ± 0.01 μM in the same respective conditions. Thus, amiloride and benzamil exhibited concentration-dependent inhibition profiles that are consistent with the block of ENaC channels; benzamil was 20 times more potent than amiloride (113, 239). Additionally, 5-N-ethyl-N-isopropyl-amiloride (EIPA), an amiloride analog that preferentially inhibits the Na^+/H^+ exchanger (NHE) at relatively low

concentrations (e.g., < 10 μM), but affects ENaC only at very high concentrations (i.e., > 100 μM) was used. Even at the highest concentration employed (30 μM), EIPA failed to affect the amiloride-sensitive I_{sc} (data not shown). Taken together, the results suggest that the Ctx-induced amiloride sensitive I_{sc} is ENaC mediated Na^+ transport.

In addition to amiloride, the effects of forskolin, bumetanide and glibenclamide on ion transport across MCF10A monolayers were tested (see Figure 2.1A). Forskolin (2 μM), an activator of adenylyl cyclase elevated I_{sc} modestly in both culture conditions. Bumetanide (20 μM), an inhibitor of $Na^+/K^+/2Cl^-$ cotransporter, and glibenclamide (300 μM; data not shown), a CFTR blocker at this concentration, caused a decline in I_{sc}. Statistical analysis ($n \geq 5$) indicated that there was no detectable difference in the effects of forskolin, bumetanide or glibenclamide between cells cultured in typical medium or in Ctx.

Ctx B subunit fails to mimic effect of holotoxin

Cells were exposed to Ctx B subunit and outcomes were compared with cells exposed to the holotoxin. Typical and summarized data are presented in Figure 2.3. Amiloride-sensitive I_{sc} was significantly greater only in the presence of the holotoxin. Ctx B subunit alone had no detectable effect on amiloride-sensitive I_{sc}. After Ussing experiments were completed, protein was isolated from MCF10A cells and Ctx B subunit immunoreactivity was detected by Western blot in lysates of cells exposed to Ctx or Ctx B subunit. Similar labeling intensity for Ctx B subunit was observed in lysates derived from both treatments (Figure 2.3C). This outcome shows that Ctx B was internalized by the cells to a similar extent in the absence and presence of Ctx A. The results suggest that Ctx A subunit or the holotoxin, the A subunit together with B subunits, is required to regulate ENaC activity in these mammary epithelial cells.

Ctx effects are not reversed by acute wash-out

MCF10A cells were exposed to vehicle or Ctx for 12 hours and either were assessed immediately in Ussing chambers or the medium was replaced with Ctx-free medium and assays were conducted 12 hours later (Figure 2.4). All monolayers that were exposed to Ctx exhibited greater spontaneous and amiloride-sensitive I_{sc}. The magnitude of this I_{sc} was not diminished by the 12 hour washout period. Results presented in Figure 1 show a slow onset for Ctx effects that approach or achieve maximal I_{sc} only with greater than two hours of exposure. Figure 2.4

demonstrates that the onset for the reversal of this effect requires greater than 12 hours as no detectable reversal was observed at this time.

Forskolin and isoproterenol do not mimic the effects of Ctx on amiloride-sensitive I_{sc}

Ctx is best known to elevate intracellular cAMP in intestinal epithelial cells by activating adenylyl cyclase and ultimately causing massive secretory diarrhea. Thus, other treatments that are thought to elevate cytosolic cAMP were evaluated. MCF10A cells were cultured in the presence or absence of Ctx or forskolin (300 nM) for 1 or 2 days prior to assessment. Amiloride-sensitive I_{sc} was significantly greater only when cells were cultured in the presence of Ctx; forskolin induced no significant difference (Figure 2.5). Furthermore, typical results show that acute exposures to either forskolin (2 μM) or Ctx (100 ng/ml) has little effect on amiloride-sensitive I_{sc}. Similarly, isoproterenol, a β-adrenergic receptor agonist, was used to determine whether increasing cAMP following the activation of a G protein-coupled receptor could mimic the effect of Ctx on MCF10A cells (158). Results presented in Figure 2.6 show that MCF10A cells exposed in culture to isoproterenol (100 nM) for 1 day had amiloride-sensitive I_{sc} that was modestly greater, but the magnitude of I_{sc} did not approach the level observed with Ctx.

To test further for a role of cAMP/PKA in the response, cells were concurrently exposed to isoproterenol, Ctx and/or R_p-cAMP, a cAMP antagonist. Results presented in Figure 2.6 show first that R_p-cAMP has no discernible effect on basal I_{sc}, but that the acute effect of isoproterenol was inhibited by greater than 60%, as would be expected. Results presented in Figure 2.6 further suggest that chronic (24 h) exposure to either Ctx or to isoproterenol elevates cAMP to the extent that acute exposure to isoproterenol is virtually without effect. Importantly, concurrent exposure to R_p-cAMP did not abrogate the effect of Ctx on amiloride inhibitable I_{sc}. In a separate set of experiments, the effect of H89 (10 μM), a PKA inhibitor was evaluated. Results presented in Figure 2.6D show that H-89 enhanced basal I_{sc} modestly. More importantly, the increment in amiloride-sensitive I_{sc} that is induced by Ctx was not inhibited by H-89. The results presented in Figures 2.5 and 2.6, when taken together, suggest quite strongly that the Ctx-associated increment in amiloride sensitive I_{sc} likely involves a cellular pathway(s) that is independent of cAMP/PKA.

Ctx elevates amiloride-sensitive I_{sc} only in the presence of cortisol

Amiloride-sensitive I_{sc} was present consistently in MCF10A monolayers and was significantly greater when cells were exposed to Ctx. The results suggest strongly that Ctx enhanced Na^+ transport across MCF10A monolayers by increasing the expression and/or the activity of ENaC. To test these possibilities, MCF10A cells were cultured in the presence or absence of cortisol and/or Ctx. Amiloride-sensitive I_{sc} was detected only when cells were cultured in the presence of the corticosteroid (Figure 2.7); in the absence of cortisol, Ctx was without effect. The outcomes show that Ctx fails to induce amiloride-sensitive I_{sc}. Rather, Ctx potentiates the magnitude of amiloride-sensitive I_{sc} that is induced by cortisol. Consistent with earlier reports (20, 182) on epithelial cell culture in general, cortisol exposure was associated also with enhanced R_{te}, which is shown by the larger I_{sc} deflections associated with the periodic voltage steps in the right panels of Figure 2.7, when cortisol was absent.

Ctx has no effect on ENaC mRNA expression

RNA was isolated following exposure to cortisol and/or Ctx and semi-quantitative RT-PCR was used to detect and quantify α-, β-, and γ-ENaC transcripts. Threshold cycle (CT) value for each ENaC subunit was normalized to the CT for 18s and $^{\Delta\Delta}$CT was used to calculate copy number of transcripts in each condition relative to the basal medium, which contains cortisol. There is little indication that Ctx affected the number of transcripts coding for any ENaC subunit. A modest trend toward greater γ-ENaC mRNA was detected, but the effect did not achieve statistical significance ($P>0.06$). Consistent with previous observations in other mammary systems (182) cortisol is associated with a doubling of mRNA coding for α-ENaC (i.e., a 50% reduction when cortisol is withdrawn) and greater that ten-fold increase in the number of mRNA copies coding for either β- or γ-ENaC (20, 182). Ultimately, the results show that Ctx does not cause a detectable change in ENaC mRNA expression, but that the effect of Ctx on amiloride-sensitive I_{sc} was dependent on the induction of ENaC expression by corticosteroids.

Cholera toxin has no effect on α-, β-, or γ-ENaC immunoreactivity

Experiments were designed to determine whether Ctx could enhance ENaC expression at the protein level independent of an effect on mRNA expression. Three ENaC subunits were examined in lysates that were derived from MCF10A monolayers exposed to Ctx or to the vehicle in the final day of culture. Intensely labeled bands of expected mobility were present in

each of the samples (Figure 2.8). Densitometric analysis showed that there were no detectable differences in band intensities for any of the ENaC subunits when normalized to occludin (65 kDa), Na/K ATPase α1 (95 kDa), or β-actin (42 kDa, not shown) as an internal standard in each lane. The results show that Ctx-enhanced Na^+ transport across MCF10A cells was not elicited by elevating the protein expression of any of the three ENaC subunits, which leaves the possibility that Ctx affects Na^+ transport across MCF10A monolayers by changing ENaC localization or channel gating.

Ctx elevates the abundance of β- and γ-ENaC at the apical cell surface

To evaluate the membrane localization of ENaC subunits, biotinylation assays were conducted in conjunction with western blot analysis. MCF10A monolayers were exposed to Ctx or typical medium followed by biotin labeling for 30 min at 4°C. Western blots revealed β-ENaC and γ-ENaC immunoreactivity in all samples. Importantly, results presented in Figure 2.9 show that both β-ENaC and γ-ENaC on the apical cell surface (AP) were elevated following exposure to Ctx for 2 hours or 1 day. There were no detectable differences in the band densities on total protein expression (whole cell lysates) between vehicle and Ctx treated cells (Veh_WCL vs Ctx2h_WCL vs Ctx1d_WCL). The double bands representing γ-ENaC (Figure 2.9B), which were present in whole cell lysates, are consistent with both the full length and the cleaved form of γ-ENaC. The single band detected with biotinylation at the apical cell surface is consistent with the cleaved form of the protein and it is elevated in Ctx treated cells compared with vehicle. Occludin was used as internal control for loading of protein samples. Although Ctx exposure does not cause a detectable change in the expression of either mRNA coding for any ENaC subunit or of the actual ENaC subunits, these results indicate that Ctx causes a change in ENaC distribution such that there is an increase in the abundance of both β- and γ-ENaC at the apical cell surface.

Effects of Ctx are not blocked by cytosolic pathway inhibitors

Experiments were conducted to test whether Ctx affects ENaC protein trafficking from the endoplasmic reticulum (ER) to the Golgi. Figure 2.10A shows that amiloride-sensitive I_{sc} across MCF10A cells was reduced by brefeldin A, a compound that disrupts cytosolic trafficking. In the presence of brefeldin A (10 mg/ml), amiloride-sensitive I_{sc} was reduced by half, both with and without Ctx exposure. Brefeldin A clearly affects the expression or activity of ENaC at the apical

cell membrane. However, the increment induced by Ctx exposure is not disproportionately affected by the trafficking disruptor. These results suggest that the effect of Ctx on ENaC distribution occurs at a post-Golgi locale.

Phosphatidylinositol-3-kinase (PI3K) is a lipid kinase that can stimulate ENaC activity (16, 174, 185). MCF10A cells were exposed to LY294002 (50 μM), a PI3K inhibitor, in the presence or absence of Ctx. Like brefeldin A, LY294002 caused a reduction in amiloride-sensitive I_{sc} both in the absence and in the presence of Ctx (Figure 2.10B). Regardless of whether LY294002 was present, the effect of Ctx was to increase amiloride sensitive I_{sc} by 5-fold relative to the baseline conditions. While some portion of the activity or expression of ENaC is sensitive to LY294002, this outcome indicates that the effect of Ctx on ENaC is not mediated by the PI3K pathway.

Ctx increases Nedd4-2 expression

Nedd4-2, a cytosolic ubiquitin ligase, can induce ENaC retrieval from the cell membrane and subsequent degradation (25, 100, 183, 266). Western blot analysis was conducted with lysates from MCF10A monolayers that had been exposed to Ctx or vehicle using primary antibodies that label both phosphorylated (inactive) and nonphosphorylated (active) Nedd4-2. Ctx appeared to increase the signal intensity for both the active nonphosphorylated (110 kDa) and the inactive phosphorylated (130 kDa) Nedd4-2 forms (Figure 2.11). Densitometric analysis showed that Ctx exposure was associated with a statistically significant increase in the relative density of the 130 kDa bands following Ctx exposure. This result suggests that Ctx increases Nedd4-2 expression, but more importantly that Ctx exhibits a more obvious effect to increase the amount of the phosphorylated form, which would be expected to reduce the relative activity of Nedd4-2 and thus reduce retrieval of ENaC from the cell membrane.

Ctx increases the mono-ubiquitination of β- and γ-ENaC

To test whether Ctx alters ENaC ubiquitination, immunoprecipitation of ubiquitin was conducted using whole cell lysates from MCF10A monolayers and was followed by Western blot analysis. β- and γ-ENaC subunits were detected by Western blot in the ubiquitin immunoprecipitates (Figure 2.12). Importantly, the results show that the most prominent form of either subunit in the immunoprecipitate is monoubiquitinated. Even with extended exposure times, polyubiquitinated forms of ENaC were not readily detected. It is obvious with the raw data shown and densitometric analysis indicates that Ctx increased β- and γ-ENaC ubiquitination

by ~ 4 fold (4.27 ± 2.01 and 3.60 ± 1.45; n=4; respectively). This result suggests that Ctx increases monoubiquitination of ENaC that may be associated with surface retention (266).

Discussion

This line of investigation demonstrates that epithelial cells derived from the human mammary gland, MCF10A cells, express ENaC and that Ctx elevates Na^+ absorption by increasing the abundance of ENaC in the apical membranes of these epithelial cells. That Ctx regulates Na^+ absorption across human mammary epithelium is a novel observation. The results demonstrate that Ctx-treated MCF10A cells exhibit greater basal ion flux and greater amiloride-sensitive ion transport indicating enhanced Na^+ absorption. However, the outcomes show that the link between Ctx and Na^+ absorption is independent of cAMP and seems not to be affected by brefeldin A. Ctx has no effect on the expression of mRNA coding for α-, β-, or γ-ENaC subunits. Furthermore, there were no detectable effects on protein expression of any of ENaC subunits when assessed by Western blot. Rather, the results show that Ctx changes the distribution of ENaC between cytosolic and apical pools. Ctx increases Nedd4-2 expression and the apparent ratio between the phosphorylated (inactive) and nonphosphorylated (inactive) forms. The greater overall amount of Nedd4-2 and the relatively greater amount of inactive Nedd4-2 may account for the elevated level of monoubiquitinated, but not polyubiquitinated ENaC subunits, which would be expected to reduce protein retrieval from the apical membrane and, subsequently, protein degradation. The underlying mechanism(s), however, remains to be defined further - in addition to reduced retrieval there could be greater insertion or potentially greater recycling of the channels back to the apical membrane. Regardless, the results demonstrate that corticosteroids substantially upregulate the expression of mRNA coding for ENaC subunits and that corticosteroids are required for amiloride-sensitive transport to be detected. The results demonstrate that Ctx enhances Na^+ absorption by elevating the proportion of ENaC in the apical membrane of these mammary epithelial cells.

A working model of human mammary epithelia to account for the low Na^+ concentration that is observed in human milk is depicted in Figure 2.13. In this model, cortisol binds to glucocorticoid receptors and regulates ENaC mRNA expression (182). In mammary epithelia, cortisol increases mRNA coding for the expression of all three ENaC subunits (20, 182), but the cortisol-induced increment differs for each subunit. β- and γ-ENaC mRNA increased more than

10 fold and α-ENaC increased about 2 fold (182). Upon translation, newly synthesized ENaC subunits assemble to form a heterotrimeric channel while processing through the endoplasmic reticulum (219). ENaC exits the endoplasmic reticulum and enters the Golgi apparatus where it can be activated by furin, which cleaves the extracellular loops of α- and γ-ENaC (91, 219). ENaC channels are trafficked to the apical membrane where they allow Na^+ to enter the cell by moving down its electrochemical gradient, which, in conjunction with Na^+/K^+ ATPase at the basolateral membrane, can account for net Na^+ transport from the apical luminal compartment to the interstitial compartment (i.e., net absorption). Nedd4-2 can bind to surface ENaC to promote retrieval via endocytosis (218). All three ENaC subunits contain a PY (PPXY) motif that can interact with Nedd4-2 WW domains (219). Since Nedd4-2 is an E3 ubiquitin ligase, the interaction with Nedd4-2 results typically in ENaC ubiquitination and ultimately to degradation via the proteasome pathway (190). Phosphorylation of Nedd4-2 prevents the interaction with ENaC. In this report, we show that Ctx elevates amiloride-sensitive I_{sc} by increasing the numbers of ENaC channels in the apical membrane and we provide evidence to suggest that the activity of Nedd4-2 is likely reduced by phosphorylation following Ctx exposure.

The structure of Ctx and its pathophysiological effects on intestinal epithelia have been well characterized (193, 199, 200). Ctx is secreted by the gram-negative bacterium *Vibrio cholera* and is responsible for massive secretory diarrhea in cholera disease. The heat labile toxin of *E. coli*, which also causes secretory diarrhea, is virtually identical in both structure and pathological mechanism (193). Ctx belongs in the AB5 toxin structure family, which is defined by one A subunit and 5 B subunits (193, 228). Ctx binds to GM1 by Ctx B subunits and is internalized via lipid rafts or by endocytosis (124). The binding site for Ctx, the ganglioside GM1, is reportedly present in the mammary gland (97). After internalization, as Figure 2.13 shows, the toxin is transported in a retrograde fashion from the apical membrane to the Golgi apparatus and then to the endoplasmic reticulum. Once in the endoplasmic reticulum lumen, the A-subunit becomes dissociated from the B subunits and retro-translocates to the cytosol. In the cytosol, the Ctx A subunit catalyzes the ADP-ribosylation of $G_s\alpha$ to activate the G-protein irreversibly and to increase the cytosolic cAMP level, which activates PKA and ultimately induces Cl^- secretion (124). The well-characterized effects of Ctx are through the cAMP/PKA dependent pathway. Ctx also has effects on A6 cells derived from *Xenopus laevis* distal nephron where it had been reported that Ctx increases the number of ENaC channels in the apical membrane by a cAMP-

dependent mechanism, but without detectable effects on the open probability of the channel (144). In PC-12 cells, Ctx also reportedly stimulates adenylyl cyclase to increase cAMP levels (217). In these cells, Ctx increased lactate production, an indicator of increased metabolic rate and the effect was inhibited by H-89 (217). The current results suggest that Ctx increases phosphorylation of Nedd4-2 (Figure 2.11), which prevents the interaction between Nedd4-2 and surface ENaC, ultimately reducing the rate of internalization. Various pathways can modulate Nedd4-2 phosphorylation, such as glucocorticoid-induced kinase (SGK) and PKA. Indeed, the current results suggest strongly that Ctx increases cAMP accumulation in these cells. However, our reported outcomes suggest that Ctx regulates Na^+ transport via a mechanism that is independent of cAMP/PKA. Inhibition of PKA by H-89 or by R_p-cAMP had no effect on Ctx increased amiloride-sensitive I_{sc}. The underlying mechanism(s) that contribute to Ctx-associated Nedd4-2 phosphorylation remains to be determined.

Numerous studies have focused on Na^+ transport through ENaC in the mammary gland, but this study is the first to demonstrate that Ctx modulates Na^+ transport through ENaC across human mammary epithelium. Four decades ago, and again more recently, a mammary epithelial model based upon *in vivo* observations with goats was proposed in which the apical membrane was freely permeable to cations, but not to anions (132, 204). In this model, cationic composition of milk was set by activity of the Na^+/K^+ ATPase at the basolateral membrane (132). An overwhelming amount of more recent evidence demonstrates that ENaC is present in the apical membranes of mammary epithelial cells, that the expression of ENaC in these membranes is regulated, and it is postulated that ENaC activity contributes to milk composition for a number of species (15, 20, 123, 181). The present study extends observations reported for bovine mammary epithelium, which showed both cation absorption and anion secretion (182, 197). The current results provide strong evidence that ENaC is expressed in MCF10A cells, which are of human origin, and contributes to regulated Na^+ transport.

An important question for this study is to determine whether Ctx increases ENaC activity by targeting the cAMP/PKA pathway. There is no doubt that Ctx can elevate cAMP level in MCF10A cells (158). Indeed, a limited number of our own observations show that Ctx is associated with elevated cAMP generation in MCF10A cells (data not shown). The duration to the effect of Ctx on elevation of amiloride-sensitive I_{sc} is consistent with the expected time course for activation of adenylyl cyclase activity (199, 200) and for the induction of intestinal

anion secretion as we showed previously (165). Thus, studies were designed to test whether forskolin, which activates adenylyl cyclase to increase cytosolic cAMP, can mimic the Ctx-induced effect by activation of the cAMP/PKA pathway. In a recent study, MCF10A cells were cultured in the presence of forskolin and showed increased intracellular cAMP level (237). The current results, however, show that forskolin did not mimic Ctx. Likewise, isoproterenol, a β-adrenergic receptor agonist, failed to mimic the Ctx effect. Both treatments elevated cAMP generation (data not shown) and both substantially reduced an acute effect of isoproterenol on I_{sc} (e.g., see Figure 2.6). To test further whether Ctx induces Na^+ absorption by activating PKA, a small array of selective inhibitors with different mechanisms of actions (H89, R_p-cAMP and KT5720) was employed in conjunction with Ctx. H89 does not reduce Ctx-potentiated amiloride-sensitive I_{sc}. Similarly, R_p-cAMP, a competitive antagonist of the cAMP activation site on PKA, did not inhibit Ctx-induced amiloride-sensitive I_{sc}, but did abolish the acute increase in I_{sc} induced by isoproterenol (156, 249). KT5720 reportedly has a similar mechanism as H89 to inhibit PKA activity (102, 156). In our study, KT5720 did not reduce Ctx-potentiated amiloride-sensitive I_{sc}, but inhibited the acute effect of isoproterenol (data not shown). Together, the results suggest that Ctx-induced Na^+ absorption across MCF10A cells is not dependent on the PKA pathway. Somewhat surprisingly, H-89 increased amiloride-sensitive I_{sc} in cells exposed only to vehicle, which could reflect an increase in channel open probability as has been reported in fetal rat alveolar type II epithelium (145). Furthermore, to verify that H89 is working by inhibiting PKA, PVD9902 cells (36) were exposed to H89 for 24 hours in a parallel experiment and the response to both 8-cpt-cAMP and forskolin was reduced, validating the effectiveness of H89 in the reported assays.

To investigate further the intracellular pathway(s) that Ctx may target, the endoplasmic reticulum associated degradation (ERAD) pathway was evaluated. Ctx and specifically its B chain were shown to increase expression of the ERAD proteins Bip, Derlin-1, and Derlin-2 (49). However, in the present study, Ctx B subunit alone did not mimic the holotoxin effect. Moreover, Western blot analysis showed that Bip expression was not changed (data not shown). Due to the specific process by which Ctx accesses cells, B subunit must bind to the cell membrane receptor in order to facilitate entry of the A subunit. Therefore, an effect of the A subunit alone is unlikely in this cell culture system. The amiloride-sensitive I_{sc} was maximized after 24 h exposure to Ctx and declined after 2 days. Although amiloride-sensitive I_{sc} decreased

with prolonged exposure to Ctx, the I_{sc} remained elevated by Ctx at all time points. The underlying mechanism(s) to account for the decline in amiloride-sensitive current after 4 days exposure to Ctx requires further investigation. The half-life of ENaC on the cell surface is reported to be from a few minutes to 8 h or more, but the functional channel is present for about 3.5 h (169, 260). The current results show greater ENaC residency in the apical membrane, which could reflect increased insertion, decreased retrieval, or increased recycling. Additional studies are required to determine whether Ctx increases half-life of ENaC on the cell membrane, although the results suggest that this is the case. Nedd4-2 is a widely studied E3 ubiquitin-protein ligase and critical for ENaC retrieval from the cell surface and ultimately for protein degradation (189, 218, 221). It has been reported that cAMP can inhibit Nedd4-2 activity by enhancing phosphorylation (221). In this study, we observed that Ctx increases phosphorylation of Nedd4-2, but inhibition of PKA has no effect on amiloride-sensitive I_{sc}. Whether Ctx-associated phosphorylation of Nedd4-2 is due to targeting the cAMP/PKA pathway or other novel mechanisms requires further study. It has been well documented that ubiquitination can regulate ENaC degradation by Nedd4-2-mediated mechanisms (139, 234, 266). There are two types of ubiquitination based on how many ubiquitin moieties attach to lysine residues on substrate proteins, monoubiquitination and polyubiquitination (184, 192). Monoubiquitination was suggested to regulate protein non-degradative activities, such as DNA repair, histone function regulation and gene expression (184, 192). Polyubiquitination appears to target proteins for degradation in the 26S proteasomes complex (88, 192). It had been shown that ENaC degradation can be regulated by mono- and polyubiquitination both in transfected cells (234, 266) and in cells expressing ENaC under native regulation (139). Our data show that β- and γ-ENaC are monoubiquitinated in MCF10A cells and Ctx increases ENaC monoubiquitination. However, we did not detect any polyubiquitinated ENaC in this study. Monoubiquitination of β-ENaC was associated elevated surface β-ENaC expression in HEK 293T cells which were transfected with mutated ubiquitin to prevent formation of polyubiquitin chains (266). Some reports suggest that different types of E3 ubiquitin-protein ligase or E2 ubiquitin conjugating enzyme alone can regulate protein monoubiquitination (184, 192). Our data suggest that Ctx increases ENaC surface expressions and decreases Nedd4-2 activities. It is possible that Ctx elevates endogenous ENaC monoubiquitination by novel mechanisms independent of an effect on Nedd4-2.

This study has implications for the pathology and treatment of mastitis. Mastitis has great impact on both human society and the dairy industry. Approximately 10% of lactating women suffer from mastitis (62). This disease is extremely painful, it influences breast milk quality and volume, and the interruption of normal breastfeeding can weaken social bonding (229). In the dairy industry, mastitis has significant effects on milk production and is the greatest financial burden of any animal disease in U.S. agriculture (209). The pathophysiology remains poorly understood. Elevated milk electrical conductivity and elevated electrolytes have been used to indicate the preclinical stages of mastitis (130). Loss of the mammary epithelial barrier is documented in mastitis (181, 264). There are ongoing questions whether mastitis compromises the epithelia barrier to induce an increase in milk electrolytes or whether mastitis induces a decrease in the activity of Na^+ absorption mechanisms to increase milk electrolytes, which causes the epithelia barrier to break down. Using an *in vitro* system employing bovine mammary epithelial cells, we showed previously that changes in Na^+ concentration on the apical (i.e., milk) side of the cells had rapid and profound impact on the epithelial barrier (181). A reduction in the apical Na^+ concentration led to an increase epithelial electrical resistance, indicating a tight epithelial barrier. Our outcomes suggest that ENaC-mediated Na^+ absorption across mammary epithelium, which is regulated by corticosteroids, can contribute to the generation and maintenance of the epithelial barrier (182). Conversely, the results suggested that a reduction in ENaC activity might contribute to mastitis disease progression. The ultimate goal for this study is to identify key intermediates by which Ctx modulates ENaC-mediated Na^+ absorption. Further elucidation of this novel pathway will identify components of the cellular systems that can be targeted to circumvent or treat this costly disease. If these signaling mechanisms are present in epithelia at other locations throughout the body, one can envision new treatments being developed potentially to target hypertension, congestive heart failure, obstructive pulmonary disease, and other diseases of Na^+ and fluid balance.

In summary, our research suggests that Ctx elevates Na^+ absorption across human mammary epithelia by increasing the abundance of ENaC in the apical membrane. The underlying mechanism is not fully defined, but likely includes phosphorylation of Nedd4-2 and it appears to be independent of the cAMP/PKA pathway. These reported outcomes constitute a novel mechanism for the regulation of net Na^+ transport that will likely have implications for epithelia throughout the body.

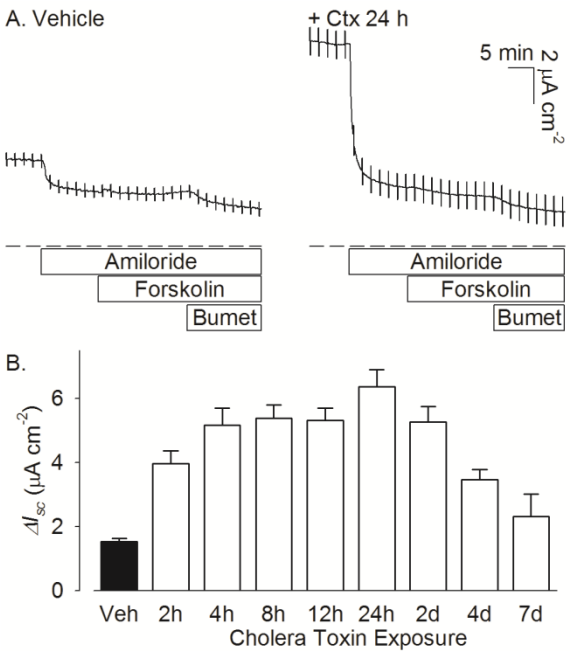

Figure 2.1 Pharmacological evidence for Na^+ absorption and anion secretion by MCF10A cells, a cell line derived from human mammary epithelium.

A. Typical tracings of short circuit current (I_{sc}; net ion transport) across MCF10A cells that were cultured for the final 24 hours in the absence or presence of Ctx. Solid lines represent I_{sc} values over time and the dashed lines represent zero current. Ctx treated monolayers show elevated baseline I_{sc} and greater amiloride sensitive I_{sc}. **B.** Summary of amiloride-sensitive I_{sc} at all time points tested. All cells were assessed 14 days post seeding and were exposed to Ctx for the indicated duration prior to assessment. A significant effect of Ctx was observed at all time points when compared to vehicle. Bars represent 5-11 observations at each duration.

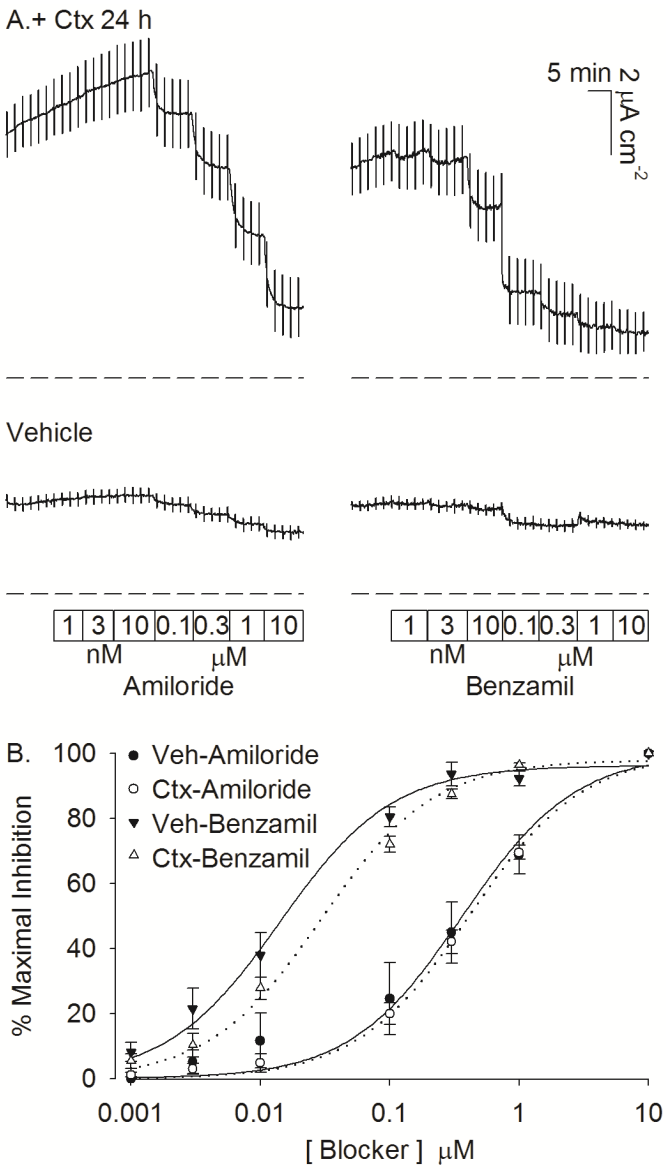

Figure 2.2 Amiloride and benzamil exhibit concentration-dependent inhibition profiles that are consistent with the block of ENaC channels.

A. Typical tracings in which MCF10A monolayers were cultured with or without Ctx and were exposed to escalating concentrations of amiloride or benzamil, as indicated. Results are representative from four observations in each condition. **B.** Summarized data and derived concentration-response curves for the block of Ctx-induced I_{sc} by amiloride and benzamil. Amiloride- or benzamil-sensitive I_{sc} for each concentration was converted to the percentage of maximal inhibited current for that monolayer. Solid lines represent the best fit of a Michaelis-Menten equation to data sets exposed only to vehicle. Dashed lines represent fits for the data from Ctx-treated cells. Data were summarized from four sets of observations in each condition. Parameters of each fit are reported in the text.

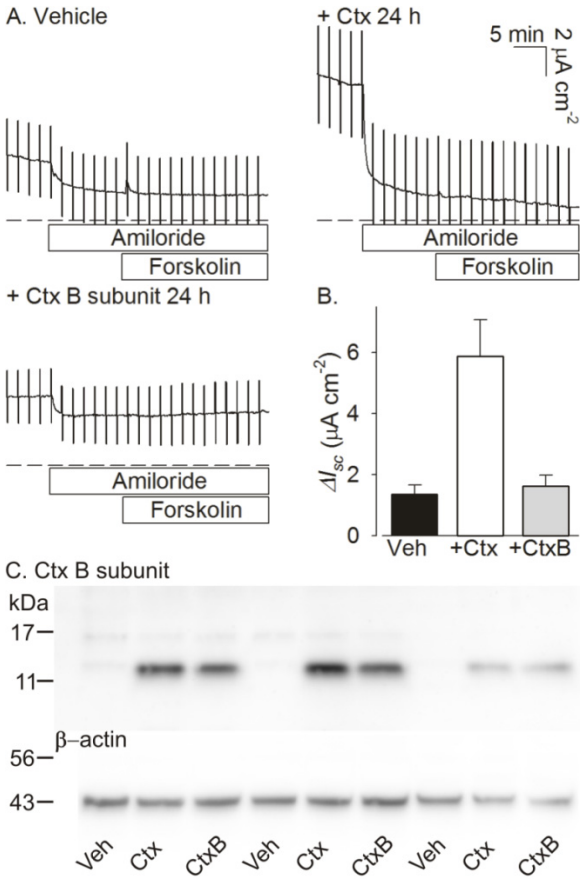

Figure 2.3 Ctx B subunit alone fails to mimic Ctx effect.

A. Typical tracings from MCF10A cells that were cultured in the absence or presence of Ctx or Ctx B subunit for 1 day. **B.** Data summarized from panel A and 4 additional experiments. Amiloride-sensitive I_{sc} was significantly greater only when cells were exposed to the holotoxin. Ctx B subunit, alone, had no detectable effect on amiloride-sensitive I_{sc}. **C.** Western blot shows Ctx B subunit immunoreactivity was detected in samples derived from cells exposed either to Ctx (holotoxin) or to Ctx B subunit alone. Results from three experiments are shown.

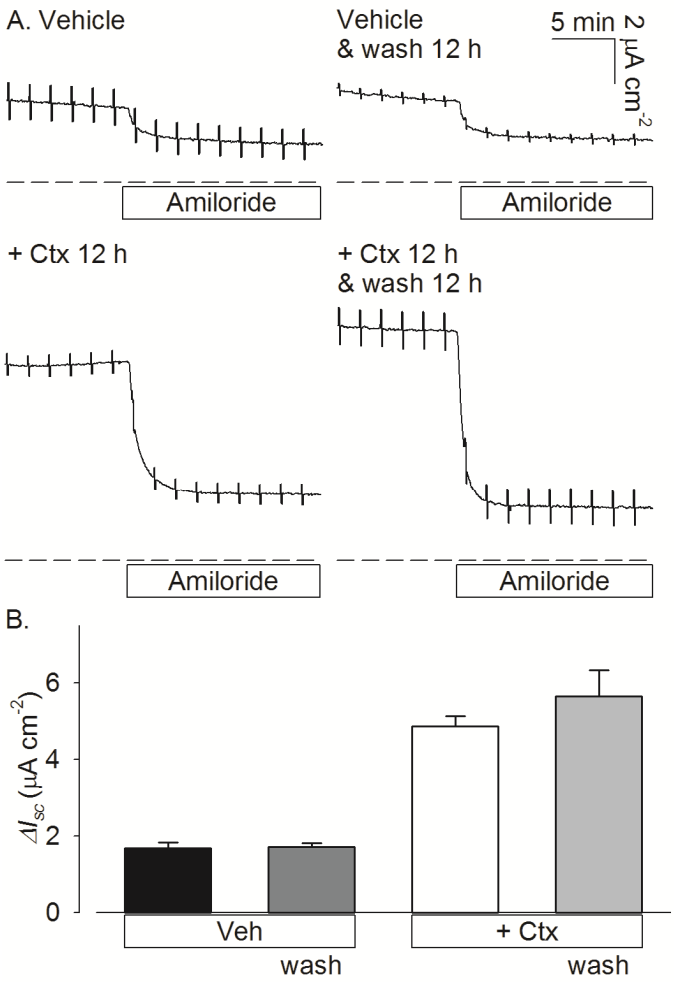

Figure 2.4 Ctx-enhanced amiloride-sensitive I_{sc} is not reduced with washing out.

A. Typical data from MCF10A cells that were exposed to vehicle or Ctx for 12 h prior to assay or followed by culturing for 12 h in typical medium. **B.** Data summarized from panel A and six similar experiments that included each of the four conditions. Ctx-enhanced amiloride-sensitive I_{sc} was not reduced with washing out.

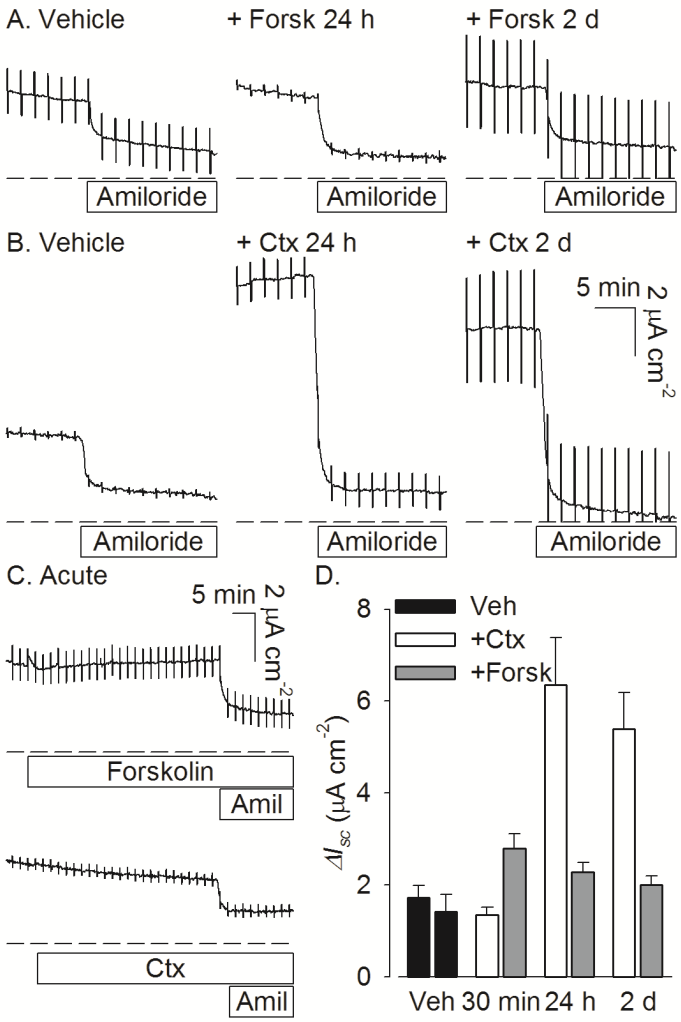

Figure 2.5 Forskolin fails to mimic Ctx effect on amiloride-sensitive I_{sc} across MCF10A cells.

A. MCF10A cells were cultured in the absence or presence of forskolin for 24 h or 2 days. Typical results showing that, in paired monolayers, there was no increment in baseline or amiloride (Amil)-sensitive I_{sc} associated with forskolin exposure. **B.** Typical results showing a clear and sustained increment in basal and amiloride-sensitive I_{sc} was associated with Ctx exposure. **C.** Typical results showing that acute (30 min) exposure to either forskolin or Ctx was without detectable effect. **D.** Data are summarized from 4 experiments in all conditions.

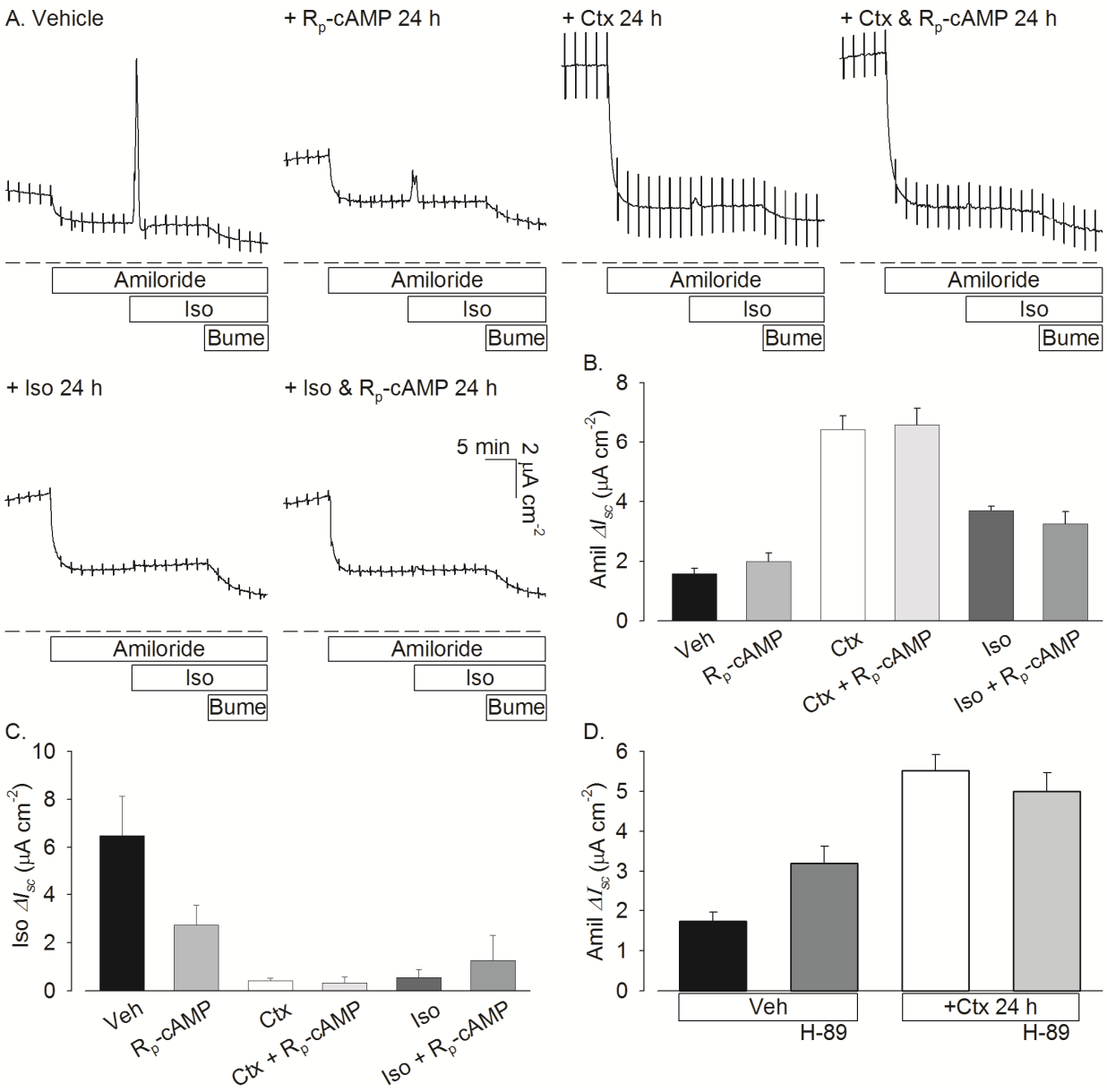

Figure 2.6 Isoproterenol fails to mimic and R_p-cAMP and H-89 fails to block the Ctx effect.

A. Typical outcomes when MCF10A cells were cultured in the presence or absence of Ctx or isoproterenol (Iso; 100 nM) in combination with R_p-cAMP (100 µM) for 24 h. Cells were exposed acutely to amiloride and isoproterenol (1 µM) as indicated. **B.** Data summarized from 8 experiments showing that amiloride-sensitive I_{sc} was significantly greater only when cells were cultured in the presence of Ctx. **C.** Rp-cAMP did not decrease Ctx induced amiloride-sensitive I_{sc}, but abolished the acute isoproterenol-induced current. **D.** MCF10A cells were cultured in the absence or presence of Ctx and/or H-89 (10 µM), a protein kinase A (PKA) inhibitor for 24 hours prior to assessment in Ussing chambers. The effect of Ctx on I_{sc} was not inhibited significantly by H-89. Data are summarized from 7 paired observations.

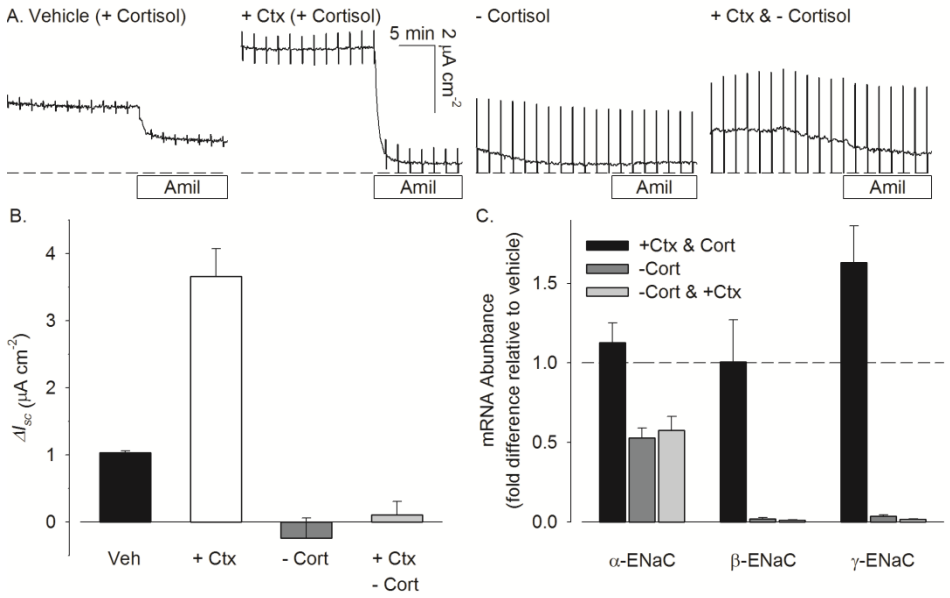

Figure 2.7 Ctx elevats amiloride-sensitive I_{sc} only in the presence of cortisol and has no effect on mRNA expression of ENaC subunits in MCF10A cells.

A. Typical tracings from MCF10A cells that were cultured in the absence or presence of cortisol and/or Ctx for one day as indicated. Amiloride-sensitive I_{sc} was detected only in cells that had been exposed to the corticosteroid and was enhanced by Ctx exposure. **B.** Results showing the effect of amiloride are summarized from panel A and five similar experiments. **C.** RNA was isolated in each culture condition. Semi-quantitative RT-PCR shows that mRNA expressions for α-, β-, or γ-ENaC subunits are detectable in all cells and exhibit cortisol-induced expression. Threshold cycle (CT) value for each ENaC subunit was normalized to 18s and the $^{\Delta\Delta}$CT method was used to determine mRNA expression level relative to cells cultured in typical cortisol-containing medium. Withdrawal of cortisol was associated with significant reduction in mRNA coding for all ENaC subunits. The effect of Ctx was not statistically significant for any ENaC subunit. Data are summarized from four experiments.

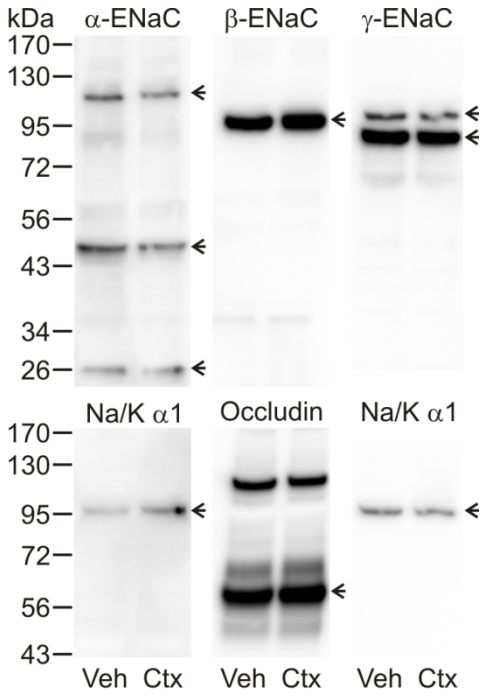

Figure 2.8 Ctx has no effect on α-, β-, or γ -ENaC expression.

Representative western blot of MCF10A cells that were exposed to Ctx or vehicle for 24 hours. Western blot analysis of whole cell lysates was conducted using primary antibodies raised against human α-, β-, or γ-ENaC, as indicated. Membranes were subsequently stripped and reprobed with antibodies to Na/K ATPase α1 or occludin, as indicated, to verify equal protein loading. Arrows indicate bands of expected mobility. Results are representative from at least four experiments for each target protein.

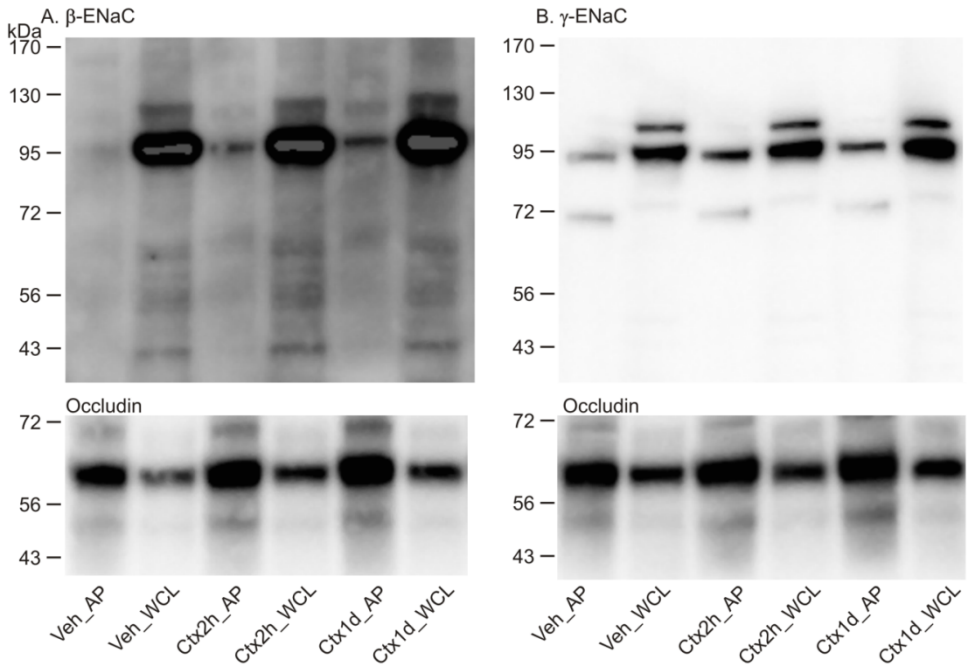

Figure 2.9 Ctx elevats the abundance of β- and γ-ENaC at the apical cell surface.

MCF10A cells were exposed to Ctx for 2 h or 1 day. Biotinylation followed by Western blot analysis was used to detect surface expression of β-ENaC (**A**) and γ-ENaC (**B**). Densitometric analysis showed that Ctx exposure was associated with increased intensities of bands that had been biotin-labeled. Occludin labeling is used as an internal standard for protein loading. Results are representative from at least 3 observations in each condition. The protein was loaded as the following sequence: vehicle with apical biotinylation (Veh_AP), vehicle whole cell lysates (Veh_WCL), Ctx 2 hours with apical biotinylation (Ctx2h_AP), Ctx 2 hours whole cell lysates (Ctx2h_WCL), Ctx 1 day with apical biotinylation (Ctx1d_AP), and Ctx 1 day whole cell lysates (Ctx1d_WCL).

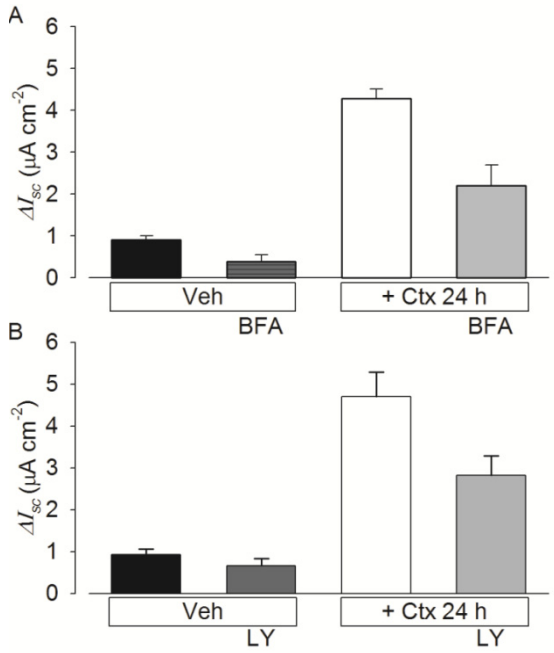

Figure 2.10 Effects of Ctx are not blocked by cytosolic pathway inhibitors.

A. Amiloride-sensitive I_{sc} across MCF10A cells was reduced by brefeldin A (BFA ; 10 mg/ml), a drug disrupting protein trafficking from ER to Golgi, but remained sensitive to Ctx exposure. Data are summarized from six observations. **B.** Data summarized from five observations show that the effect Ctx was not blocked by a phosphatidylinositol-3-kinase (PI3K) inhibitor, LY294002 (LY; 50 μM).

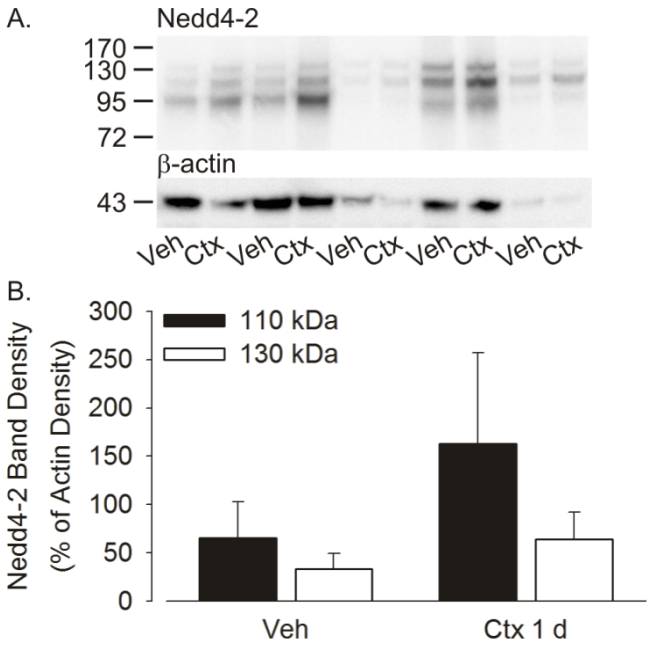

Figure 2.11 Ctx increases Nedd4-2 phosphorylation.

A. Western blot of lysates from five paired MCF10A monolayers exposed to either vehicle or Ctx for 1 day using antibodies raised against Nedd4-2 and β-actin. **B.** Densitometric analysis showed Ctx increased apparent Nedd4-2 expression of both the phosphorylated (130 kDa) and the non-phosphorylated (110 kDa) forms of Nedd4-2 although only the effect of Ctx on 130 kDa phosphorylated form achieved statistical significance. Densities were expressed relative to the intensity of β-actin and are summarized from 5 paired samples.

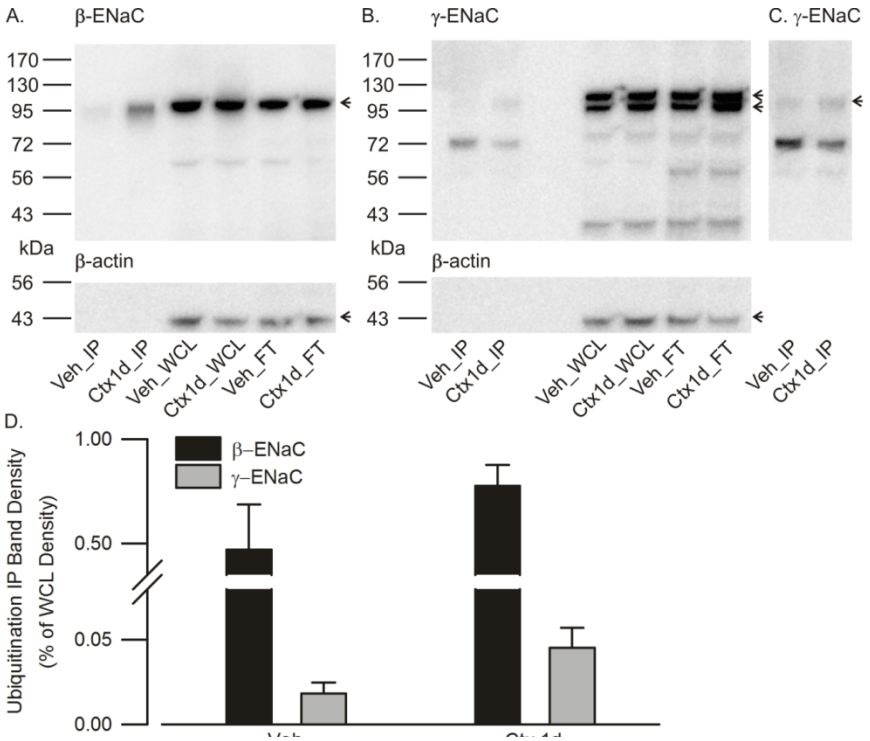

Figure 2.12 Ctx elevates β- and γ-ENaC monoubiquitination.

A. Ubiquitinated β-ENaC was detected by immunoprecipitation of ubiquitin and followed by Western blot of lysates from MCF10A monolayers exposed to either vehicle or Ctx for 1 day using antibodies raised against β-ENaC. **B.** Ubiquitinated γ-ENaC was detected similarly. **C.** Increasing membrane exposure time from 20 sec (B.) to 60 sec, the Ctx induced increment of the signal of γ-ENaC pulled down by immunoprecipitation of ubiquitin is more evident. **D.** Densitometric analysis showed Ctx increased β- and γ-ENaC monoubiquitination although only the effect of Ctx on γ-ENaC reached statistical significance. Densities were expressed relative to the intensity of whole cell lysates and are summarized from 4 paired samples.

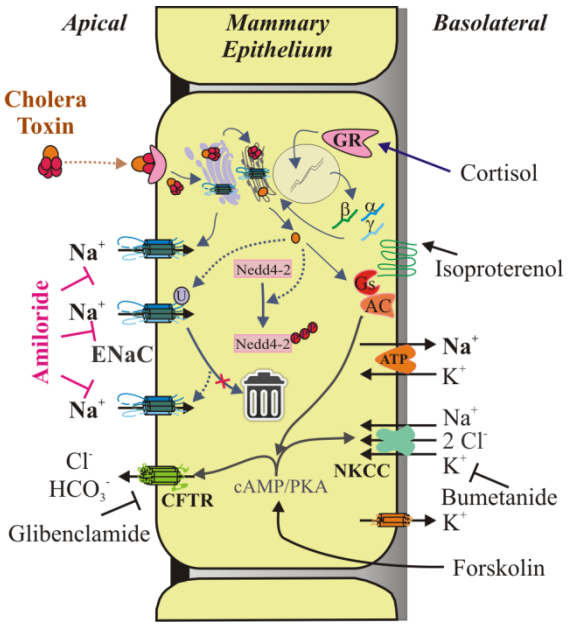

Figure 2.13 Mammary cell model to account for monovalent ion transport and especially for Ctx enhanced Na^+ absorption.

In this model, cortisol binds to glucocorticoid receptor and induces (β and γ) or enhances (α) the expression of mRNA coding for ENaC subunits, which are transcribed in the endoplasmic reticulum, processed through the Golgi apparatus and trafficked to the apical membrane. Under normal conditions, Nedd4-2 binds to ENaC in the apical membrane to induce its retrieval and, upon ubiquitination, its degradation. Ctx elevates amiloride-sensitive I_{sc} by increasing the number of ENaC channels in the apical membrane. As depicted, Ctx is composed of one A subunit and 5 B subunits and binds to GM1 by Ctx B subunits to internalize into cells. After internalization, Ctx is transported in a retrograde fashion from the apical membrane to the Golgi apparatus and then to the endoplasmic reticulum where the A-subunit becomes dissociated from the B subunits and translocates to the cytosol. In the cytosol, the Ctx A subunit catalyzes the ADP-ribosylation of Gsα to irreversibly activate the G-protein and increase cAMP level that activates PKA. However, the effect of Ctx on increased amiloride-sensitive I_{sc} is independent of the cAMP/PKA pathway. Ctx increases phosphorylation of Nedd4-2, which would decrease its ability to promote retrieval of ENaC from the apical membrane, although the underlying mechanism is not defined. Ctx elevates monoubiquitination of ENaC, which may lead to more surface ENaC expression. Solid lines represent pathways that have been defined and short dash lines represent predicted pathways. GR, glucocorticoid receptor. α, β and γ represent ENaC mRNAs.

Chapter 3 - Primary Culture of Caprine and Bovine Mammary Gland Epithelia

Abstract

Primary cultures of mammary gland epithelia represent a valuable tool to study mammary function. The goal of this research is to develop and begin to optimize a protocol to isolate mammary gland epithelia from dairy goats and cows for subsequent *in vitro* culture, which can be used to identify and characterize barrier function, secretory functions, and ion transport processes along with associated regulatory cascades. Caprine and bovine mammary tissue were digested enzymatically and the resulting epithelial cultures were enriched by partial sedimentation and by serial exposure to collagenase when passaged. Cells were seeded initially on solid substrates and were subcultured in types of media that have been used previously in the laboratory for either human mammary cells (THM) or bovine mammary cells (TBM). When grown on permeable supports cells formed electrically tight monolayers. Caprine mammary epithelia (1°CME) were passaged up to 12 times and each passage was evaluated with electrophysiological techniques. When grown in THM, 1°CME formed higher resistance (R_{te}) monolayers than when grown in TBM. Amiloride-sensitive short circuit current (I_{sc}) was detected only in monolayers that were cultured in THM. 1°CME responded to forskolin with an increase in I_{sc} that was partially sensitive to bumetanide. These results suggest that 1°CME exhibit Na^+ absorption *via* the epithelial Na^+ channel, ENaC, and cAMP-stimulated anion secretion. In a separate experiment, bovine mammary epithelia (1°BME) were obtained and subcultured for 19 passages in TBM in the absence or presence of dexamethasone, which was associated with greater R_{te}. There was little detectable amiloride-sensitive I_{sc} in either culture condition. However, 1°BME responded to norepinephrine and carbamylcholine with rapid and substantial increases in I_{sc}. Taken together, these results demonstrate that both 1°CME and 1°BME can be isolated, expanded in culture and passaged to generate electrically tight monolayers that can be used to assess net ion transport or other epithelial functions. Either system likely can be optimized to focus on either acini or duct epithelia. Further, conditions might be optimized with the use of hormones or growth factors to assess changes that occur during lactation or in mastitis.

Introduction

Mammary gland epithelia are essential for milk production, although mechanisms of ion transport across mammary epithelia are not well characterized. The complex structure and development of the mammary gland make it challenging to isolate and culture mammary epithelial cells (204). Rodent and human mammary cell cultures are often used as model systems to elucidate gland function that might contribute to breast cancer (230). However, fewer studies are designed to develop systems that assess epithelial function in the context of lactation. Most mammary epithelial cell lines have been developed in the past three decades. For example, the MCF10A cell line was derived from non-neoplastic human mammary tissue and was characterized in 1990 (225). The BME-UV cell line was derived from a lactating Holstein cow and was first described in 1996 (262). The 31EG4 cell line, which is an untransformed nontumorigenic mouse mammary cell line, can be grown as tight monolayers that respond to lactogenic hormones (186, 236, 263). Although many cell lines have been developed to study mammary function, certain limitations cannot be eliminated, such as loss of their responsiveness to characteristic hormones and growth factors. Moreover, cell lines are derived from single individuals, which makes inferences to a large population tenuous, at best. Although cell lines have been selected for the ability to proliferate in culture and to maintain a high level of differentiation, many characteristics of mammary epithelia change with increasing passage number.

The above-mentioned limitations of mammary cell lines underscore the value of epithelial cultures for studies of mammary function. Importantly, primary cells allow for inferences to the population from which they were derived. However, isolation of mammary gland epithelial cells is challenging and there is no standard protocol to assess the methodology of primary mammary epithelia isolation and cell culture. This study is designed to develop and optimize a protocol to isolate and culture primary mammary gland epithelia from lactating dairy animals - goats and cows.

Milk composition varies widely across species, epically the Na^+ concentrations (132). One of the major goals for the laboratory is to define mechanisms of ion transport, especially Na^+ transport, across mammary epithelia. A necessary tool is an appropriate *in vitro* system that is amenable to appropriate experimental approaches. In the present study, epithelial cells were isolated from multiple gland samples from a lactating goat and a lactating cow. Caprine

(1°CME) and bovine mammary epithelial cells (1°BME) were enriched by partial sedimentation and then cultured on solid substrates for 12 and 20 passages, respectively. With each passage, a portion of the cells was cultured on permeable supports to study ion epitheilal transport. The outcomes suggest the capacity for agonist-stimulated anion secretion in cells from both species for more than four passages. Caprine mammary epithelia exhibit net Na^+ transport, whereas 1°BME failed to show a similar response. This study establishes a working technique to isolate, culture, subculture and assess mammary gland epithelia from both species.

Methods

Cell culture media and experimental solutions

The method for cell isolation and passage will be summarized in the Results sections. All chemicals were obtained from Sigma-Aldrich (Sigma-Aldrich, St. Louis, MO) unless indicated otherwise. Bovine mammary gland samples were collected immediately post-mortem from a lactating cow at a commercial slaughter facility by Dr. Ronette Gehring (Kansas State University). Ten to thirty cubic cm were collected from four locations in the gland and placed in ice-cold Hanks buffered salt solution (HBSS (in mM): 137 NaCl; 5.4 KCl; 0.4 KH_2PO_4; 0.6 Na_2HPO_4; 5.5 glucose) supplemented with antibiotics (20 µg/ml gentamicin, 1% penicillin and streptomycin, and 2 µg/ml fungizone; all from Gibco, Grand Island, NY). Samples were transported to the laboratory (~4 h) on ice. The caprine mammary samples were obtained immediately post mortem by Dr. O. A. Chiesa (US FDA, Center for Veterinary Medicine, Laurel, MD), placed in ice cold HBSS and sent *via* courier to the laboratory for processing the following day.

Cells were cultured in media of three different compositions. The first medium, typical human medium (THM), was used previously in the laboratory to grow MCF10A cells (225, 251). THM contained DMEM/F-12 (Cellgro, Herndon, VA), horse serum (5%; Gibco), insulin-transferrin-sodium selenite (0.7%), penicillin and streptomycin (1%; Gibco), L-Glutamine (2 mM), hydrocortisone (cortisol, 0.5 µg/ml), and epidermal growth factor (20 ng/ml; RD Systems, Minneapolis, MN). The second medium, typical bovine medium (TBM), has been described previously (181, 182, 197, 262), and was used when cells were cultured on solid substrates. TBM contained a 5:3:2 mixture of DMEM/Ham's F-12: RPMI medium: NCTC-135 medium (Gibco) supplemented with 10% fetal bovine serum (Atlanta Biologicals, Flowery Branch, GA), 3% of

newborn calf serum (Gibco), 2% iron-supplemented bovine calf serum (Gibco), 1% insulin-transferrin-sodium selenite media supplement solution, 1% penicillin and streptomycin, 1 mg/ml lactalbumin hydrosylate, 10 µg/ml L-ascorbic acid and 3 mM lactose. The third medium, apical bovine medium (ABM), was used in the mucosal compartment when cells were cultured on a permeable supports with TBM in the serosal compartment. ABM is a complex medium that was designed to reduce electrolyte concentrations when compared to typical commercially available media. The composition was published in detail previously (181, 197) and mirrors the composition of TBM except that Na^+ concentration is 60 mEq/l and lactose is introduced (160 mM) to maintain osmolality at ~300 mosm•kgH_2O. In some experiments, cells were exposed to dexamethasone (100 nM) in culture for 72 h prior to experimental analysis. When passing cells, epithelial cells were detached using trypsin in phosphate buffered saline (PBS) with disodium EDTA (2.4 mM; Gibco) for 7-10 min at 37°C, suspended in culture medium, and seeded on permeable supports (Snapwell or Transwell; 1.13 cm^2 or 4.67 cm^2, respectively; Corning). Cells were maintained at 37°C in a humidified atmosphere containing 5% CO_2. Media were refreshed every day until experimentation, which typically was 14 days post-seeding.

A modified Ussing-style system was used to measure active net transepithelial ion transport and electrical resistance as detailed previously (181, 182, 197, 251). Briefly, the cultured monolayer on its permeable support was inserted to separate the two halves of an acrylic chamber (DCV9; Navicyte, San Diego, CA). The mucosal and serosal hemichambers were filled with equal volumes of Ringer solution (composition in mM; 120 NaCl, 25 $NaHCO_3$, 3.33 KH_2PO_4, 0.83 K_2HPO_4, 1.2 $CaCl_2$, 1.2 $MgCl_2$). Each hemichamber was mixed continually by an air lift system (5% CO_2 with 95% O_2) that also maintained a stable pH (7.4). The system was maintained at 37°C. Custom-made voltage-sensing and current-injecting electrodes were placed in each chamber and connected to a voltage clamp (model 558C; University of Iowa, Department of Bioengineering, Iowa City, IA) to determine open circuit voltage, to clamp the voltage and to measure short circuit current (I_{sc}). Monolayers were clamped to 0 mV with the exception of an intermittent 1 mV bipolar pulse per 100 seconds to allow for the determination of transepithelial electrical resistance (R_{te}). Voltage and current measurements were acquired digitally at 1 Hz (MP100A-CE interface and Aqknowledge software, ver. 3.2.6; BIOPAC Systems, Santa Barbara, CA) throughout all experiments. Ion transport modulators were added as 1000x stock solutions to achieve the reported working concentrations either to the mucosal hemichamber

(amiloride), to the serosal hemichamber (bumetanide), or symmetrically (forskolin, Calbiochem, Gibbstown, NJ; glibenclamide).

Data Analysis

Statistical analysis was conducted using SigmaPlot (ver. 10.0, Systat Software, Inc. Chicago, IL) and Excel (ver. 14.0.6129.5000, Microsoft, Redmond, WA). Students t-test for unpaired or paired data were used, as appropriate. Summarized data are presented as mean ± standard error of the mean. Treatment effects were considered significant when the probability of the type I error was ≤ 0.05.

Results

Cultured primary caprine mammary epithelia form an electrically tight epithelial barrier and exhibit net ion transport.

Freshly dissected caprine mammary gland tissues were obtained from different sections of one goat udder, including proximal, middle, distal anterior and posterior. However, the experimental design did not make comparisons between these regions and all tissues were treated similarly. Upon arrival at the laboratory, tissues were washed with ice-cold HBSS. Then small specimens (3-4 cm^3) of mammary tissues were obtained and placed in ice-cold HBSS supplemented with antibiotics. These small specimens were washed with HBSS plus antibiotics four times in a Petri dish. Two small cubes of tissue (2 mm^3) were cut, placed in a Petri dish, and minced finely with a scalpel. Minced tissues were incubated with 5 ml cell isolation enzyme solution (300 U/ml collagenase [Gibco] and trypsin in PBS with disodium EDTA [2.65 mM, Gibco]) in a 50 ml tube at 37°C for 90 minutes. During the incubation, tubes were shaken gently by hand for 20 seconds, every 15 minutes. Dissociated cells were collected by passing through a 100 μm cell strainer (BD Falcon #352360) placed on a new 50 ml tube. The resulting cell suspensions were centrifuged at 600 RCF for 5 minutes. The supernatant was carefully removed and pelleted cells were suspended in 2 mL of either THM or TBM. Cells were seeded on a 6 well plate (Falcon, Becton Dickinson Labware, Franklin Lakes, NJ) and placed in a cell culture incubator (37°C, 5% CO_2, humidified). After 30 min, the media and any unattached cells were moved to a second well and fresh medium was added to the first well. This 30-min sedimentation procedure was conducted a second time resulting in three wells derived from each initial seeding.

Two types of cells, based on morphology, were isolated from these mammary tissues, epithelial cells and fibroblasts. Epithelial cells are cuboidal and exhibit a 'cobble stone' appearance and they grow together to form islands. Fibroblasts are spindle- or stellate-shaped and grow over greater distances. Ultimately, it was determined that populations of cells attached in the first two sedimentations contained a substantial proportion that exhibited fibroblast morphology. Thus, these cells were discarded. Cells in the third sedimentation were allowed to grow to >70% confluency (3-7 days) before being passaged. The cultures appeared to contain some spindle or stellate cells. Thus, a differential digestion technique was used to remove these cells selectively (171). Cultures were exposed to trypsin in PBS with disodium EDTA for 5 min at room temperature. Any cells that detached were discarded and the cells were washed with PBS. This step to preferentially remove fibroblasts was conducted a second time. Remaining cells were then exposed to the enzyme solution for 7-10 min at 37°C to dislodge all remaining cells. Cells were suspended in culture medium and seeded on a vented, 25 cm^2 tissue culture flask or the wells of a 6-well plate and maintained at 37°C in the cell culture incubator. Subsequent passages were made by exposing cultures to the enzyme solution for 7-10 min at 37°C to dislodge all cells. When passing cells, half of the cells were seeded on Transwell (6 to 12 at 0.33 cm^2, each) or Snapwell (4 to 6 at 1.13 cm^2, each) permeable supports (Costar) and the remaining cells were seeded on a subsequent culture well or flask. Cells were subcultured or passaged 12 times (denoted P2-P13) with electrophysiological assessment of R_{te} and I_{sc} at each passage.

Primary (1°) CME were cultured on solid and permeable substrates in either THM or TBM. For the cells that were grown in TBM, when cells growing on permeable supports were fed, TBM was added only to the serosal aspect of the cells and ABM was added to the mucosal aspect of the cells (the asymmetrical media feeding method was introduced in detail by Quesnell, et al. (181)). Media (both sides) were refreshed every day until experimentation, which typically was 14 days post-seeding. Dexamethasone (100 nM) was included in the medium for some wells during the final 72 hours prior to assessment.

Primary (1°) CME formed electrically tight epithelial monolayers when cultured in either THM or TBM (Figure 3.1). Cells cultured in THM exhibited a positive I_{sc} (4.56 or 8.43 μA cm^{-2}, cultured for the final 72 hours in the absence (vehicle) or presence of dexamethasone, respectively) indicative of net cation absorption or anion secretion. In contrast, when 1°CME were grown in TBM, the beginning baseline I_{sc} (0.97 or 1.7 μA cm^{-2}, cultured for the final 72

hours in the absence or presence of dexamethasone, respectively) was redundant and there was no obvious response to amiloride. Using Ohms law, R_{te} was calculated based on the current associated with each periodic 1 mV bipolar pulse. Figure 3.2 summarizes R_{te} for 3 groups, each comprising 4 passages, each under vehicle- and dexamethasone-stimulated conditions. Initial passages cultured in THM exhibited the greatest R_{te} with the greatest R_{te} being observed at P2 (>2000 Ω cm^2 either with or without dexamethasone). Initial passages did not show dexamethasone-enhanced R_{te} in either medium, whereas a significant difference was detected for TBM in P6-9 and P10-13, and for THM for P10-13. The cells cultured in TBM exhibited the highest resistance at P3 (484 ± 13 Ω cm^2 or 488 ± 50 Ω cm^2, n=3, vehicle and dexamethasone, respectively).

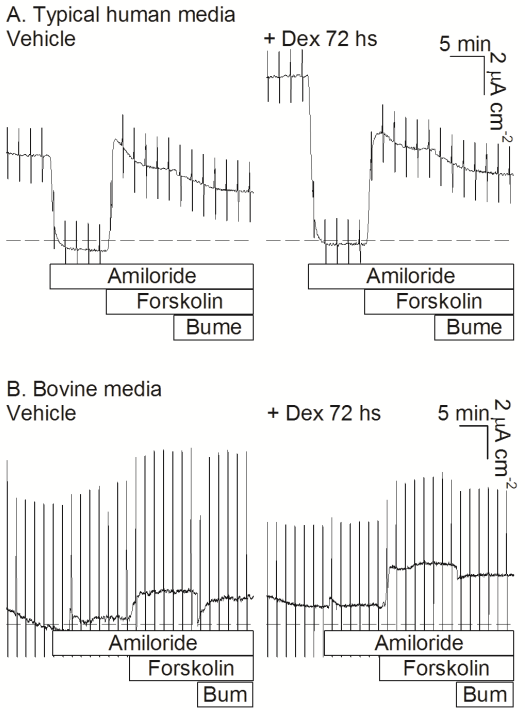

Figure 3.1 1°CME cells form tight monolayers that respond to ion transport modulators.

A. Typical tracings of short circuit current (I_{sc}) across 1°CME cells that were cultured in typical human media in the absence (vehicle) or presence of dexamethasone (Dex). Solid lines represent I_{sc} and dashed lines represent zero current. Monolayers exposed to Dex showed greater amiloride-sensitive I_{sc}. Forskolin stimulated I_{sc} that was reduced by bumetanide (Bum). **B.** Typical tracings of I_{sc} across 1°CME cells that were cultured in bovine media in the absence or presence of Dex. There was no detectable amiloride-sensitive I_{sc} in either condition. Again, forskolin-stimulated I_{sc} was reduced by bumetanide.

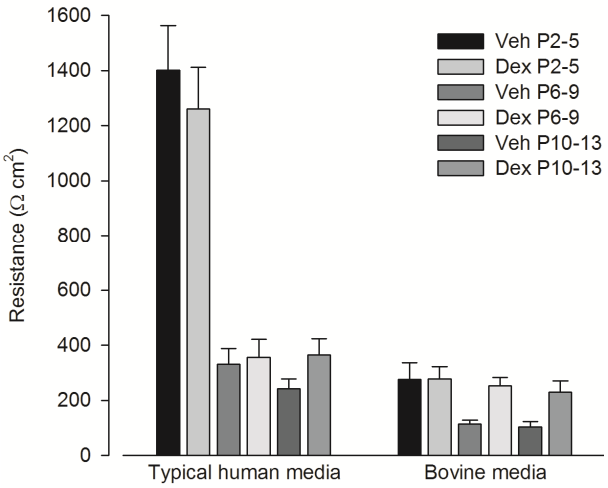

Figure 3.2 1°CME cells form electrically tight epithelial barriers in all culture conditions.

Results are summarized from 15-32 Ussing-style experiments and presented in groups of 4 passages. 1°CME formed electrically resistive monolayers whether cultured in either medium and in the absence (Veh) or presence of dexamethasone (Dex).

Amiloride (10 μM), which blocks the epithelial Na^+ channel (ENaC), was added to the apical medium during each recording. Typical outcomes presented in Figure 3.1 suggest that amiloride-sensitive I_{sc} can be detected readily only in monolayers cultured in THM. More-over, Figure 3.1 shows that cells cultured in the presence of dexamethasone-supplemented THM exhibited greater amiloride-sensitive I_{sc} (8.67 μA cm^{-2}) when compared to their untreated counterparts (4.89 μA cm^{-2}). When summarized, the highest amiloride-sensitive I_{sc} was observed at P7 in THM-cultured monolayers (2.44 ± 0.98 μA

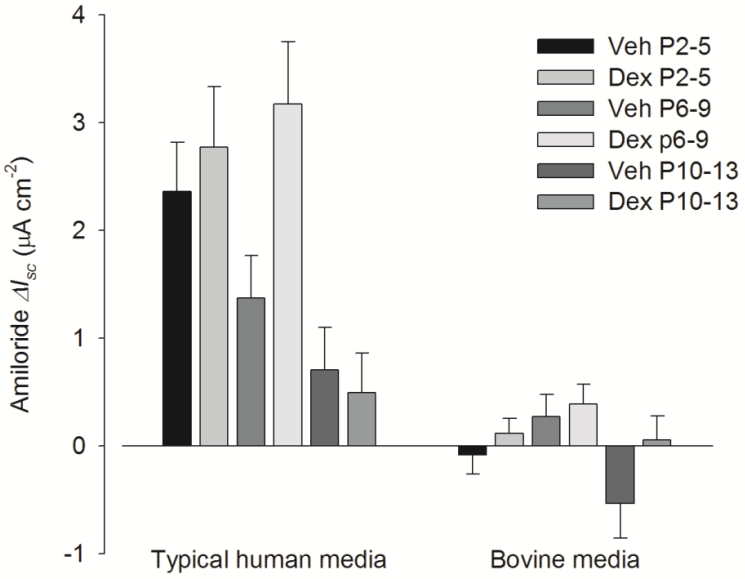

Figure 3.3 Amiloride-sensitive I_{sc} is detected across 1°CME only in typical human media.

Results are summarized from 15-32 Ussing-style experiments and presented in groups of 4 passages. Primary (1°) CME exhibited obvious amiloride-sensitive I_{sc} when grown in typical human media. There is a detectable trend suggesting that Dex increased amiloride-sensitive I_{sc} in either culture condition.

cm^{-2} vs 5.00 ± 1.16 μA cm^{-2}, n=8, in vehicle and dexamethasone, respectively). In general, 1°CME cells cultured in THM exhibited decreased amiloride-sensitive I_{sc} as the passage number increased in vehicle treatment group. However, dexamethasone increased amiloride-sensitive I_{sc} only at P2-5 and P6-9. The highest passages (P10-13) exhibited the smallest amiloride-sensitive I_{sc} and there is no effect of dexamethasone. Primary (1°) CME monolayers cultured in TBM exhibited no consistent detectable amiloride-sensitive I_{sc} regardless of whether dexamethasone was present. These data suggest that cell culture media composition may affect epithelial function. Typical human media contains hydrocortisone, which can induce or increase ENaC expression in both bovine and human mammary gland epithelia (20, 182, 251). Although 1°CME cells were exposed to dexamethasone-supplemented TBM for 72 hours, there was little effect on the magnitude of amiloride-sensitive I_{sc} (Figure 3.3). In summary, 1°CME cells exhibited markedly higher amiloride-sensitive I_{sc} when cultured in typical human media than those cultured in bovine media.

Forskolin (2 μM), an activator of adenylyl cyclase, elevated I_{sc} in all culture conditions. Typical tracings of forskolin-stimulated I_{sc} show a rapid transient peak followed by a sustained plateau (Figure 3.1). Summarized data are presented at Figure 3.4. Primary (1°) CME cells grown in THM exhibited increased forskolin-stimulated, sustained I_{sc} with increased passage number (Figure 3.4A). Dexamethasone had no significant effect on either the forskolin-stimulated sustained I_{sc} or the transient peak I_{sc}.

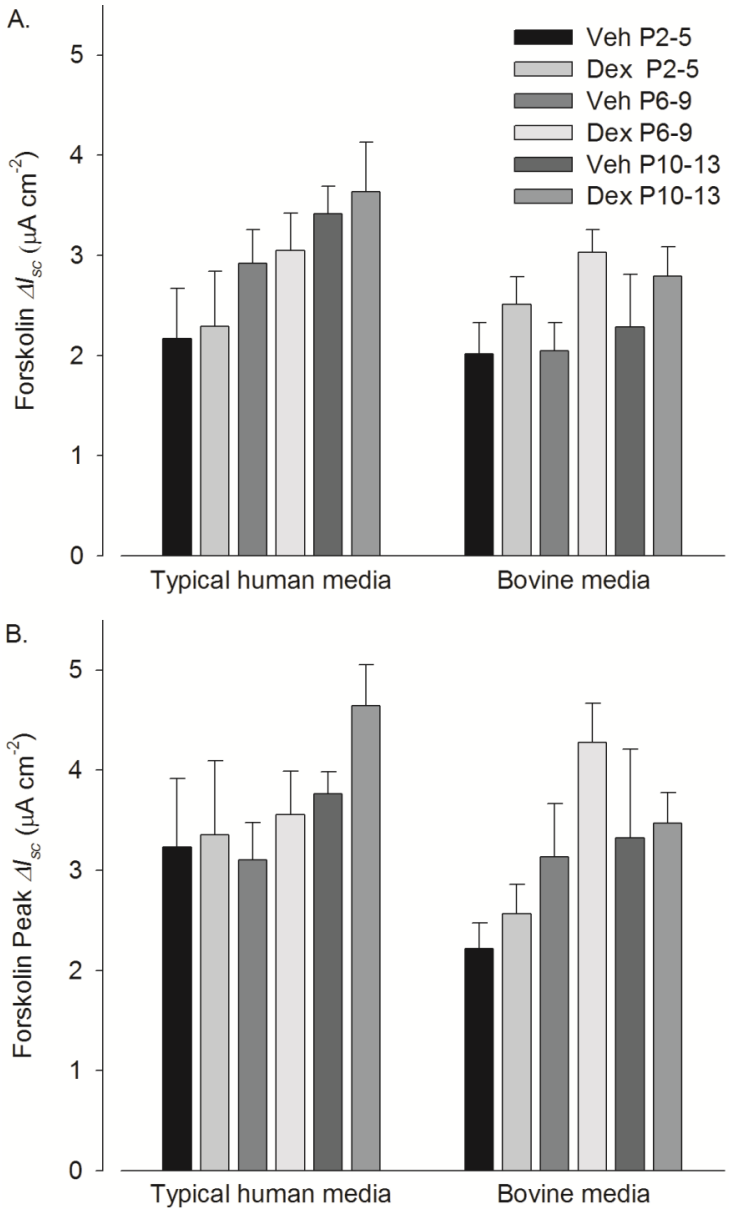

Figure 3.4 Forskolin stimulates I_{sc} across 1°CME in typical human media and bovine media.

Results are summarized from 15-32 Ussing-style experiments and presented in groups of 4 passages. Forskolin stimulated both sustained (**A**) and transient (**B**) I_{sc} across all monolayers tested. No obvious effect of medium composition, dexamethasone (Dex) or passage number is suggested.

When cells were cultured in TBM, the maximum forskolin-stimulated sustained I_{sc} was observed at P7 (P7: 3.79 ± 0.39 μA cm^{-2} when cultured with dexamethasone). When 4 passages were grouped, dexamethasone significantly increased forskolin-induced sustained I_{sc} on P6-9 (n=24, unpaired). However, there was no significant effect of dexamethasone on forskolin-stimulated peak I_{sc} when cells were grown in TBM (Figure 3.4B). When comparing THM and TBM for the effect of forskolin, outcomes in Figure 3.4 suggest that no significant difference.

Bumetanide (20 μM), an inhibitor of the $Na^+/K^+/2Cl^-$ cotransporter that is added to the serosal medium during each recording, caused a decline in I_{sc} (Figure 3.1). Outcomes summarized and shown in Figure 3.5 suggest that cells cultured in THM exhibited increased bumetanide-sensitive I_{sc} with increasing cell passages. In contrast, cells grown in TBM, exhibited the highest bumetanide-sensitive I_{sc} between P6-9. There was no significant effect of dexamethasone on bumetanide-sensitive I_{sc} in either culture medium.

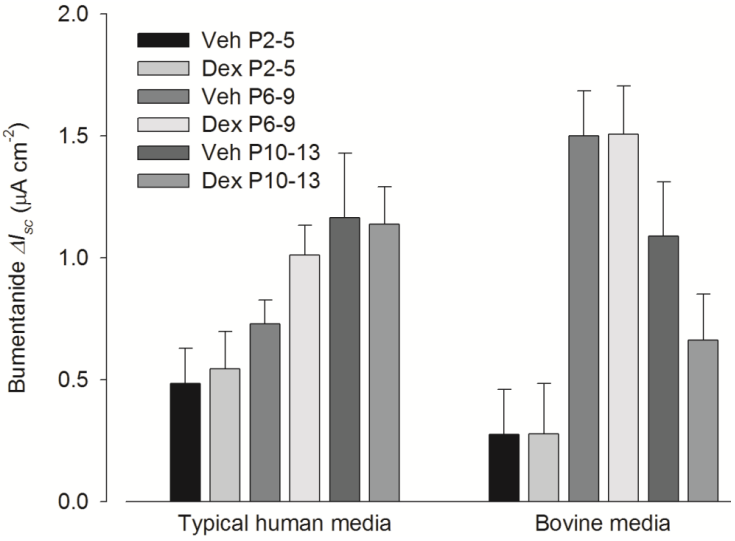

Figure 3.5 Bumetanide-sensitive I_{sc} across 1°CME in both media culture conditions.

Results are summarized from 15-32 Ussing-style experiments and presented in groups of 4 passages. Bumetanide reduced forskolin-stimulated I_{sc} across all monolayers tested.

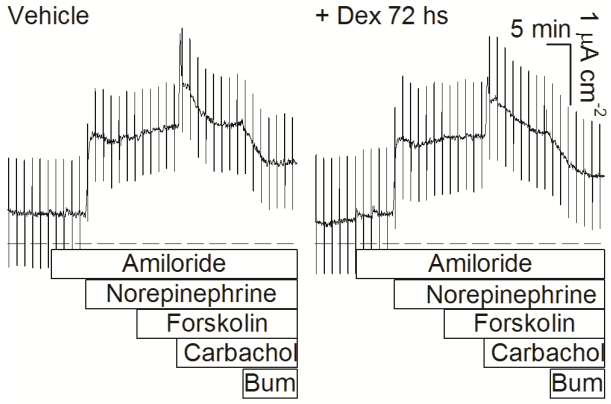

Figure 3.6 1°BME cells form tight monolayers in bovine media and responded to neurotransmitters with increases in anion secretion.

Typical tracings of I_{sc} across 1°BME cells that were cultured in typical bovine media and in the absence or presence of dexamethasone (Dex). Solid lines represent I_{sc} and dashed lines represent zero current. Amiloride was without effect. Norepinephrine and carbamylcholine caused sharp and sustained increases in I_{sc} that were partially sensitive to bumetanide (bum).

Cultured primary bovine mammary epithelia form an electrically tight epithelial barrier and exhibit net ion transport.

The goal of this set of observations is testing the effect of dexamethasone on 1°BME and different compounds over different subculture passages. Epithelial cells derived from one of two cows were cultured *in vitro* successfully. Primary (1°) BME were isolated using the method described for 1° CME and grown on permeable supports in TBM, with ABM on the mucosal aspect of the cells for 14 days and in the absence or presence of dexamethasone for the final 72 hours. Monolayers were mounted in Ussing-style flux chambers to test for electrogenic ion transport. Cells were maintained for 19 passages (P2-P20). Figure 3.6 shows a typical tracing from 1°BME. This tracing illustrates the typical responses of 1°BME and highlight the electrically tight epithelial barrier and net ion

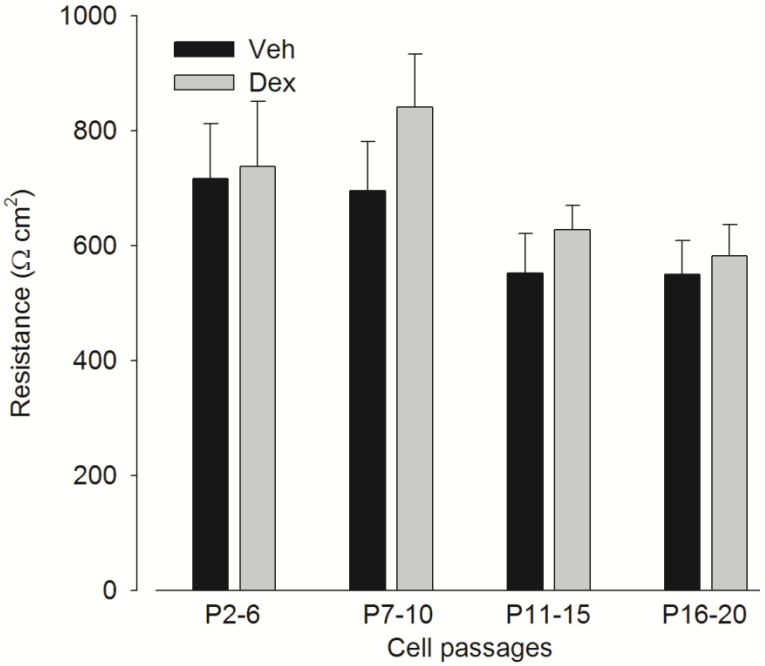

Figure 3.7 1°BME form electrically tight epithelial barrier.

Results are summarized from 16-40 Ussing-style experiments and presented in groups of 4 or 5 passages. Primary (1°) BME cells formed electrically tight monolayers. Dex indicates dexamethasone for 72 hrs in culture.

transport (beginning I_{sc}: 0.56 or 0.37 μA cm^{-2}, observed when cells were cultured for the final 72 hours in the absence or presence of dexamethasone, respectively). Cultured 1°BME monolayers did not respond to amiloride, regardless of culture conditions (*i.e.*, absence or presence of dexamethasone). However, 1°BME responded to an adrenergic agonist, norepinephrine and to a cholinergic agonist, carb-amylcholine, with rapid increases in I_{sc}. There is no statistical difference in R_{te} amongst cell passages in the absence or presence of dexamethasone (Figure 3.7). However, dexamethasone-treated cells exhibited higher R_{te} when compared to their counterparts. Cells from P7-10 that had been exposed to dexamethasone exhibited the highest R_{te} (841 ± 92 Ω cm^2, n=11) among all the monolayers tested.

Experiments were conducted to determine the effect of adrenergic receptor agonist on 1°BME monolayers. Basolateral norepinephrine (10 μM) exposure was associated with an acute increase in I_{sc} (Figure 3.6). The response to norepinephrine was consistent with activation of adrenergic receptors, which were reported in cultured BME-UV cells (197). Figure 3.8 summarizes these data. No effect of dexamethasone was detected. There is a trend toward decreasing responses to norepinephrine as cell passage number increased. At P16 and above, monolayers failed to exhibit a response to norepinephrine. Forskolin (2 μM) was applied after norepinephrine and had no effect. These outcomes are consistent with a norepinephrine-induced increase in cytosolic cAMP concentration and activated anion secretion across 1°BME. Furthermore, the absence of response to both norepinephrine and forskolin in the higher passages

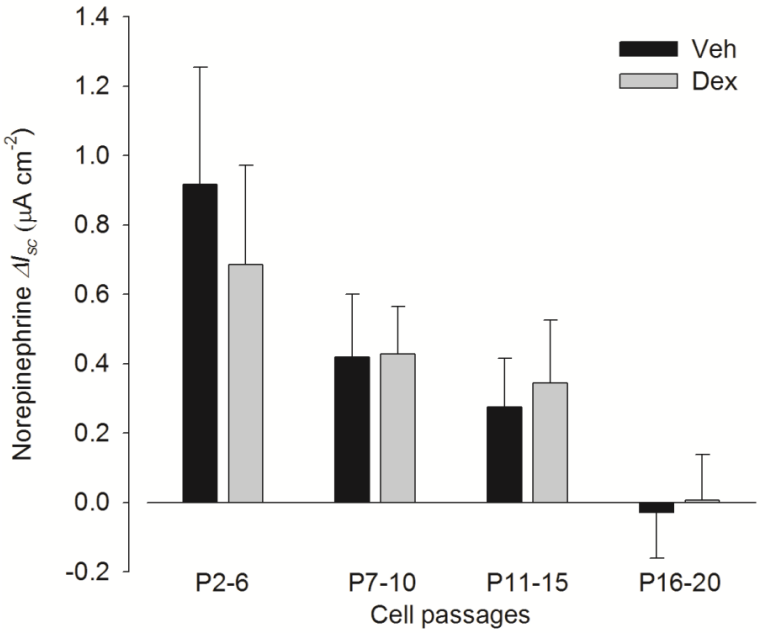

Figure 3.8 Norepinephrine stimulates I_{sc} across 1°BME decreased as cell passages increased.

Results are summarized from 16-40 Ussing-style experiments and presented in groups of 4 or 5 passages. 1°BME exhibited norepinephrine-stimulated I_{sc}. The effect of dexamethasone (Dex) was not statistically significant on norepinephrine-stimulated I_{sc}. There is a trend of decreased response to norepinephrine as cell passages increased.

suggests that these cells lack one or more elements of the second messenger pathway or the ion transport pathway, but not merely a loss of the adrenergic receptor.

Carbamylcholine (100 μM) produced a sharp increase in I_{sc}, when added in the ongoing presence of norepinephrine and forskolin (Figure 3.6). The response to carbamylcholine is consistent with activation of cholinergic receptors although selective inhibitors were not tested (56). Figure 3.9 summarizes these data. Dexamethasone produced no detectable effect of on carbamylcholine-stimulated I_{sc}. The maximum response of carbamylcholine was observed at P11-15. The magnitude of carbamylcholine-stimulated I_{sc} was increased from cell passages from 2 to 15 and began declining at the most advanced passage group (P16-20).

Bumetanide (20 μM), was used also with 1°BME cells to test for the activity of the $Na^+/K^+/2Cl^-$ cotransporter. An obvious decline in bumentanide-sensitive I_{sc} was observed in initial passages (*e.g.*, see Figure 3.6), but not in later passages. Summarized outcomes shown in Figure 3.10 suggest that the magnitude of bumetanide-inhibited I_{sc} declined with increasing cell passage increased. With norepinephrine and carbamylcholine, dexamethasone had no detectable effect on bumetanide-inhibited I_{sc}.

Figure 3.9 Carbamylcholine stimulates I_{sc} across 1°BME cell monolayers.

Results are summarized from 16-40 Ussing-style experiments and presented in groups of 4 or 5 passages. The magnitude of carbamylcholine-stimulated I_{sc} increased from P2-15 and declined from P16-20. Dex indicates dexamethasone for 72 hrs in culture.

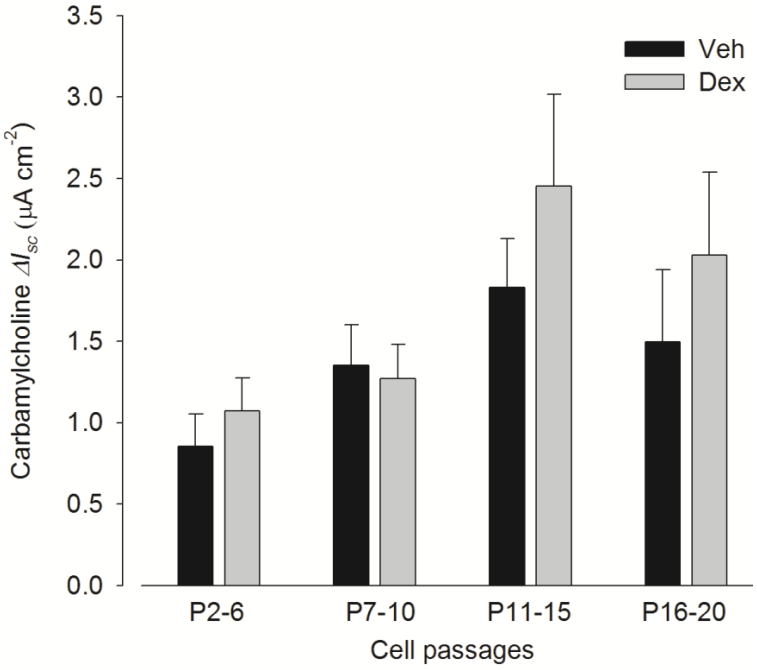

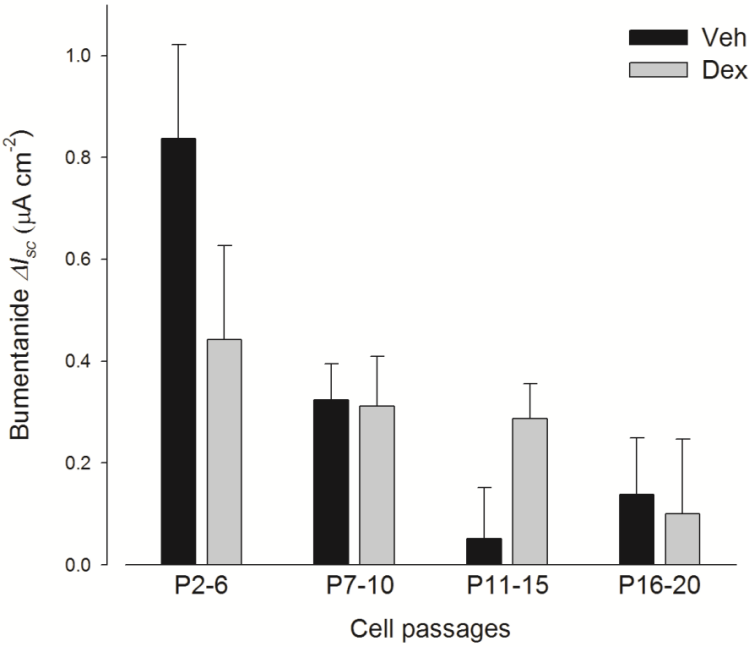

Figure 3.10 Primary (1°) BME exhibit bumetanide sensitive I_{sc}.

Results are summarized from 16-40 Ussing-style experiments and presented in groups of 4 or 5 passages. Primary (1°) BME exhibited bumetanide-sensitive I_{sc} following exposure to norepinephrine, forskolin and carbamylcholine. Dexamethasone (Dex) in culture was without effect. There is a trend of decreased response to bumetanide as cell passages increased.

Discussion

The present study seeks to define a protocol that can be used routinely to isolate and culture mammary epithelia from dairy goats or cows that can be used to study ion transport and other secretory processes that contribute to normal gland function. This report provides evidence that 1°CME and 1°BME develop electrically tight monolayers when cultured on permeable supports and exhibit active net ion transport. When compared to cells grown in TBM, 1°CME monolzyers cultured in THM exhibited greater baseline R_{te}. Moreover, 1°CME exhibited amiloride-sensitive Na^+ transport, suggesting that ENaC activity contributes to a portion of the ion transport machinery. Amiloride-sensitive transport was detected in cells cultured in THM, but not in TBM. In contrast, 1°BME failed to exhibit amiloride-sensitive ion transport - regardless of whether the culture medium contained corticosteroids. Importantly, 1°BME responded to both adrenergic and cholinergic stimulation, thereby suggesting the presence of adrenergic and cholinergic receptor in 1°BME. In addition to these key observations, the results show that cells isolated from the mammary gland can be expanded and propagated through a number of subcultures. Discrete and apparently continuous differences in the magnitude of outcomes were observed depending on the culture medium and passage number, with higher passages showing diminished responses to corticosteroids (1°CME), adrenergic stimuli and, in the case of 1°BME, bumetanide. Nonetheless, this report provides a valid protocol to isolate and culture 1°CME and 1°BME.

This pilot study clearly has many limitations. Most notably, all data were derived from a cell isolation protocol performed on one day with samples from one individual, each, for caprine and bovine tissue. Additionally, the identity and origins of cells in the cultures were not defined. Based on general morphology, both epithelial cells and fibroblasts were present in the cultures. There is a strong possibility that myoepithelial cells were present also. Although the observations that a measurable electrical resistance and the expression of directional ion transport that can be stimulated with physiological and/or pharmacological agents provides strong evidence for cultures that are substantially epithelial in nature, the presence of other cell types that affect the responses, or potentially modify the response, cannot be ruled out. It has been speculated that alveolar and duct cells in the mammary gland perform distinct secretory and/or absorptive functions (142). Whether one or the other cell type predominated in these cultures and whether there might be differences in the proportions as passage number increased is unknown.

Additional studies are required to demonstrate repeatability of results and to address these gaps in our knowledge. Nonetheless, numerous conclusions can be drawn.

Many papers have focused on the isolation and culture of epithelial cells derived from bovine mammary gland (1, 147, 216, 224). However, none have focused on ion transport across 1°BME. The current study is the first report ion transport across these primary cultures. The results indicate that 1°BME can form an electrically tight monolayer that exhibits active ion transport. It is intriguing that 1°BME exhibit very small amiloride-sensitive I_{sc} in the absence or presence of dexamethasone. In another report from this laboratory, BME-UV cells, an immortalized bovine mammary epithelial cell line, expressed mRNA coding for all ENaC subunits. (197). More importantly, it was demonstrated that glucocorticoids upregulated BME-UV ENaC expression and amiloride-sensitive I_{sc} (182). The current results provide modest support for the conclusion that ENaC is expressed also in freshly isolated cells that are taken through primary culture. Again, it must be emphasized that the cells were derived from a single isolation protocol, which leaves open the possibility that the BME-UV cells are changed fundamentally upon immortalization, that there is substantial animal-to-animal variation in the responses, that there are regional differences in the udder regarding the expression of transport mechanism and/or that the cell isolation protocol selected for a particular cell type that did not express some component of the glucocorticoid and ENaC signaling or response pathways. Therefore, it is necessary to obtain more bovine mammary gland donors to examine the ENaC-mediated Na^+ transport across 1°BME.

The presence of adrenergic receptors was demonstrated previously in BME-UV cells (197) and the response of 1°BME monolayers to norepinephrine is similar. After exposure to norepinephrine, forskolin failed to cause an additional increment in I_{sc}. The simplest interpretation is that norepinephrine stimulates the cAMP second messenger pathway maximally to achieve anion secretion such that there is either no increase in cAMP with forskolin or that the anion secretory machinery is functioning at maximal capacity. Five major types of adrenergic receptors have been characterized; α_1, α_2, β_1, β_2, and β_3. Alpha- receptors are further divided into seven subtypes based upon their pharmacology and/or gene structure: α_{1A}, α_{1B}, α_{1C} and α_{1D}, and α_{2A}, α_{2B}, and α_{2C} (95). The mRNA expressions of almost all adrenergic receptors (except α_{1D}) have been detected in lactating bovine mammary tissues (95). However, mRNA coding for β_2-adrenergic receptors is the most abundant (95). *In vivo* studies led to the conclusion that β-

receptor stimulation increases milk removal (10, 17) while α-receptor activation decreases milk yield and peak flow (26, 27). In this current study, we have observed that adrenergic stimuli induce a secretory response, as indicated by an increase in anion secretion, in 1°BME cell monolayers. However, the underlying cellular mechanisms that account for the regulation and the ion transport remain to be defined. Carbamylcholine or carbachol is a muscarinic agonist and can stimulate Ca^{2+}-induced Cl^- secretion by many epithelia (58, 99). This study demonstrates for the first time that muscarinic receptors are present in 1°BME and are linked to changes in ion transport. This observation is particularly exciting because it suggests a novel mechanism with acute affects that can modify milk volume or composition. Clearly, the mechanisms of regulation in bovine mammary gland by muscarinic agonists required further investigation.

The current protocol to isolate and culture 1°CME and 1°BME was derived from previously published reports (1, 85, 147, 194, 198, 259). This study is valuable because it includes the assessment of ion transport across 1°CME and 1°BME. Due to the sample size of this study (n=1 for each species), the optimization of culture conditions will require additional work. Certainly, culture conditions will have effects on gene expression that will lead to changes in ion transport and ultimately to changes in milk volume and composition (224). The comparison of two growth media for 1°CME suggests that THM is better suited for the examination of ion transport. Further investigation is needed to determine whether THM is also suitable to culture BME.

One of the challenges from this study is removing fibroblasts and/or enriching the proportion of epithelial cells after isolation. The current protocol uses two steps to remove fibroblasts. The first step is sedimentation of fibroblasts at isolation because fibroblasts settle and attach more quickly than epithelial cells. Because fibroblasts will detach more readily than epithelial cells, the second step is trypsinization when passing cells The limitation of this method the loss many epithelial cells in the process of removing fibroblasts. In addition, increasing passage number of epithelial cells is associated with the loss of some initial epithelial characteristics. Although this is not unexpected, the current results suggest a practical limit of four or six passages before key characteristics are lost.

Many cell lines have been developed to elucidate mammary function. Immortalized bovine mammary epithelial cell lines are commonly used to characterize bovine mammary functions, such as BME-UV (262), HH2A (93), MAC-T (94) and L-1 (68). These cell lines provide valuable models, but each has distinct shortcomings. BME-UV cells were grown successfully on

permeable supports and provide a good model to study ion transport and responsiveness to steroid hormones, including the withdrawal of progesterone (181, 182, 197). Unfortunately, this cell line requires a complex medium with 15% serum and daily feeding, which makes them both cumbersome and costly to maintain. HH2A was the first cell line reported to expresses mammary-derived growth inhibitor (MDGI) and can be grown to form a three-dimensional structure in collagen gel (93). However, HH2A formed monolayers only when cultured in the contact with other cell types (*e.g.* fibroblasts) (93) and failed to synthesize detectable levels of milk proteins (262). MAC-T cells have been used to study insulin-like growth factor function (187), but a response to growth factor was not detected (262). Furthermore, MAC-T cells failed to form electrically resistive monolayers when first assessed in this laboratory. L-1 cells were reported to establish a duct-like structure in special cell culture gels, Matrigel (68), but there is no report to indicate that this cell line can form a resistive monolayer. Therefore, primary culture of bovine mammary epithelial cells may provide a better model to define key mammary functions. Caprine mammary epithelial cell lines are not used commonly, although tissue culture and *in vivo* studies were conducted with goat mammary gland (131, 134, 173). A goat mammary gland epithelial cell line (GMGE) was cultured on a solid substrate and used to study glycosylation of human erythropoietin, which was transfected into the cells (194). The caprine mammary epithelial cell line (CMEC) was derived from a lactating goat (171). Although these cells exhibited epithelial morphology on a solid substrate, there are no functional data regarding an epithelial barrier or ion transport. Current research provides functional data to indicate that 1°CME cells form electrically tight monolayers on permeable supports. Thus, this model system may provide a 'best' model to define ion transport in the caprine mammary gland.

In summary, this research provides a protocol to isolate and culture mammary gland epithelial cells. Primary (1°) CME and 1°BME were grown on permeable supports and formed electrically tight monolayers. However, the isolation and culture systems need to be optimized for the best media composition to grow 1°CME and 1°BME. The current data suggest that Na^+ transport is present in 1°CME, but was not detected in 1°BME. The establishment of a protocol to isolate and grow mammary gland epithelia is critical in order to define mammary gland function.

Chapter 4 - Discussion

This dissertation reports Na^+ transport across mammary gland epithelial cells that come from two different systems, an immortalized cell line and primary cultures. Results in Chapter 2 describe a novel pathway (Figure 2.13) through which cholera toxin (Ctx) upregulates epithelial Na^+ channel (ENaC)-mediated Na^+ absorption across MCF10A cells, a human mammary gland epithelial cell line. Ctx increases amiloride-sensitive short circuit current (I_{sc}), indicating enhanced Na^+ absorption. The outcomes suggest that Ctx enhances ENaC residency in the apical membrane and that the underlying mechanism is independent of the cyclic AMP and protein kinase A (cAMP/PKA) pathway. Ctx is secreted by the gram-negative bacterium *Vibrio cholera* and is responsible for massive secretory diarrhea. The heat labile toxin of *E. coli*, which also causes secretory diarrhea, is virtually identical in both structure and pathological mechanism (193). In general, Ctx is thought to act through cAMP/PKA-dependent pathway. In A6 cells, a cell line derived from *Xenopus laevis* kidney, Ctx increases the number of ENaC channels in the apical membrane by a cAMP-dependent mechanism, but without detectable effects on the open probability of the channel (144). However, in this report, cAMP antagonists did not inhibit Ctx-induced amiloride-sensitive I_{sc}, although a cAMP agonist did mimic the effect of Ctx. Similarly, the effect of Ctx was not blocked by inhibitors of PKA, phosphatidylinositol-4,5-bisphosphate 3-kinase (PI3K) and protein trafficking. Furthermore, Ctx effected neither the expression of mRNA encoding α-, β-, or γ-ENaC subunits nor levels of total protein for any of these subunits. Rather, the results show that Ctx changes the distribution of ENaC between cytosolic and apical pools. Ctx increases Nedd4-2 expression and the apparent ratio between the phosphorylated (inactive) and nonphosphorylated (inactive) forms. The greater overall amount of Nedd4-2 and the relatively greater amount of inactive Nedd4-2 may account for the elevated level of monoubiquitinated, but not polyubiquitinated ENaC subunits, which would be expected to reduce protein retrieval from the apical membrane and, subsequently, protein degradation. Regardless, the results demonstrate that corticosteroids substantially upregulate the expression of mRNA coding for ENaC subunits and that corticosteroids are required for amiloride-sensitive transport to be detected. The results demonstrate that Ctx enhances Na^+ absorption by elevating the proportion of ENaC in the apical membrane of these mammary epithelial cells.

Results in Chapter 3 provide preliminary data on hormonal regulation of ENaC mediated Na^+ transport across freshly isolated caprine and bovine mammary epithelial cells. A protocol to isolate and culture mammary gland epithelial cells on permeable supports is reported. Caprine (1°CME) and bovine mammary epithelia (1°BME) formed electrically tight epithelial barriers and they were grown as tight monolayers in multiple subcultures. In the presence of corticosteroids, 1°CME exhibited amiloride-sensitive I_{sc} suggesting ENaC mediated Na^+ transport. However, 1°BME exhibited no detectable amiloride-sensitive I_{sc} in the absence or presence of dexamethasone. Rather, 1°BME responded to an adrenergic agonist, norepinephrine, and a cholinergic agonist, carbamylcholine, with rapid increases in I_{sc}. The outcomes demonstrated that 1°CME and1°BME can develop as electrically tight monolayers capable of transporting ions in response to hormone or neurotransmitters exposure. Thus, this cell isolation and culture protocol can be used to generate tightly paired samples for transport and secretion studies.

It is a challenge to investigate hormonal regulation of ion transport across mammary epithelial cells. First, the combinations of steroid and protein hormones and growth factors that can regulate mammary epithelial function are complex during all stages of mammary development. Second, the mammary gland structures are complex, which makes *in situ* or *ex vivo* measurement very difficult. Together, these factors have left the molecular mechanisms of ion transport across mammary epithelia largely uncharacterized. Therefore, this dissertation, which focuses on defining the mechanisms of Na^+ transport in mammary glands by using *in vitro* cell models, provides valuable information regarding the mechanisms that can be observed and and the procedures that might be used to generate new tools for further characterizing the system. MCF10A cells provide a good *in vitro* model to study human mammary epithelial ion transport. This cell line is immortal, but was not transformed (225). It responds to hormones and growth factors during culture (225). This cell line also expresses prolactin receptor (154), but lacks estrogen receptor (44). Based on these features, MCF10A cells often are used as control cells in *in vitro* breast cancer studies. Moreover, MCF10A cells have the ability to grow in three-dimensional (3D) culture, and thereby are capable of recapitulating (45, 86). Importantly, MCF10A cells can grow as electrically tight monolayers that exhibit hormone-sensitive ion transport. However, milk proteins were not reported to be expressed in MCF10A cells (252). Casein expression was detected when MCF10A cells were co-cultured with human mammary

fibroblasts and adipose-derived stem cells in a 3D culture system (252). Taken together, MCF10A monolayer cultures provide a good model to study ion transport across human mammary epithelia but has clear limitations. Therefore, we sought to optimize conditions to isolate and grow primary mammary gland epithelial cells from dairy animals.

In Chapter 3, only one bovine and one goat mammary gland were obtained for the study, which accounts for substantial limitations on the conclusions that can be drawn. Nonetheless, the data provide meaningful direction for future studies. A protocol to isolate and grow primary mammary epithelial cells as electrically tight monolayers on permeable supports was demonstrated and can be optimized. Much work remains to be done in order to establish a primary cell culture system to study hormonal-sensitive ion transport across mammary gland epithelia. We exposed mammary tissues to enzymatic solutions for 90 minutes to isolate cells, which may not be optimal. Others reported enzymatic digestion times varying from 30 minutes (259) to 1 hour (171), and to even as long as14 hours (1). It is possible that there are species-specific digestion times to dissociate healthy epithelial cells from mammary tissues. Moreover, we employed a single set of enzyme concentrations, 300 U/ml collagenase and trypsin in PBS with disodium EDTA. Additional work is needed to assess alternate enzyme conditions. Further, it is challenging to obtain homogeneous epithelial cell samples from a heterogeneous cell population in fresh mammary tissue. Currently we reported a two-step process to separate epithelial cells from fibroblasts. The first step included sedimentation for 30 minutes, twice, to allow fibroblasts to attach when epithelial cells remain suspended (214). Following this step and the establishement of cell proliferation, we used selective trypsinization to enrich epithelial cell population when cells were passed (53, 171). Several methods can be used to enrich epithelial cells populations. A reported protocol for isolation of mammary epithelial cells from non-lactating pregnant cows implemented the use of antibody against milk fat globule membrane protein, PAS III, in flow cytometry to obtain an homogeneous epithelial cell population (69). Density gradient centrifugation also was used to separate epithelial cells from nonepithelial elements (151). Rat and cow mammary epithelial cell cultures were generated using this method to separate cells and tissues in colloidal silica media which contain particular density region to sediment epithelial cells population (151). Moreover, a gravity sedimentation approach has been used to separate cells from connective tissue after digestion (137). Thus, many options are available that could be tested to optimize the procedure further.

Mammary culture media are complex when compared to culture media for many other cell types. One of the goals for this study is to optimize culture conditions to grow primary mammary epithelial cells. Two different media compositions were used to grow 1°CME. The first medium, typical human media (THM), has been used to grow MCF10A cells. This medium contains 5% horse serum, hydrocortisone and EGF. The second medium, TBM, which was used to culture a bovine mammary cell line, BME-UV, includes a combination of four commercially available base media with three types of serum, but lacks hydrocortisone and EGF. The data suggest that 1°CME exhibited higher electrical resistance in THM, compared to TBM. Moreover, amiloride-sensitive I_{sc} was detected only when 1°CME were grown in THM. These data suggest that THM may be better suited to grow 1°CME, or at least to induce a measurable level of ion transport, when compared to the bovine medium. Tissues from lactating cows were reported to pose special challenges in cell isolation and culture because the cells were fragile in enzymatic solution; cells did not grow if tissues were exposed to digestive enzymes longer than 90 minutes (137). In the current report, we isolated and grew 1°BME on permeable supports successfully using tissues enzymatic dissociated for 90 minutes. The 1°BME formed electrically tight monolayers and responded to adrenergic and cholinergic agonists. Reports from this laboratory demonstrated that glucocorticoids induce amiloride-sensitive I_{sc} across BME-UV cell monolayers (182, 197). However, 1°BME failed to respond to dexamethasone with amiloride-sensitive I_{sc}. From these limited observations, it is difficult to make conclusions regarding the effect of steroid hormones on primary bovine mammary epithelial cells. More experiments should be conducted to characterize hormone-sensitive ion transport across mammary epithelial cells derived from multiple individuals and epithelial cells derived from different portions of the gland. Importantly, this report defines a protocol that was successful in isolation and growing 1°CME and 1°BME on permeable supports as electrically tight monolayers.

Na^+ transport has a close relationship with mammary gland health. The link between Na^+ transport and mammary epithelial integrative has been shown by using an *in vitro* system employing BME-UVcells in this laboratory (182, 197). Changes in Na^+ concentration on the apical (*i.e.*, milk) side of the cells had a rapid and profound impact on the epithelial barrier (181). A reduction in the apical Na^+ concentration led to an increase in epithelial electrical resistance, indicating a tight epithelial barrier. Loss of the mammary epithelial barrier is documented in mastitis, which is the most costly disease in the dairy industry in North America (181, 264). The

pathophysiology of mastitis remains poorly understood. Elevated milk electrical conductivity and elevated electrolytes have been used to indicate the preclinical stages of mastitis (130). There are ongoing questions whether mastitis compromises the epithelia barrier to induce an increase in milk electrolytes or whether mastitis induces a decrease in the activity of Na^+ absorption mechanisms to increase milk electrolytes, thereby causing the epithelia barrier to break down. Our outcomes suggest that ENaC-mediated Na^+ absorption across mammary epithelium, which is regulated by corticosteroids, can contribute to the generation and maintenance of the epithelial barrier (182). Conversely, the results suggested that a reduction in ENaC activity might contribute to mastitis disease progression. *Escherichia coli,* which are Gram-negative bacteria, commonly cause bovine mastitis (89). Although cholera toxin is not a common pathogen found in mastitic cows, its structure and response pathway are similar to *Escherichia coli* heat labile toxin (228). Therefore, the identity of key intermediates by which Ctx modulates ENaC-mediated Na^+ absorption might provide novel targets to treat or prevent mastitis. *In vitro* cell models of primary mammary gland epithelial cells can be developed to study the cellular mechanisms for treating and/or preventing mastitis.

In summary, this dissertation focuses on identifying mechanisms that regulate Na^+ transport across mammary gland epithelial cells. Corticosteroids induce mammary epithelia to express ENaC at significant levels, which can account for low Na^+ concentration in human milk. Ctx potentiates the effect by enhancing ENaC localization in the apical membrane. This signaling mechanism is independent of cAMP/PKA and reflects a novel pathway characterized by prevention of ENaC degradation and enhancement of channel monoubiquitination. In the mammary gland, these processes are expected to either further reduce the Na^+ concentration in milk or reduce the fluid volume that is secreted. This novel regulation of Na^+ transport across human mammary epithelial cells establishes a foundation for understanding human milk composition and potentially has broad implications for the regulation of fluid and electrolyte balance throughout the body. This new regulatory pathway may provide new targets to treat or prevent mastitis. Moreover, optimization and development of a method to isolate and grow primary mammary gland epithelial cells will provide valuable *in vitro* cell models to study mechanisms of hormone-sensitive ion transport across mammary gland.

Appendix A - Glossary of Acronyms

5-HT	5-hydroxytryptamine or serotonin
βCN1-28	β-casein 1 to 28
AngII	Angiotensin II
ASDN	aldosterone-sensitive distal nephron
CF	Cystic fibrosis
CFTR	Cystic fibrosis transmembrane conductance regulator
Ctx	Cholera toxin
EGF	Epidermal growth factor
ENaC	Epithelial Na^+ channel
ERK	Extracellular signal-regulated kinases
FIL	Feedback inhibitor of lactation
HME	Human mammary epithelial cells
hTERT	Human telomerase
I_{sc}	Short circuit current
JAK2	Janus kinase 2
MAPK	Mitogen-activated protein kinases
MFG	Milk fat globule
mTORC-2	mammalian target of rapamycin complex-2
NEDD4	Neural precursor cells expressed developmentally downregulated
PHA-1	Pseudohypoaldosteronism type 1
PI3K	phosphatidylinositol 3'-kinase
PKA	Protein kinase A or cAMP-dependent protein kinase
R_{te}	Transepithelial electrical resistance
SERT	Serotonin reuptake transporter
SGK	Serum and glucocorticoid-induced kinase
STAT5	Signal transducer and activator of transcription 5
T-HME	see HME

References

1. **Ahn JY, Aoki N, Adachi T, Mizuno Y, Nakamura R, and Matsuda T.** Isolation and culture of bovine mammary epithelial cells and establishment of gene transfection conditions in the cells. *Biosci Biotechnol Biochem* 59: 59-64, 1995.
2. **Ahn YJ, Brooker DR, Kosari F, Harte BJ, Li J, Mackler SA, and Kleyman TR.** Cloning and functional expression of the mouse epithelial sodium channel. *Am J Physiol* 277: F121-129, 1999.
3. **Alvarez de la Rosa D, Zhang P, Naray-Fejes-Toth A, Fejes-Toth G, and Canessa CM.** The serum and glucocorticoid kinase sgk increases the abundance of epithelial sodium channels in the plasma membrane of Xenopus oocytes. *J Biol Chem* 274: 37834-37839, 1999.
4. **Babini E, Geisler HS, Siba M, and Grunder S.** A new subunit of the epithelial Na+ channel identifies regions involved in Na+ self-inhibition. *J Biol Chem* 278: 28418-28426, 2003.
5. **Ball RK, Friis RR, Schoenenberger CA, Doppler W, and Groner B.** Prolactin regulation of beta-casein gene expression and of a cytosolic 120-kd protein in a cloned mouse mammary epithelial cell line. *EMBO J* 7: 2089-2095, 1988.
6. **Barker PM, Nguyen MS, Gatzy JT, Grubb B, Norman H, Hummler E, Rossier B, Boucher RC, and Koller B.** Role of gammaENaC subunit in lung liquid clearance and electrolyte balance in newborn mice. Insights into perinatal adaptation and pseudohypoaldosteronism. *J Clin Invest* 102: 1634-1640, 1998.
7. **Baudracco J, Lopez-Villalobos N, Holmes CW, Comeron EA, Macdonald KA, Barry TN, and Friggens NC.** e-Cow: an animal model that predicts herbage intake, milk yield and live weight change in dairy cows grazing temperate pastures, with and without supplementary feeding. *Animal* 6: 980-993, 2012.
8. **Bauman DE and Currie WB.** Partitioning of nutrients during pregnancy and lactation: a review of mechanisms involving homeostasis and homeorhesis. *J Dairy Sci* 63: 1514-1529, 1980.
9. **Bentley PJ.** Amiloride: a potent inhibitor of sodium transport across the toad bladder. *J Physiol* 195: 317-330, 1968.
10. **Bernabe J and Peeters G.** Studies on the motility of smooth muscles of the teats in lactating cows. *J Dairy Res* 47: 259-275, 1980.
11. **Bertog M, Cuffe JE, Pradervand S, Hummler E, Hartner A, Porst M, Hilgers KF, Rossier BC, and Korbmacher C.** Aldosterone responsiveness of the epithelial sodium channel (ENaC) in colon is increased in a mouse model for Liddle's syndrome. *J Physiol* 586: 459-475, 2008.
12. **Bertog M, Smith DJ, Bielfeld-Ackermann A, Bassett J, Ferguson DJ, Korbmacher C, and Harris A.** Ovine male genital duct epithelial cells differentiate in vitro and express functional CFTR and ENaC. *Am J Physiol Cell Physiol* 278: C885-894, 2000.
13. **Bhalla V and Hallows KR.** Mechanisms of ENaC regulation and clinical implications. *J Am Soc Nephrol* 19: 1845-1854, 2008.
14. **Bisbee CA.** Prolactin effects on ion transport across cultured mouse mammary epithelium. *Am J Physiol* 240: C110-115, 1981.
15. **Blaug S, Hybiske K, Cohn J, Firestone GL, Machen TE, and Miller SS.** ENaC- and CFTR-dependent ion and fluid transport in mammary epithelia. *Am J Physiol Cell Physiol* 281: C633-648, 2001.

16. **Blazer-Yost BL and Nofziger C.** The role of the phosphoinositide pathway in hormonal regulation of the epithelial sodium channel. *Adv Exp Med Biol* 559: 359-368, 2004.
17. **Blum JW, Schams D, and Bruckmaier R.** Catecholamines, oxytocin and milk removal in dairy cows. *J Dairy Res* 56: 167-177, 1989.
18. **Boucher RC, Cotton CU, Gatzy JT, Knowles MR, and Yankaskas JR.** Evidence for reduced Cl- and increased Na+ permeability in cystic fibrosis human primary cell cultures. *J Physiol* 405: 77-103, 1988.
19. **Boulkroun S, Ruffieux-Daidie D, Vitagliano JJ, Poirot O, Charles RP, Lagnaz D, Firsov D, Kellenberger S, and Staub O.** Vasopressin-inducible ubiquitin-specific protease 10 increases ENaC cell surface expression by deubiquitylating and stabilizing sorting nexin 3. *Am J Physiol Renal Physiol* 295: F889-900, 2008.
20. **Boyd C and Naray-Fejes-Toth A.** Steroid-mediated regulation of the epithelial sodium channel subunits in mammary epithelial cells. *Endocrinology* 148: 3958-3967, 2007.
21. **Briand P, Petersen OW, and Van Deurs B.** A new diploid nontumorigenic human breast epithelial cell line isolated and propagated in chemically defined medium. *In Vitro Cell Dev Biol* 23: 181-188, 1987.
22. **Brisken C, Park S, Vass T, Lydon JP, O'Malley BW, and Weinberg RA.** A paracrine role for the epithelial progesterone receptor in mammary gland development. *Proc Natl Acad Sci U S A* 95: 5076-5081, 1998.
23. **Brooks HL, Allred AJ, Beutler KT, Coffman TM, and Knepper MA.** Targeted proteomic profiling of renal Na(+) transporter and channel abundances in angiotensin II type 1a receptor knockout mice. *Hypertension* 39: 470-473, 2002.
24. **Brouard M, Casado M, Djelidi S, Barrandon Y, and Farman N.** Epithelial sodium channel in human epidermal keratinocytes: expression of its subunits and relation to sodium transport and differentiation. *J Cell Sci* 112 (Pt 19): 3343-3352, 1999.
25. **Bruce MC, Kanelis V, Fouladkou F, Debonneville A, Staub O, and Rotin D.** Regulation of Nedd4-2 self-ubiquitination and stability by a PY motif located within its HECT-domain. *Biochem J* 415: 155-163, 2008.
26. **Bruckmaier R, Mayer H, and Schams D.** Effects of alpha- and beta-adrenergic agonists on intramammary pressure and milk flow in dairy cows. *J Dairy Res* 58: 411-419, 1991.
27. **Bruckmaier RM, Wellnitz O, and Blum JW.** Inhibition of milk ejection in cows by oxytocin receptor blockade, alpha-adrenergic receptor stimulation and in unfamiliar surroundings. *J Dairy Res* 64: 315-325, 1997.
28. **Butte NF, Hopkinson JM, Mehta N, Moon JK, and Smith EO.** Adjustments in energy expenditure and substrate utilization during late pregnancy and lactation. *Am J Clin Nutr* 69: 299-307, 1999.
29. **Butterworth MB, Edinger RS, Frizzell RA, and Johnson JP.** Regulation of the epithelial sodium channel by membrane trafficking. *Am J Physiol Renal Physiol* 296: F10-24, 2009.
30. **Cailleau R, Young R, Olive M, and Reeves WJ, Jr.** Breast tumor cell lines from pleural effusions. *J Natl Cancer Inst* 53: 661-674, 1974.
31. **Caldwell RA, Boucher RC, and Stutts MJ.** Serine protease activation of near-silent epithelial Na+ channels. *Am J Physiol Cell Physiol* 286: C190-194, 2004.
32. **Canessa CM.** Structural biology: unexpected opening. *Nature* 449: 293-294, 2007.
33. **Canessa CM, Horisberger JD, and Rossier BC.** Epithelial sodium channel related to proteins involved in neurodegeneration. *Nature* 361: 467-470, 1993.

34. **Canessa CM, Schild L, Buell G, Thorens B, Gautschi I, Horisberger JD, and Rossier BC.** Amiloride-sensitive epithelial Na+ channel is made of three homologous subunits. *Nature* 367: 463-467, 1994.
35. **Carlin RW, Lee JH, Marcus DC, and Schultz BD.** Adenosine stimulates anion secretion across cultured and native adult human vas deferens epithelia. *Biol Reprod* 68: 1027-1034, 2003.
36. **Carlin RW, Sedlacek RL, Quesnell RR, Pierucci-Alves F, Grieger DM, and Schultz BD.** PVD9902, a porcine vas deferens epithelial cell line that exhibits neurotransmitter-stimulated anion secretion and expresses numerous HCO3(-) transporters. *Am J Physiol* 290: C1560-1571, 2006.
37. **Champigny G, Voilley N, Lingueglia E, Friend V, Barbry P, and Lazdunski M.** Regulation of expression of the lung amiloride-sensitive Na+ channel by steroid hormones. *EMBO J* 13: 2177-2181, 1994.
38. **Chang SS, Grunder S, Hanukoglu A, Rosler A, Mathew PM, Hanukoglu I, Schild L, Lu Y, Shimkets RA, Nelson-Williams C, Rossier BC, and Lifton RP.** Mutations in subunits of the epithelial sodium channel cause salt wasting with hyperkalaemic acidosis, pseudohypoaldosteronism type 1. *Nat Genet* 12: 248-253, 1996.
39. **Chen SY, Bhargava A, Mastroberardino L, Meijer OC, Wang J, Buse P, Firestone GL, Verrey F, and Pearce D.** Epithelial sodium channel regulated by aldosterone-induced protein sgk. *Proc Natl Acad Sci U S A* 96: 2514-2519, 1999.
40. **Collawn JF, Lazrak A, Bebok Z, and Matalon S.** The CFTR and ENaC debate: how important is ENaC in CF lung disease? *Am J Physiol Lung Cell Mol Physiol* 302: L1141-1146, 2012.
41. **Collier RJ, Hernandez LL, and Horseman ND.** Serotonin as a homeostatic regulator of lactation. *Domest Anim Endocrinol* 43: 161-170, 2012.
42. **Cordas E, Naray-Fejes-Toth A, and Fejes-Toth G.** Subcellular location of serum- and glucocorticoid-induced kinase-1 in renal and mammary epithelial cells. *Am J Physiol Cell Physiol* 292: C1971-1981, 2007.
43. **Couloigner V, Fay M, Djelidi S, Farman N, Escoubet B, Runembert I, Sterkers O, Friedlander G, and Ferrary E.** Location and function of the epithelial Na channel in the cochlea. *Am J Physiol Renal Physiol* 280: F214-222, 2001.
44. **Cvetkovic D, Dragan M, Leith SJ, Mir ZM, Leong HS, Pampillo M, Lewis JD, Babwah AV, and Bhattacharya M.** KISS1R induces invasiveness of estrogen receptor-negative human mammary epithelial and breast cancer cells. *Endocrinology* 154: 1999-2014.
45. **Debnath J, Muthuswamy SK, and Brugge JS.** Morphogenesis and oncogenesis of MCF-10A mammary epithelial acini grown in three-dimensional basement membrane cultures. *Methods* 30: 256-268, 2003.
46. **Debonneville C, Flores SY, Kamynina E, Plant PJ, Tauxe C, Thomas MA, Munster C, Chraibi A, Pratt JH, Horisberger JD, Pearce D, Loffing J, and Staub O.** Phosphorylation of Nedd4-2 by Sgk1 regulates epithelial Na(+) channel cell surface expression. *EMBO J* 20: 7052-7059, 2001.
47. **Deng J, Wang DX, Deng W, Li CY, Tong J, and Ma H.** Regulation of alveolar fluid clearance and ENaC expression in lung by exogenous angiotensin II. *Respir Physiol Neurobiol* 181: 53-61, 2011.
48. **Dinudom A, Young JA, and Cook DI.** Amiloride-sensitive Na+ current in the granular duct cells of mouse mandibular glands. *Pflugers Arch* 423: 164-166, 1993.

49. **Dixit G, Mikoryak C, Hayslett T, Bhat A, and Draper RK.** Cholera toxin up-regulates endoplasmic reticulum proteins that correlate with sensitivity to the toxin. *Exp Biol Med (Maywood)* 233: 163-175, 2008.
50. **Driscoll M and Chalfie M.** The mec-4 gene is a member of a family of Caenorhabditis elegans genes that can mutate to induce neuronal degeneration. *Nature* 349: 588-593, 1991.
51. **Duc C, Farman N, Canessa CM, Bonvalet JP, and Rossier BC.** Cell-specific expression of epithelial sodium channel alpha, beta, and gamma subunits in aldosterone-responsive epithelia from the rat: localization by in situ hybridization and immunocytochemistry. *J Cell Biol* 127: 1907-1921, 1994.
52. **Ebner KE, Hageman EC, and Larson BL.** Functional biochemical changes in bovine mammary cell cultures. *Exp Cell Res* 25: 555-570, 1961.
53. **Ebner KE, Hoover CR, Hageman EC, and Larson BL.** Cultivation and properties of bovine mammary cell cultures. *Exp Cell Res* 23: 373-385, 1961.
54. **Firsov D, Robert-Nicoud M, Gruender S, Schild L, and Rossier BC.** Mutational analysis of cysteine-rich domains of the epithelium sodium channel (ENaC). Identification of cysteines essential for channel expression at the cell surface. *J Biol Chem* 274: 2743-2749, 1999.
55. **Firsov D, Schild L, Gautschi I, Merillat AM, Schneeberger E, and Rossier BC.** Cell surface expression of the epithelial Na channel and a mutant causing Liddle syndrome: a quantitative approach. *Proc Natl Acad Sci U S A* 93: 15370-15375, 1996.
56. **Fischer H, Illek B, Negulescu PA, Clauss W, and Machen TE.** Carbachol-activated calcium entry into HT-29 cells is regulated by both membrane potential and cell volume. *Proc Natl Acad Sci U S A* 89: 1438-1442, 1992.
57. **Flezar M and Heisler S.** P2-purinergic receptors in human breast tumor cells: coupling of intracellular calcium signaling to anion secretion. *J Pharmacol Exp Ther* 265: 1499-1510, 1993.
58. **Flores CA, Melvin JE, Figueroa CD, and Sepulveda FV.** Abolition of Ca2+-mediated intestinal anion secretion and increased stool dehydration in mice lacking the intermediate conductance Ca2+-dependent K+ channel Kcnn4. *J Physiol* 583: 705-717, 2007.
59. **Fogg VC, Liu CJ, and Margolis B.** Multiple regions of Crumbs3 are required for tight junction formation in MCF10A cells. *J Cell Sci* 118: 2859-2869, 2005.
60. **Forouharmehr A, Harkinezhad T, and Qasemi-Panahi B.** Effect of Aflatoxin B1 on growth of bovine mammary epithelial cells in 3D and monolayer culture system. *Adv Pharm Bull* 3: 143-146, 2013.
61. **Fowler KJ, Walker F, Alexander W, Hibbs ML, Nice EC, Bohmer RM, Mann GB, Thumwood C, Maglitto R, Danks JA, and et al.** A mutation in the epidermal growth factor receptor in waved-2 mice has a profound effect on receptor biochemistry that results in impaired lactation. *Proc Natl Acad Sci U S A* 92: 1465-1469, 1995.
62. **Foxman B, D'Arcy H, Gillespie B, Bobo JK, and Schwartz K.** Lactation mastitis: occurrence and medical management among 946 breastfeeding women in the United States. *Am J Epidemiol* 155: 103-114, 2002.
63. **Fuller CM, Awayda MS, Arrate MP, Bradford AL, Morris RG, Canessa CM, Rossier BC, and Benos DJ.** Cloning of a bovine renal epithelial Na+ channel subunit. *Am J Physiol* 269: C641-654, 1995.
64. **Furuya K, Enomoto K, Furuya S, Yamagishi S, Edwards C, and Oka T.** Single calcium-activated potassium channel in cultured mammary epithelial cells. *Pflugers Arch* 414: 118-124, 1989.

65. **Gaffney EV.** A cell line (HBL-100) established from human breast milk. *Cell Tissue Res* 227: 563-568, 1982.
66. **Garty H and Palmer LG.** Epithelial sodium channels: function, structure, and regulation. *Physiol Rev* 77: 359-396, 1997.
67. **Gebre-Egziabher A, Wood HC, Robar JD, and Blankenagel G.** Evaluation of automatic mastitis detection equipment. *J Dairy Sci* 62: 1108-1114, 1979.
68. **German T and Barash I.** Characterization of an epithelial cell line from bovine mammary gland. *In Vitro Cell Dev Biol Anim* 38: 282-292, 2002.
69. **Gibson CA, Vega JR, Baumrucker CR, Oakley CS, and Welsch CW.** Establishment and characterization of bovine mammary epithelial cell lines. *In Vitro Cell Dev Biol* 27A: 585-594, 1991.
70. **Gjorevski N and Nelson CM.** Integrated morphodynamic signalling of the mammary gland. *Nat Rev Mol Cell Biol* 12: 581-593, 2011.
71. **Golestaneh N, Nicolas C, Picaud S, Ferrari P, and Mirshahi M.** The epithelial sodium channel (ENaC) in rodent retina, ontogeny and molecular identity. *Curr Eye Res* 21: 703-709, 2000.
72. **Gonzalez-Recio O, Ugarte E, and Bach A.** Trans-generational effect of maternal lactation during pregnancy: a Holstein cow model. *PLoS One* 7: e51816, 2013.
73. **Gordon KE, Binas B, Chapman RS, Kurian KM, Clarkson RW, Clark AJ, Lane EB, and Watson CJ.** A novel cell culture model for studying differentiation and apoptosis in the mouse mammary gland. *Breast Cancer Res* 2: 222-235, 2000.
74. **Gottardi CJ, Dunbar LA, and Caplan MJ.** Biotinylation and assessment of membrane polarity: caveats and methodological concerns. *Am J Physiol* 268: F285-295, 1995.
75. **Graham JD, Mote PA, Salagame U, Balleine RL, Huschtscha LI, and Clarke CL.** Hormone-responsive model of primary human breast epithelium. *J Mammary Gland Biol Neoplasia* 14: 367-379, 2009.
76. **Grotjohann I, Schulzke JD, and Fromm M.** Electrogenic Na+ transport in rat late distal colon by natural and synthetic glucocorticosteroids. *Am J Physiol* 276: G491-498, 1999.
77. **Grubb BR, O'Neal WK, Ostrowski LE, Kreda SM, Button B, and Boucher RC.** Transgenic hCFTR expression fails to correct beta-ENaC mouse lung disease. *Am J Physiol Lung Cell Mol Physiol* 302: L238-247, 2011.
78. **Grunder S, Firsov D, Chang SS, Jaeger NF, Gautschi I, Schild L, Lifton RP, and Rossier BC.** A mutation causing pseudohypoaldosteronism type 1 identifies a conserved glycine that is involved in the gating of the epithelial sodium channel. *EMBO J* 16: 899-907, 1997.
79. **Habran S, Pomeroy PP, Debier C, and Das K.** Changes in trace elements during lactation in a marine top predator, the grey seal. *Aquat Toxicol* 126: 455-466, 2012.
80. **Hackett AJ, Smith HS, Springer EL, Owens RB, Nelson-Rees WA, Riggs JL, and Gardner MB.** Two syngeneic cell lines from human breast tissue: the aneuploid mammary epithelial (Hs578T) and the diploid myoepithelial (Hs578Bst) cell lines. *J Natl Cancer Inst* 58: 1795-1806, 1977.
81. **Hansson JH, Nelson-Williams C, Suzuki H, Schild L, Shimkets R, Lu Y, Canessa C, Iwasaki T, Rossier B, and Lifton RP.** Hypertension caused by a truncated epithelial sodium channel gamma subunit: genetic heterogeneity of Liddle syndrome. *Nat Genet* 11: 76-82, 1995.
82. **Hanukoglu A.** Type I pseudohypoaldosteronism includes two clinically and genetically distinct entities with either renal or multiple target organ defects. *J Clin Endocrinol Metab* 73: 936-944, 1991.

83. **Hapon MB, Simoncini M, Via G, and Jahn GA.** Effect of hypothyroidism on hormone profiles in virgin, pregnant and lactating rats, and on lactation. *Reproduction* 126: 371-382, 2003.
84. **Hassiotou F and Geddes D.** Anatomy of the human mammary gland: Current status of knowledge. *Clin Anat* 26: 29-48, 2012.
85. **He YL, Wu YH, He XN, Liu FJ, He XY, and Zhang Y.** An immortalized goat mammary epithelial cell line induced with human telomerase reverse transcriptase (hTERT) gene transfer. *Theriogenology* 71: 1417-1424, 2009.
86. **Hebner C, Weaver VM, and Debnath J.** Modeling morphogenesis and oncogenesis in three-dimensional breast epithelial cultures. *Annu Rev Pathol* 3: 313-339, 2008.
87. **Hennighausen L and Robinson GW.** Information networks in the mammary gland. *Nat Rev Mol Cell Biol* 6: 715-725, 2005.
88. **Hershko A and Ciechanover A.** The ubiquitin system. *Annu Rev Biochem* 67: 425-479, 1998.
89. **Hogan J and Larry Smith K.** Coliform mastitis. *Vet Res* 34: 507-519, 2003.
90. **Holt C.** Swelling of Golgi vesicles in mammary secretory cells and its relation to the yield and quantitative composition of milk. *J Theor Biol* 101: 247-261, 1983.
91. **Hughey RP, Bruns JB, Kinlough CL, Harkleroad KL, Tong Q, Carattino MD, Johnson JP, Stockand JD, and Kleyman TR.** Epithelial sodium channels are activated by furin-dependent proteolysis. *J Biol Chem* 279: 18111-18114, 2004.
92. **Hummler E, Barker P, Gatzy J, Beermann F, Verdumo C, Schmidt A, Boucher R, and Rossier BC.** Early death due to defective neonatal lung liquid clearance in alpha-ENaC-deficient mice. *Nat Genet* 12: 325-328, 1996.
93. **Huynh H and Pollak M.** HH2A, an immortalized bovine mammary epithelial cell line, expresses the gene encoding mammary derived growth inhibitor (MDGI). *In Vitro Cell Dev Biol Anim* 31: 25-29, 1995.
94. **Huynh HT, Robitaille G, and Turner JD.** Establishment of bovine mammary epithelial cells (MAC-T): an in vitro model for bovine lactation. *Exp Cell Res* 197: 191-199, 1991.
95. **Inderwies T, Pfaffl MW, Meyer HH, Blum JW, and Bruckmaier RM.** Detection and quantification of mRNA expression of alpha- and beta-adrenergic receptor subtypes in the mammary gland of dairy cows. *Domest Anim Endocrinol* 24: 123-135, 2003.
96. **Ismailov, II, Awayda MS, Jovov B, Berdiev BK, Fuller CM, Dedman JR, Kaetzel M, and Benos DJ.** Regulation of epithelial sodium channels by the cystic fibrosis transmembrane conductance regulator. *J Biol Chem* 271: 4725-4732, 1996.
97. **Iwamori M, Takamizawa K, Momoeda M, Iwamori Y, and Taketani Y.** Gangliosides in human, cow and goat milk, and their abilities as to neutralization of cholera toxin and botulinum type A neurotoxin. *Glycoconj J* 25: 675-683, 2008.
98. **Ji HL, Zhao RZ, Chen ZX, Shetty S, Idell S, and Matalon S.** delta ENaC: a novel divergent amiloride-inhibitable sodium channel. *Am J Physiol Lung Cell Mol Physiol* 303: L1013-1026, 2012.
99. **Joo NS, Saenz Y, Krouse ME, and Wine JJ.** Mucus secretion from single submucosal glands of pig. Stimulation by carbachol and vasoactive intestinal peptide. *J Biol Chem* 277: 28167-28175, 2002.
100. **Kabra R, Knight KK, Zhou R, and Snyder PM.** Nedd4-2 induces endocytosis and degradation of proteolytically cleaved epithelial Na+ channels. *J Biol Chem* 283: 6033-6039, 2008.

101. **Kamynina E, Debonneville C, Bens M, Vandewalle A, and Staub O.** A novel mouse Nedd4 protein suppresses the activity of the epithelial Na+ channel. *FASEB J* 15: 204-214, 2001.
102. **Kase H, Iwahashi K, Nakanishi S, Matsuda Y, Yamada K, Takahashi M, Murakata C, Sato A, and Kaneko M.** K-252 compounds, novel and potent inhibitors of protein kinase C and cyclic nucleotide-dependent protein kinases. *Biochem Biophys Res Commun* 142: 436-440, 1987.
103. **Kellenberger S, Gautschi I, Rossier BC, and Schild L.** Mutations causing Liddle syndrome reduce sodium-dependent downregulation of the epithelial sodium channel in the Xenopus oocyte expression system. *J Clin Invest* 101: 2741-2750, 1998.
104. **Kellenberger S and Schild L.** Epithelial sodium channel/degenerin family of ion channels: a variety of functions for a shared structure. *Physiol Rev* 82: 735-767, 2002.
105. **Kemendy AE, Kleyman TR, and Eaton DC.** Aldosterone alters the open probability of amiloride-blockable sodium channels in A6 epithelia. *Am J Physiol* 263: C825-837, 1992.
106. **Keydar I, Chen L, Karby S, Weiss FR, Delarea J, Radu M, Chaitcik S, and Brenner HJ.** Establishment and characterization of a cell line of human breast carcinoma origin. *Eur J Cancer* 15: 659-670, 1979.
107. **Kim H, Farris J, Christman SA, Kong BW, Foster LK, O'Grady SM, and Foster DN.** Events in the immortalizing process of primary human mammary epithelial cells by the catalytic subunit of human telomerase. *Biochem J* 365: 765-772, 2002.
108. **Kim SH, Kim KX, Raveendran NN, Wu T, Pondugula SR, and Marcus DC.** Regulation of ENaC-mediated sodium transport by glucocorticoids in Reissner's membrane epithelium. *Am J Physiol Cell Physiol* 296: C544-557, 2009.
109. **Kim SH and Marcus DC.** Endolymphatic sodium homeostasis by extramacular epithelium of the saccule. *J Neurosci* 29: 15851-15858, 2009.
110. **Kim SH and Marcus DC.** Regulation of sodium transport in the inner ear. *Hear Res* 280: 21-29, 2011.
111. **Kimura S, Morimoto K, Okamoto H, Ueda H, Kobayashi D, Kobayashi J, and Morimoto Y.** Development of a human mammary epithelial cell culture model for evaluation of drug transfer into milk. *Arch Pharm Res* 29: 424-429, 2006.
112. **Kitchen BJ.** Review of the progress of dairy science: bovine mastitis: milk compositional changes and related diagnostic tests. *J Dairy Res* 48: 167-188, 1981.
113. **Kleyman TR and Cragoe EJ, Jr.** Cation transport probes: the amiloride series. *Methods Enzymol* 191: 739-755, 1990.
114. **Kleyman TR, Cragoe EJ, Jr., and Kraehenbuhl JP.** The cellular pool of Na+ channels in the amphibian cell line A6 is not altered by mineralocorticoids. Analysis using a new photoactive amiloride analog in combination with anti-amiloride antibodies. *J Biol Chem* 264: 11995-12000, 1989.
115. **Kleyman TR, Ernst SA, and Coupaye-Gerard B.** Arginine vasopressin and forskolin regulate apical cell surface expression of epithelial Na+ channels in A6 cells. *Am J Physiol* 266: F506-511, 1994.
116. **Kleyman TR, Sheng S, Kosari F, and Kieber-Emmons T.** Mechanism of action of amiloride: a molecular prospective. *Semin Nephrol* 19: 524-532, 1999.
117. **Kleyman TR, Smith PR, and Benos DJ.** Characterization and localization of epithelial Na+ channels in toad urinary bladder. *Am J Physiol* 266: C1105-1111, 1994.
118. **Knight CH, Peaker M, and Wilde CJ.** Local control of mammary development and function. *Rev Reprod* 3: 104-112, 1998.

119. **Koefoed-Johnsen V and Ussing HH.** The nature of the frog skin potential. *Acta Physiol Scand* 42: 298-308, 1958.
120. **Kosari F, Sheng S, Li J, Mak DO, Foskett JK, and Kleyman TR.** Subunit stoichiometry of the epithelial sodium channel. *J Biol Chem* 273: 13469-13474, 1998.
121. **Kretz O, Barbry P, Bock R, and Lindemann B.** Differential expression of RNA and protein of the three pore-forming subunits of the amiloride-sensitive epithelial sodium channel in taste buds of the rat. *J Histochem Cytochem* 47: 51-64, 1999.
122. **Kuhn NJ.** Progesterone withdrawal as the lactogenic trigger in the rat. *J Endocrinol* 44: 39-54, 1969.
123. **Lee SY, Palmer ML, Maniak PJ, Jang SH, Ryu PD, and O'Grady SM.** P2Y receptor regulation of sodium transport in human mammary epithelial cells. *Am J Physiol Cell Physiol* 293: C1472-1480, 2007.
124. **Lencer WI, Hirst TR, and Holmes RK.** Membrane traffic and the cellular uptake of cholera toxin. *Biochim Biophys Acta* 1450: 177-190, 1999.
125. **Liddle GW BT, Coppage WS Jr.** A familial renal disorder simulating primary aldosteronism but with negligible aldosterone secretion. *transactions of the association of american physicians* 76: 199-213, 1963.
126. **Lin W, Finger TE, Rossier BC, and Kinnamon SC.** Epithelial Na+ channel subunits in rat taste cells: localization and regulation by aldosterone. *J Comp Neurol* 405: 406-420, 1999.
127. **Lindemann B.** Receptors and transduction in taste. *Nature* 413: 219-225, 2001.
128. **Lindemann B.** Taste reception. *Physiol Rev* 76: 718-766, 1996.
129. **Lindemann B and Van Driessche W.** Sodium-specific membrane channels of frog skin are pores: current fluctuations reveal high turnover. *Science* 195: 292-294, 1977.
130. **Linzell JL and Peaker M.** Day-to-day variations in milk composition in the goat and cow as a guide to the detection of subclinical mastitis. *Br Vet J* 128: 284-295, 1972.
131. **Linzell JL and Peaker M.** The effects of oxytocin and milk removal on milk secretion in the goat. *J Physiol* 216: 717-734, 1971.
132. **Linzell JL and Peaker M.** Mechanism of milk secretion. *Physiol Rev* 51: 564-597, 1971.
133. **Linzell JL and Peaker M.** The permeability of mammary ducts. *J Physiol* 216: 701-716, 1971.
134. **Linzell JL and Peaker M.** Permeability of mammary ducts in the lactating goat. *J Physiol* 213: 48P-49P, 1971.
135. **Loffing J and Korbmacher C.** Regulated sodium transport in the renal connecting tubule (CNT) via the epithelial sodium channel (ENaC). *Pflugers Arch* 458: 111-135, 2009.
136. **Long W, Wagner KU, Lloyd KC, Binart N, Shillingford JM, Hennighausen L, and Jones FE.** Impaired differentiation and lactational failure of Erbb4-deficient mammary glands identify ERBB4 as an obligate mediator of STAT5. *Development* 130: 5257-5268, 2003.
137. **Mackenzie DD, Forsyth IA, Brooker BE, and Turvey A.** Culture of bovine mammary epithelial cells on collagen gels. *Tissue Cell* 14: 231-241, 1982.
138. **Mackenzie DD and Lascelles AK.** The movement of solutes across the epithelium of the ducts and cisterns in the mammary gland of the ewe. *Aust J Biol Sci* 18: 1035-1044, 1965.
139. **Malik B, Yue Q, Yue G, Chen XJ, Price SR, Mitch WE, and Eaton DC.** Role of Nedd4-2 and polyubiquitination in epithelial sodium channel degradation in untransfected renal A6 cells expressing endogenous ENaC subunits. *Am J Physiol Renal Physiol* 289: F107-116, 2005.

140. **Mall M, Grubb BR, Harkema JR, O'Neal WK, and Boucher RC.** Increased airway epithelial Na+ absorption produces cystic fibrosis-like lung disease in mice. *Nat Med* 10: 487-493, 2004.
141. **Marshall AM, Nommsen-Rivers LA, Hernandez LL, Dewey KG, Chantry CJ, Gregerson KA, and Horseman ND.** Serotonin transport and metabolism in the mammary gland modulates secretory activation and involution. *J Clin Endocrinol Metab* 95: 837-846.
142. **Marshall AM, Pai VP, Sartor MA, and Horseman ND.** In vitro multipotent differentiation and barrier function of a human mammary epithelium. *Cell Tissue Res* 335: 383-395, 2009.
143. **Martin RH and Oakey RE.** The role of antenatal oestrogen in post-partum human lactogenesis: evidence from oestrogen-deficient pregnancies. *Clin Endocrinol (Oxf)* 17: 403-408, 1982.
144. **Marunaka Y and Eaton DC.** Effects of vasopressin and cAMP on single amiloride-blockable Na channels. *Am J Physiol* 260: C1071-1084, 1991.
145. **Marunaka Y and Niisato N.** H89, an inhibitor of protein kinase A (PKA), stimulates Na+ transport by translocating an epithelial Na+ channel (ENaC) in fetal rat alveolar type II epithelium. *Biochem Pharmacol* 66: 1083-1089, 2003.
146. **Matalon S and O'Brodovich H.** Sodium channels in alveolar epithelial cells: molecular characterization, biophysical properties, and physiological significance. *Annu Rev Physiol* 61: 627-661, 1999.
147. **Matitashvili E and Bauman DE.** Culture of primary bovine mammary epithelial cells. *In Vitro Cell Dev Biol Anim* 35: 431-434, 1999.
148. **McDonald FJ, Price MP, Snyder PM, and Welsh MJ.** Cloning and expression of the beta- and gamma-subunits of the human epithelial sodium channel. *Am J Physiol* 268: C1157-1163, 1995.
149. **McDonald FJ, Snyder PM, McCray PB, Jr., and Welsh MJ.** Cloning, expression, and tissue distribution of a human amiloride-sensitive Na+ channel. *Am J Physiol* 266: L728-734, 1994.
150. **McDonald FJ, Yang B, Hrstka RF, Drummond HA, Tarr DE, McCray PB, Jr., Stokes JB, Welsh MJ, and Williamson RA.** Disruption of the beta subunit of the epithelial Na+ channel in mice: hyperkalemia and neonatal death associated with a pseudohypoaldosteronism phenotype. *Proc Natl Acad Sci U S A* 96: 1727-1731, 1999.
151. **McGrath MF.** A novel system for mammary epithelial cell culture. *J Dairy Sci* 70: 1967-1980, 1987.
152. **McManaman JL and Neville MC.** Mammary physiology and milk secretion. *Adv Drug Deliv Rev* 55: 629-641, 2003.
153. **McManaman JL, Reyland ME, and Thrower EC.** Secretion and fluid transport mechanisms in the mammary gland: comparisons with the exocrine pancreas and the salivary gland. *J Mammary Gland Biol Neoplasia* 11: 249-268, 2006.
154. **Meng J, Tsai-Morris CH, and Dufau ML.** Human prolactin receptor variants in breast cancer: low ratio of short forms to the long-form human prolactin receptor associated with mammary carcinoma. *Cancer Res* 64: 5677-5682, 2004.
155. **Mulac-Jericevic B, Mullinax RA, DeMayo FJ, Lydon JP, and Conneely OM.** Subgroup of reproductive functions of progesterone mediated by progesterone receptor-B isoform. *Science* 289: 1751-1754, 2000.

156. **Murray AJ.** Pharmacological PKA inhibition: all may not be what it seems. *Sci Signal* 1: re4, 2008.
157. **Naray-Fejes-Toth A, Canessa C, Cleaveland ES, Aldrich G, and Fejes-Toth G.** SGK is an aldosterone-induced kinase in the renal collecting duct. Effects on epithelial na+ channels. *J Biol Chem* 274: 16973-16978, 1999.
158. **Nedvetsky PI, Kwon SH, Debnath J, and Mostov KE.** Cyclic AMP regulates formation of mammary epithelial acini in vitro. *Mol Biol Cell* 23: 2973-2981, 2012.
159. **Neville MC.** Anatomy and physiology of lactation. *Pediatr Clin North Am* 48: 13-34, 2001.
160. **Neville MC.** The physiological basis of milk secretion. *Ann N Y Acad Sci* 586: 1-11, 1990.
161. **Neville MC, McFadden TB, and Forsyth I.** Hormonal regulation of mammary differentiation and milk secretion. *J Mammary Gland Biol Neoplasia* 7: 49-66, 2002.
162. **Nguyen DA and Neville MC.** Tight junction regulation in the mammary gland. *J Mammary Gland Biol Neoplasia* 3: 233-246, 1998.
163. **Nicco C, Wittner M, DiStefano A, Jounier S, Bankir L, and Bouby N.** Chronic exposure to vasopressin upregulates ENaC and sodium transport in the rat renal collecting duct and lung. *Hypertension* 38: 1143-1149, 2001.
164. **Nicholas K, Sharp J, Watt A, Wanyonyi S, Crowley T, Gillespie M, and Lefevre C.** The tammar wallaby: a model system to examine domain-specific delivery of milk protein bioactives. *Semin Cell Dev Biol* 23: 547-556, 2012.
165. **O'Donnell EK, Sedlacek RL, Singh AK, and Schultz BD.** Inhibition of enterotoxin-induced porcine colonic secretion by diarylsulfonylureas in vitro. *Am J Physiol Gastrointest Liver Physiol* 279: G1104-1112, 2000.
166. **Oda Y, Imanzahrai A, Kwong A, Komuves L, Elias PM, Largman C, and Mauro T.** Epithelial sodium channels are upregulated during epidermal differentiation. *J Invest Dermatol* 113: 796-801, 1999.
167. **Oftedal OT.** Milk composition, milk yield, and energy output at peak lactation: A comparative review. *Physiological Strategies in lactation* edited by Peaker M, Vernon RG and Knight CH, London. Academic Press: p. 33-85, 1984.
168. **Ontsouka CE, Bruckmaier RM, and Blum JW.** Fractionized milk composition during removal of colostrum and mature milk. *J Dairy Sci* 86: 2005-2011, 2003.
169. **Palmer LG, Patel A, and Frindt G.** Regulation and dysregulation of epithelial Na+ channels. *Clin Exp Nephrol* 16: 35-43, 2011.
170. **Palmer ML, Peitzman ER, Maniak PJ, Sieck GC, Prakash YS, and O'Grady SM.** K(Ca)3.1 channels facilitate K+ secretion or Na+ absorption depending on apical or basolateral P2Y receptor stimulation. *J Physiol* 589: 3483-3494, 2011.
171. **Pantschenko AG, Woodcock-Mitchell J, Bushmich SL, and Yang TJ.** Establishment and characterization of a caprine mammary epithelial cell line (CMEC). *In Vitro Cell Dev Biol Anim* 36: 26-37, 2000.
172. **Park S, Mazina O, Kitagawa A, Wong P, and Matsumura F.** TCDD causes suppression of growth and differentiation of MCF10A, human mammary epithelial cells by interfering with their insulin receptor signaling through c-Src kinase and ERK activation. *J Biochem Mol Toxicol* 18: 322-331, 2004.
173. **Paterson JY and Linzell JL.** The secretion of cortisol and its mammary uptake in the goat. *J Endocrinol* 50: 493-499, 1971.

174. **Paunescu TG, Blazer-Yost BL, Vlahos CJ, and Helman SI.** LY-294002-inhibitable PI 3-kinase and regulation of baseline rates of Na(+) transport in A6 epithelia. *Am J Physiol Cell Physiol* 279: C236-247, 2000.
175. **Peaker M and Taylor JC.** Milk secretion in the rabbit: changes during lactation and the mechanism of ion transport. *J Physiol* 253: 527-545, 1975.
176. **Phillips ML and Schultz BD.** Steroids modulate transepithelial resistance and Na(+) absorption across cultured porcine vas deferens epithelia. *Biol Reprod* 66: 1016-1023, 2002.
177. **Piacentini GL, Boner AL, Richelli CC, and Gaburro D.** Artificial feeding: progresses and problems. *Ann Ist Super Sanita* 31: 411-418, 1995.
178. **Pierucci-Alves F, Akoyev V, Stewart JC, 3rd, Wang LH, Janardhan KS, and Schultz BD.** Swine models of cystic fibrosis reveal male reproductive tract phenotype at birth. *Biol Reprod* 85: 442-451, 2011.
179. **Pondugula SR, Raveendran NN, Ergonul Z, Deng Y, Chen J, Sanneman JD, Palmer LG, and Marcus DC.** Glucocorticoid regulation of genes in the amiloride-sensitive sodium transport pathway by semicircular canal duct epithelium of neonatal rat. *Physiol Genomics* 24: 114-123, 2006.
180. **Puoti A, May A, Canessa CM, Horisberger JD, Schild L, and Rossier BC.** The highly selective low-conductance epithelial Na channel of Xenopus laevis A6 kidney cells. *Am J Physiol* 269: C188-197, 1995.
181. **Quesnell RR, Erickson J, and Schultz BD.** Apical electrolyte concentration modulates barrier function and tight junction protein localization in bovine mammary epithelium. *Am J Physiol* 292: C305-318, 2007.
182. **Quesnell RR, Han X, and Schultz BD.** Glucocorticoids stimulate ENaC upregulation in bovine mammary epithelium. *Am J Physiol* 292: C1739-1745, 2007.
183. **Raikwar NS and Thomas CP.** Nedd4-2 isoforms ubiquitinate individual epithelial sodium channel subunits and reduce surface expression and function of the epithelial sodium channel. *Am J Physiol Renal Physiol* 294: F1157-1165, 2008.
184. **Ramanathan HN and Ye Y.** Cellular strategies for making monoubiquitin signals. *Crit Rev Biochem Mol Biol* 47: 17-28, 2011.
185. **Record RD, Froelich LL, Vlahos CJ, and Blazer-Yost BL.** Phosphatidylinositol 3-kinase activation is required for insulin-stimulated sodium transport in A6 cells. *Am J Physiol* 274: E611-617, 1998.
186. **Reichmann E, Ball R, Groner B, and Friis RR.** New mammary epithelial and fibroblastic cell clones in coculture form structures competent to differentiate functionally. *J Cell Biol* 108: 1127-1138, 1989.
187. **Robinson RM, Akers RM, and Forsten KE.** Real-time detection of insulin-like growth factor-1 stimulation of the MAC-T bovine mammary epithelial cell line. *Endocrine* 13: 345-352, 2000.
188. **Rohrwasser A, Morgan T, Dillon HF, Zhao L, Callaway CW, Hillas E, Zhang S, Cheng T, Inagami T, Ward K, Terreros DA, and Lalouel JM.** Elements of a paracrine tubular renin-angiotensin system along the entire nephron. *Hypertension* 34: 1265-1274, 1999.
189. **Rotin D, Kanelis V, and Schild L.** Trafficking and cell surface stability of ENaC. *Am J Physiol Renal Physiol* 281: F391-399, 2001.
190. **Rotin D and Staub O.** Nedd4-2 and the regulation of epithelial sodium transport. *Front Physiol* 3: 212, 2012.

191. **Roudier-Pujol C, Rochat A, Escoubet B, Eugene E, Barrandon Y, Bonvalet JP, and Farman N.** Differential expression of epithelial sodium channel subunit mRNAs in rat skin. *J Cell Sci* 109 (Pt 2): 379-385, 1996.
192. **Sadowski M, Suryadinata R, Tan AR, Roesley SN, and Sarcevic B.** Protein monoubiquitination and polyubiquitination generate structural diversity to control distinct biological processes. *IUBMB Life* 64: 136-142, 2011.
193. **Sanchez J and Holmgren J.** Cholera toxin structure, gene regulation and pathophysiological and immunological aspects. *Cell Mol Life Sci* 65: 1347-1360, 2008.
194. **Sanchez O, Montesino R, Toledo JR, Rodriguez E, Diaz D, Royle L, Rudd PM, Dwek RA, Gerwig GJ, Kamerling JP, Harvey DJ, and Cremata JA.** The goat mammary glandular epithelial (GMGE) cell line promotes polyfucosylation and N,N'-diacetyllactosediaminylation of N-glycans linked to recombinant human erythropoietin. *Arch Biochem Biophys* 464: 322-334, 2007.
195. **Schild L.** The epithelial sodium channel: from molecule to disease. *Rev Physiol Biochem Pharmacol* 151: 93-107, 2004.
196. **Schild L, Lu Y, Gautschi I, Schneeberger E, Lifton RP, and Rossier BC.** Identification of a PY motif in the epithelial Na channel subunits as a target sequence for mutations causing channel activation found in Liddle syndrome. *EMBO J* 15: 2381-2387, 1996.
197. **Schmidt CR, Carlin RW, Sargeant JM, and Schultz BD.** Neurotransmitter-stimulated ion transport across cultured bovine mammary epithelial cell monolayers. *J Dairy Sci* 84: 2622-2631, 2001.
198. **Sedlacek RL, Carlin RW, Singh AK, and Schultz BD.** Neurotransmitter-stimulated ion transport by cultured porcine vas deferens epithelium. *Am J Physiol Renal Physiol* 281: F557-570, 2001.
199. **Sharp GW and Hynie S.** Stimulation of intestinal adenyl cyclase by cholera toxin. *Nature* 229: 266-269, 1971.
200. **Sharp GW, Hynie S, Lipson LC, and Parkinson DK.** Action of cholera toxin to stimulate adenyl cyclase. *Trans Assoc Am Physicians* 84: 200-211, 1971.
201. **Sharp GW and Leaf A.** Biological Action of Aldosterone in Vitro. *Nature* 202: 1185-1188, 1964.
202. **Shennan DB.** Mammary gland membrane transport systems. *J Mammary Gland Biol Neoplasia* 3: 247-258, 1998.
203. **Shennan DB and Gow IF.** Volume-activated K(+)(Rb(+)) efflux in lactating rat mammary tissue. *Biochim Biophys Acta* 1509: 420-428, 2000.
204. **Shennan DB and Peaker M.** Transport of milk constituents by the mammary gland. *Physiol Rev* 80: 925-951, 2000.
205. **Shi H, Asher C, Yung Y, Kligman L, Reuveny E, Seger R, and Garty H.** Casein kinase 2 specifically binds to and phosphorylates the carboxy termini of ENaC subunits. *Eur J Biochem* 269: 4551-4558, 2002.
206. **Shi PP, Cao XR, Sweezer EM, Kinney TS, Williams NR, Husted RF, Nair R, Weiss RM, Williamson RA, Sigmund CD, Snyder PM, Staub O, Stokes JB, and Yang B.** Salt-sensitive hypertension and cardiac hypertrophy in mice deficient in the ubiquitin ligase Nedd4-2. *Am J Physiol Renal Physiol* 295: F462-470, 2008.
207. **Shiffman ML, Seale TW, Flux M, Rennert OR, and Swender PT.** Breast-milk composition in women with cystic fibrosis: report of two cases and a review of the literature. *Am J Clin Nutr* 49: 612-617, 1989.

208. **Shillingford JM, Miyoshi K, Robinson GW, Grimm SL, Rosen JM, Neubauer H, Pfeffer K, and Hennighausen L.** Jak2 is an essential tyrosine kinase involved in pregnancy-mediated development of mammary secretory epithelium. *Mol Endocrinol* 16: 563-570, 2002.
209. **Shim EH, Shanks RD, and Morin DE.** Milk loss and treatment costs associated with two treatment protocols for clinical mastitis in dairy cows. *J Dairy Sci* 87: 2702-2708, 2004.
210. **Shimkets RA, Warnock DG, Bositis CM, Nelson-Williams C, Hansson JH, Schambelan M, Gill JR, Jr., Ulick S, Milora RV, Findling JW, and et al.** Liddle's syndrome: heritable human hypertension caused by mutations in the beta subunit of the epithelial sodium channel. *Cell* 79: 407-414, 1994.
211. **Silanikove N, Shamay A, Shinder D, and Moran A.** Stress down regulates milk yield in cows by plasmin induced beta-casein product that blocks K+ channels on the apical membranes. *Life Sci* 67: 2201-2212, 2000.
212. **Silanikove N, Shapiro F, and Shinder D.** Acute heat stress brings down milk secretion in dairy cows by up-regulating the activity of the milk-borne negative feedback regulatory system. *BMC Physiol* 9: 13, 2009.
213. **Sjaastad MD, Zettl KS, Parry G, Firestone GL, and Machen TE.** Hormonal regulation of the polarized function and distribution of Na/H exchange and Na/HCO3 cotransport in cultured mammary epithelial cells. *J Cell Biol* 122: 589-600, 1993.
214. **Smalley MJ.** Isolation, culture and analysis of mouse mammary epithelial cells. *Methods Mol Biol* 633: 139-170, 2010.
215. **Smith KM, McNeillie SA, and Shennan DB.** K+ (Rb+) transport by a mammary secretory cell apical membrane fraction isolated from goats' milk. *Exp Physiol* 75: 349-358, 1990.
216. **Smits E, Cifrian E, Guidry AJ, Rainard P, Burvenich C, and Paape MJ.** Cell culture system for studying bovine neutrophil diapedesis. *J Dairy Sci* 79: 1353-1360, 1996.
217. **Snider RM, McKenzie JR, Kraft L, Kozlov E, Wikswo JP, and Cliffel DE.** The effects of cholera toxin on cellular energy metabolism. *Toxins (Basel)* 2: 632-648, 2010.
218. **Snyder PM.** The epithelial Na+ channel: cell surface insertion and retrieval in Na+ homeostasis and hypertension. *Endocr Rev* 23: 258-275, 2002.
219. **Snyder PM.** Minireview: regulation of epithelial Na+ channel trafficking. *Endocrinology* 146: 5079-5085, 2005.
220. **Snyder PM, McDonald FJ, Stokes JB, and Welsh MJ.** Membrane topology of the amiloride-sensitive epithelial sodium channel. *J Biol Chem* 269: 24379-24383, 1994.
221. **Snyder PM, Olson DR, Kabra R, Zhou R, and Steines JC.** cAMP and serum and glucocorticoid-inducible kinase (SGK) regulate the epithelial Na(+) channel through convergent phosphorylation of Nedd4-2. *J Biol Chem* 279: 45753-45758, 2004.
222. **Snyder PM, Olson DR, and Thomas BC.** Serum and glucocorticoid-regulated kinase modulates Nedd4-2-mediated inhibition of the epithelial Na+ channel. *J Biol Chem* 277: 5-8, 2002.
223. **Snyder PM, Price MP, McDonald FJ, Adams CM, Volk KA, Zeiher BG, Stokes JB, and Welsh MJ.** Mechanism by which Liddle's syndrome mutations increase activity of a human epithelial Na+ channel. *Cell* 83: 969-978, 1995.
224. **Sorg D, Potzel A, Beck M, Meyer HH, Viturro E, and Kliem H.** Effects of cell culture techniques on gene expression and cholesterol efflux in primary bovine mammary epithelial cells derived from milk and tissue. *In Vitro Cell Dev Biol Anim* 48: 550-553, 2012.

225. **Soule HD, Maloney TM, Wolman SR, Peterson WD, Jr., Brenz R, McGrath CM, Russo J, Pauley RJ, Jones RF, and Brooks SC.** Isolation and characterization of a spontaneously immortalized human breast epithelial cell line, MCF-10. *Cancer Res* 50: 6075-6086, 1990.
226. **Soule HD, Vazguez J, Long A, Albert S, and Brennan M.** A human cell line from a pleural effusion derived from a breast carcinoma. *J Natl Cancer Inst* 51: 1409-1416, 1973.
227. **Soundararajan R, Lu M, and Pearce D.** Organization of the ENaC-regulatory machinery. *Crit Rev Biochem Mol Biol* 47: 349-359, 2012.
228. **Spangler BD.** Structure and function of cholera toxin and the related Escherichia coli heat-labile enterotoxin. *Microbiol Rev* 56: 622-647, 1992.
229. **Spencer JP.** Management of mastitis in breastfeeding women. *Am Fam Physician* 78: 727-731, 2008.
230. **Stampfer MR and Yaswen P.** Culture models of human mammary epithelial cell transformation. *J Mammary Gland Biol Neoplasia* 5: 365-378, 2000.
231. **Staruschenko A, Medina JL, Patel P, Shapiro MS, Booth RE, and Stockand JD.** Fluorescence resonance energy transfer analysis of subunit stoichiometry of the epithelial Na+ channel. *J Biol Chem* 279: 27729-27734, 2004.
232. **Staruschenko A, Pochynyuk O, Vandewalle A, Bugaj V, and Stockand JD.** Acute regulation of the epithelial Na+ channel by phosphatidylinositide 3-OH kinase signaling in native collecting duct principal cells. *J Am Soc Nephrol* 18: 1652-1661, 2007.
233. **Staub O, Dho S, Henry P, Correa J, Ishikawa T, McGlade J, and Rotin D.** WW domains of Nedd4 bind to the proline-rich PY motifs in the epithelial Na+ channel deleted in Liddle's syndrome. *EMBO J* 15: 2371-2380, 1996.
234. **Staub O, Gautschi I, Ishikawa T, Breitschopf K, Ciechanover A, Schild L, and Rotin D.** Regulation of stability and function of the epithelial Na+ channel (ENaC) by ubiquitination. *EMBO J* 16: 6325-6336, 1997.
235. **Stelwagen K, McFadden HA, and Demmer J.** Prolactin, alone or in combination with glucocorticoids, enhances tight junction formation and expression of the tight junction protein occludin in mammary cells. *Mol Cell Endocrinol* 156: 55-61, 1999.
236. **Strange R, Li F, Friis RR, Reichmann E, Haenni B, and Burri PH.** Mammary epithelial differentiation in vitro: minimum requirements for a functional response to hormonal stimulation. *Cell Growth Differ* 2: 549-559, 1991.
237. **Stull MA, Pai V, Vomachka AJ, Marshall AM, Jacob GA, and Horseman ND.** Mammary gland homeostasis employs serotonergic regulation of epithelial tight junctions. *Proc Natl Acad Sci U S A* 104: 16708-16713, 2007.
238. **Svennersten-Sjaunja K and Olsson K.** Endocrinology of milk production. *Domest Anim Endocrinol* 29: 241-258, 2005.
239. **Tan CD, Selvanathar IA, and Baines DL.** Cleavage of endogenous gammaENaC and elevated abundance of alphaENaC are associated with increased Na(+) transport in response to apical fluid volume expansion in human H441 airway epithelial cells. *Pflugers Arch* 462: 431-441, 2011.
240. **Taylor-Papadimitriou J, Purkis P, and Fentiman IS.** Cholera toxin and analogues of cyclic AMP stimulate the growth of cultured human mammary epithelial cells. *J Cell Physiol* 102: 317-321, 1980.

241. **Tchepichev S, Ueda J, Canessa C, Rossier BC, and O'Brodovich H.** Lung epithelial Na channel subunits are differentially regulated during development and by steroids. *Am J Physiol* 269: C805-812, 1995.
242. **Thomas KL and Ellingrod VL.** Pharmacogenetics of selective serotonin reuptake inhibitors and associated adverse drug reactions. *Pharmacotherapy* 29: 822-831, 2009.
243. **Ussing HH and Zerahn K.** Active transport of sodium as the source of electric current in the short-circuited isolated frog skin. *Acta Physiol Scand* 23: 110-127, 1951.
244. **Vasquez MM, Mustafa SB, Choudary A, Seidner SR, and Castro R.** Regulation of epithelial Na+ channel (ENaC) in the salivary cell line SMG-C6. *Exp Biol Med (Maywood)* 234: 522-531, 2009.
245. **Venkatesh VC and Katzberg HD.** Glucocorticoid regulation of epithelial sodium channel genes in human fetal lung. *Am J Physiol* 273: L227-233, 1997.
246. **Volk KA, Husted RF, Snyder PM, and Stokes JB.** Kinase regulation of hENaC mediated through a region in the COOH-terminal portion of the alpha-subunit. *Am J Physiol Cell Physiol* 278: C1047-1054, 2000.
247. **Waldmann R, Champigny G, Bassilana F, Voilley N, and Lazdunski M.** Molecular cloning and functional expression of a novel amiloride-sensitive Na+ channel. *J Biol Chem* 270: 27411-27414, 1995.
248. **Wang J, Barbry P, Maiyar AC, Rozansky DJ, Bhargava A, Leong M, Firestone GL, and Pearce D.** SGK integrates insulin and mineralocorticoid regulation of epithelial sodium transport. *Am J Physiol Renal Physiol* 280: F303-313, 2001.
249. **Wang LY, Salter MW, and MacDonald JF.** Regulation of kainate receptors by cAMP-dependent protein kinase and phosphatases. *Science* 253: 1132-1135, 1991.
250. **Wang Q and Schultz BD.** Cholera Toxin Enhances Na+ Absorption across MCF10A Human Mammary Epithelia. *Am J Physiol Cell Physiol* 306: C471-484, 2013.
252. **Wang X, Sun L, Maffini MV, Soto A, Sonnenschein C, and Kaplan DL.** A complex 3D human tissue culture system based on mammary stromal cells and silk scaffolds for modeling breast morphogenesis and function. *Biomaterials* 31: 3920-3929, 2010.
253. **Wangemann P, Itza EM, Albrecht B, Wu T, Jabba SV, Maganti RJ, Lee JH, Everett LA, Wall SM, Royaux IE, Green ED, and Marcus DC.** Loss of KCNJ10 protein expression abolishes endocochlear potential and causes deafness in Pendred syndrome mouse model. *BMC Med* 2: 30, 2004.
254. **Welch MJ, Phelps DL, and Osher AB.** Breast-feeding by a mother with cystic fibrosis. *Pediatrics* 67: 664-666, 1981.
255. **Wilde CJ, Addey CV, Boddy LM, and Peaker M.** Autocrine regulation of milk secretion by a protein in milk. *Biochem J* 305 (Pt 1): 51-58, 1995.
256. **Yang HY, Charles RP, Hummler E, Baines DL, and Isseroff RR.** The epithelial sodium channel mediates the directionality of galvanotaxis in human keratinocytes. *J Cell Sci* 126: 1942-1951, 2013.
257. **Yang J, Richards J, Guzman R, Imagawa W, and Nandi S.** Sustained growth in primary culture of normal mammary epithelial cells embedded in collagen gels. *Proc Natl Acad Sci U S A* 77: 2088-2092, 1980.
258. **Yang LM, Rinke R, and Korbmacher C.** Stimulation of the epithelial sodium channel (ENaC) by cAMP involves putative ERK phosphorylation sites in the C termini of the channel's beta- and gamma-subunit. *J Biol Chem* 281: 9859-9868, 2006.

259. **Yang W, Molenaar A, Kurts-Ebert B, and Seyfert HM.** NF-kappaB factors are essential, but not the switch, for pathogen-related induction of the bovine beta-defensin 5-encoding gene in mammary epithelial cells. *Mol Immunol* 43: 210-225, 2006.
260. **Yu L, Helms MN, Yue Q, and Eaton DC.** Single-channel analysis of functional epithelial sodium channel (ENaC) stability at the apical membrane of A6 distal kidney cells. *Am J Physiol Renal Physiol* 295: F1519-1527, 2008.
261. **Zaika O, Mamenko M, Staruschenko A, and Pochynyuk O.** Direct activation of ENaC by angiotensin II: recent advances and new insights. *Curr Hypertens Rep* 15: 17-24, 2012.
262. **Zavizion B, van Duffelen M, Schaeffer W, and Politis I.** Establishment and characterization of a bovine mammary epithelial cell line with unique properties. *In Vitro Cell Dev Biol Anim* 32: 138-148, 1996.
263. **Zettl KS, Sjaastad MD, Riskin PM, Parry G, Machen TE, and Firestone GL.** Glucocorticoid-induced formation of tight junctions in mouse mammary epithelial cells in vitro. *Proc Natl Acad Sci U S A* 89: 9069-9073, 1992.
264. **Zhao X and Lacasse P.** Mammary tissue damage during bovine mastitis: causes and control. *J Anim Sci* 86: 57-65, 2008.
265. **Zheng YM, He XY, and Zhang Y.** Characteristics and EGFP expression of goat mammary gland epithelial cells. *Reprod Domest Anim* 45: e323-331, 2010.
266. **Zhou R, Patel SV, and Snyder PM.** Nedd4-2 catalyzes ubiquitination and degradation of cell surface ENaC. *J Biol Chem* 282: 20207-20212, 2007.
267. **Ziska SE, Bhattacharjee M, Herber RL, Qasba PK, and Vonderhaar BK.** Thyroid hormone regulation of alpha-lactalbumin: differential glycosylation and messenger ribonucleic acid synthesis in mouse mammary glands. *Endocrinology* 123: 2242-2248, 1988.